U.PORTO
FEUP FACULDADE DE ENGENHARIA
UNIVERSIDADE DO PORTO

Master in Mechanical Engineering

Reinforcement of CFRP SLJs using Metal Laminates and Adhesive Layers

Mário António Morgado dos Santos Pereira

Supervised by
Lucas Filipe Martins da Silva

Co-Supervised by
Ricardo João Camilo Carbas

June, 2019

Resumo

O uso de materiais compósitos em componentes estruturais tem crescido significantemente nos ultimos anos. Esta tendência é bem representada na indústria aeronáutica, onde à semelhança da indústria autmóvel, os fabricantes aspiram obter melhores consumos de combustível e reduzir as suas emissões, através de projetos mais leves e eficientes.

No entanto, a ocorrência de delaminação em juntas adesivas de materiais compósitos é ainda uma limitação para um projeto ótimo, sem o sobredimensionamento de componentes.

Duas técnicas de reforço de juntas de sobreposição simples de fibra de carbono foram analisadas para duas velocidades de teste, uma quase-estatica (1mm/min) e outra a impacto (3m/s). Os reforços têm como objetivo principal melhorar a resistência ao arrancamento em materiais compósitos e prevenir delaminação.

As metodologias de reforço foram inspiradas pelo conceito de *Fibre Metal Laminates* (FML), materiais híbridos compostos por laminados de metal e materiais compósitos, que tentam combinar as melhores propriedades de cada componente.

A primeira, mais parecida com FMLs, utiliza como reforços placas de alumínio, de uma liga comummente usada na indústria aeronática e aeroespacial, para reforçar os topos dos aderentes. A segunda, sugere a utilização de camadas adicionais de adesivo em diferentes posições ao longo da espessura do aderente de modo a melhorar as propriedades transversais do compósito. O desempenho das juntas reforçadas foi comparado ao de juntas de fibra de carbono tradicional com a mesma geometria.

As diferentes configurações foram fabricadas e experimentalmente testadas usando uma máquina de tracção para a condição quase-estática (1mm/min) e uma máquina de queda de massa para a condição de impacto a baixa velocidade (3m/s).

Adicionalmente, modelos numéricos usando o software ABAQUS foram desenvolvidos de modo a estudar o comportamento das juntas, prever forças de rutura e o modo de falha para cada configuração sugerida.

No geral, e apesar da ocorrência de delaminação não ter sido possível de evitar para todas as configurações e condições testadas, as juntas reforçadas demonstraram melhorias consideráveis. Esta melhoria foi manifestada principalmente através do aumento das forças de rotura e deslocamento máximo.

Apesar de, para as mesmas condições de teste e mesmo adesivo, terem sido obtidos melhores resultados para o reforço usando laminados de metal do que para as juntas reforçadas com adesivo, ambas as técnicas podem vir a ser implementadas com sucesso em diferentes circunstâncias.

Abstract

Usage of composite materials like Fibre Reinforced Plastics for structural applications has been increasing in recent years. This trend can clearly be seen in the aeronautics industry, with Fibre Reinforced Plastics, accounting for an increasingly more representative share of the final structural weight of the aircraft, as manufacturers pursue improvements in fuel economy and lighter more efficient designs.

Nevertheless, delamination of adhesively bonded composite joints is still a concern, as it causes premature failure of the bond inhibiting the use of its full potential, leading to inefficient over-designed components.

Two reinforcement techniques for CFRP single lap joints are examined for quasi-static and impact conditions. The reinforcements aim to increase the joint strength in the through thickness direction, minimise peel stresses and limit delamination.

The methods were inspired by the Fibre Metal Laminates concept, a hybrid composite metallic material technology that aims to combine the best properties of FRPs and metal alloys.

The first, more closely linked to FMLs, uses an aluminium alloy commonly used in the aeronautics industry and FML configurations, to reinforce the tops of adherends. The second, uses additional adhesive layers in different configurations throughout the transverse direction of the substrate. The performance of the reinforced techniques was benchmarked against a traditional CFRP-only single lap joint with the same geometry.

The different configurations were manufactured and experimentally tested using a universal testing machine for a crosshead speed of 1mm/min and a drop-weight machine for an impact speed of 3m/s.

Numerical models were developed, using the ABAQUS software, to study the behaviour of all configurations studied. The numerical predictions of failure loads and modes were compared to the experimentally obtained results.

Overall, although the occurrence of delamination could not be avoided for all conditions and configurations, both reinforcement techniques improved the delamination resistance of the tested joint. These improvements were mainly seen through increases of the maximum failure loads and the energy absorption capabilities of the CFRP single lap joint.

Although, for the same conditions and using the same adhesive, metal laminate reinforcement joints outperformed adhesively reinforced configurations, each technique offers its own set of advantages which can possibly see both viably implemented in different circumstances.

Acknowledgements

Firstly, I hereby express my gratitude to my supervisor, Professor Lucas da Silva, for the invaluable guidance, and for the expertise and knowledge shared throughout the project.

Secondly, I would like to thank Ricardo Carbas, my co-supervisor, for all his dedication, patience and hours spent in the laboratory sharing his experience with me.

To all ADFEUP members for their availability and support for the duration of my dissertation. In particular, I thank Eduardo Marques, José Machado, Paulo Nunes, Alireza Akhavan, Mateus Reis and Diogo Antunes. To my master thesis partners, Catarinas, for their companionship in whining and dining.

I would also like to express my gratefulness to LOME, namely Pedro Moreira, Paulo Tavares and Nuno Viriato for the help given in acquiring slow-motion footage of impact tests with the high-speed camera.

To all my good friends, both from my hometown, Viseu, and FEUP, for all their support and friendship.

And finally to my good family, especially my parents and brother, for unconditionally supporting me throughout all my life.

Contents

List of Figures

List of Tables

Nomenclature

Acronyms

ALR - Adhesive Layer Reinforcement

ARALL – Aramid reinforced aluminium laminate

CARALL – Carbon reinforced aluminium laminate

CBBM - Compliance based beam method

CFRP – Carbon fibre reinforced plastic/polymer

CML - Composite Metal Laminate

CZE – Cohesive zone elements

CZM – Cohesive zone model

DCB – Double cantilever beam

ENF – End notched flexure

FEA – Finite element analysis

FEM – Finite elements method

FML – Fibre metal laminate

FRP – Fibre reinforced polymer/plastic

GLARE – Glass reinforced aluminium

P-δ - Load-Displacement

R-Curve - Crack growth resistance curve

SLJ – Single lap joint

TAST – Thick adherend shear test

Symbols

a - Crack length

a_{eq} - Equivalent crack length

δ - Displacement

E - Young's Modulus

E_f - Corrected bending modulus

G - Shear Modulus

G_{IC} - Fracture energy in mode I

G_{IIC} - Fracture energy in mode II

P - Load

ν - Poisson's ratio

1 Introduction

1.1 Background and motivation

The importance of composite materials in modern engineering cannot be overstated. While their use was limited throughout early history, their capabilities were expanded significantly throughout the 20th century and they are nowadays an important material group for any designer/engineer with their interesting properties such as high specific stiffness or excellent strength to weight ratio, fatigue behaviour and corrosion resistance. This makes them very attractive for applications where weight is a significant constraint. Fortunately for the composite industry, these applications have been growing in size and relevance with the automotive industry shifting to lightweight materials that allow their vehicles to meet mileage targets and emission standards. Once only an option for high-end sports cars, the potential for implementation in other segments could see them seize a sizeable market share in the automotive industry, one of the biggest grossing over 1500 billion US dollars for the top 10 leading automakers, something they already have in the aviation and aerospace industries.

In the aerospace industry, the Airbus A350, figure 1, has a composite material weight ratio of 52% while Boeing has models, such as the Boeing 787 Dreamliner in which composites account for half the structural weight, helping fuel economy by almost 20% [1–3].

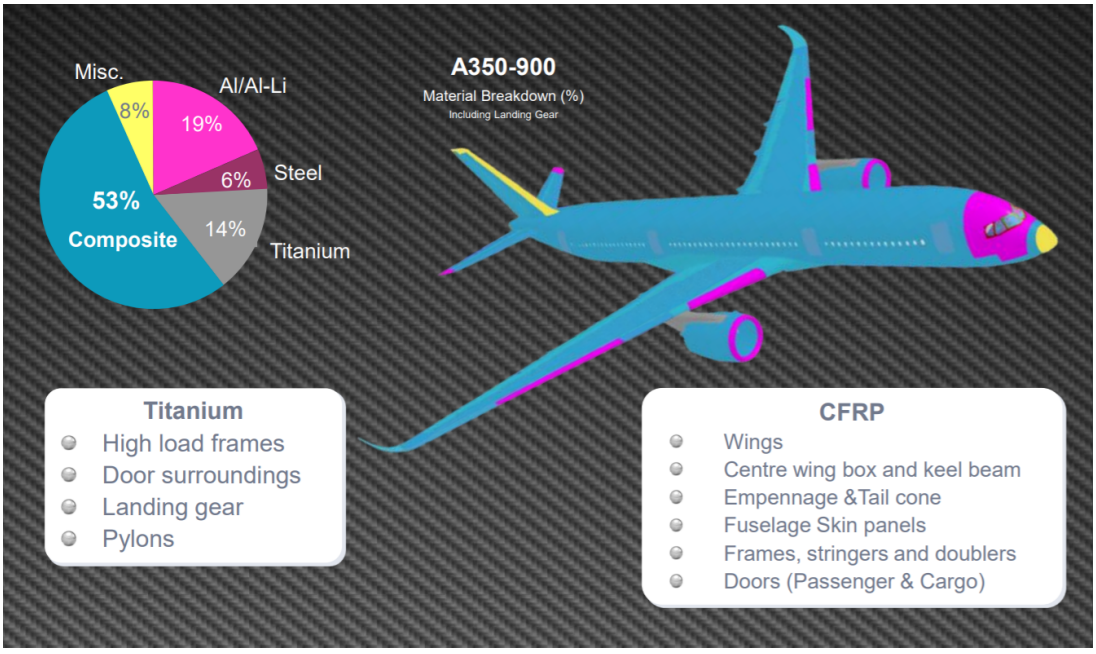

Figure 1: Airbus A350 material breakdown in percentage [2]

With composite materials comes adhesion technology. Many joining methods used for other materials like welding, riveting and bolting do not have the same success when applied to composites either by concept failure (welding/brazing) or due to composites higher notch sensitivity and low shear strength (stress concentration), decreasing the

overall strength of the joint. In components expected to be submitted to high stress loads a combination of mechanical fasteners and adhesives is used, but in many cases, like in automotive manufacturing, figure 2, the joining will be guaranteed by adhesive bonding only, with adhesives taking on a critical structural role.

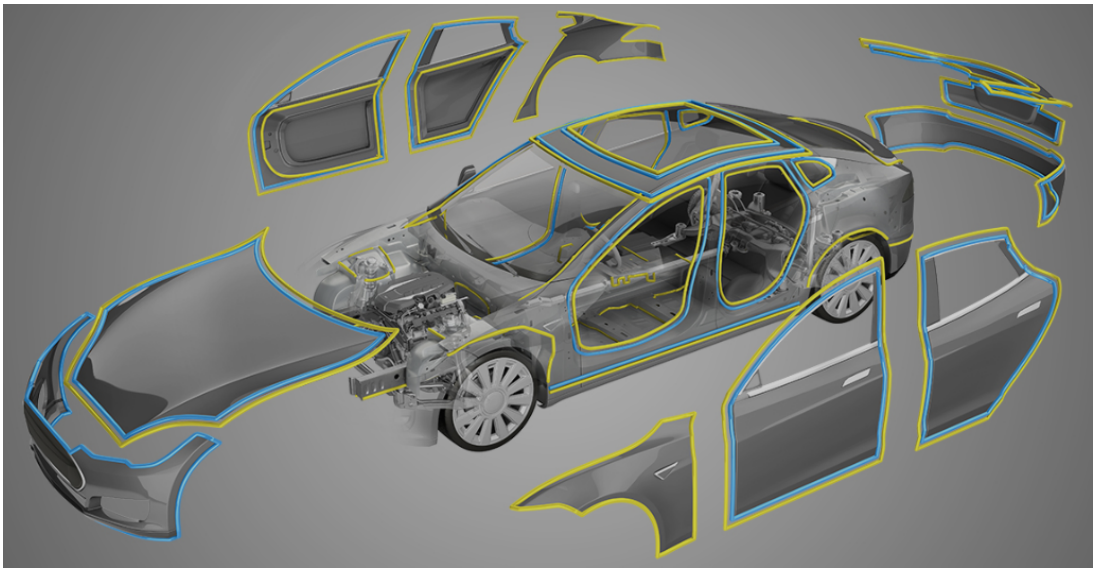

Figure 2: Adhesive use in the automotive industry [4]

Additionally, using adhesives in vehicle manufacturing provides the added benefit of damping vibrations and noise. Cadillac boasts the use of more than 387 feet (118 m) in its 2014 CTS luxury sedan claiming that their use with aluminium had contributed to a "better ride, handling and reduced cabin noise" and had helped "reduce overall weight" in two of the automaker's models [5].

The anisotropic nature of composites adds an extra layer of complexity to the use of these materials with possible out-of-plane/interlaminar loadings leading to delamination – a transversal failure mode due to peel stresses and poor bonding between the fibres and polymeric matrix.

The aim of this thesis is exactly to research methods that could minimise or eliminate this phenomenon, that is hindering the true potential of adhesive bound joints in composite materials by failing the joint prematurely. Although there are several technologies that try to address this, such as z-pins or more complex joint configurations, this project will focus on the possible role of Fibre Metal Laminate technology (FML) in delamination prevention.

This master thesis was developed within the ADFEUP group, the Adhesion Research and Development group at the Faculty of Engineering of the University of Porto (FEUP), where mechanical properties of FMLs and joints reinforced with Interlaminar Adhesive Layers (IAL) under quasi-static loading conditions were previously studied.

Two single lap joint (SLJ) configurations inspired by the concept will be studied. The first uses aluminium sheets while the second uses layers of the adhesive itself.

Even though these techniques were directly influenced by these two material technologies they are different in some aspects of the geometry preventing the use of the same name. In figure 3, these differences can visually be seen.

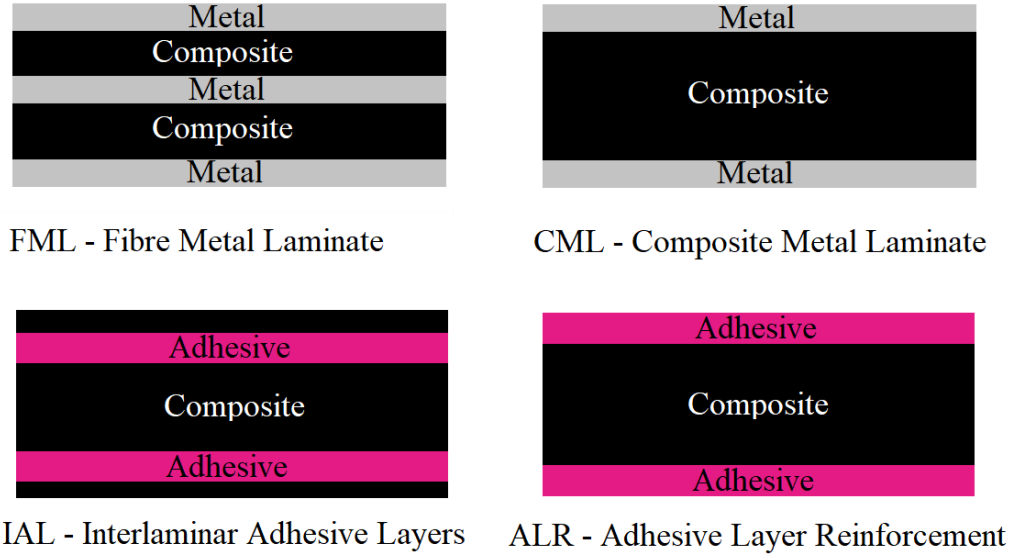

Figure 3: Nomenclature of the two reinforcement approaches

The configuration using metal laminates as reinforcement, only does so at the tops of the adherend, i.e. the interface of the adhesive and adherend in order to reduce delamination, unlike common FMLs which have metal sheets laminated directly into the adherend. As such, this technique was given the name of CML - Composite Metal Laminate.

Regarding the second approach, although no previous article has been published in scientific journals, "Interlaminar Adhesive Layers" nomenclature was previously used in a previous master thesis at FEUP. Since the continuous development of this technique for this thesis resulted in a configuration more akin to the CML method and the adhesive reinforcement was not applied in between composite plies, said reinforcement is not interlaminar. Consequently, it has been renamed to ALR - Adhesive Layer Reinforcement.

Both CML and ALR are to be applied to the adherend geometry, replacing CFRP-only adherends of the same thickness.

The concept of Interlaminar Adhesive Layers did not completely eliminate delamination in previous studies, but was shown to improve the maximum failure load up to almost 20 % in quasi-static conditions [6]. Additionally, the added adhesive layers would not significantly increase the weight of joints and could be interesting in severely weight restricted applications not uncommon in the industry segments where composites are already being used.

FML technology allows for the combination of mechanical properties of both composites and metals. While metals contribute with strength, toughness, resilience and impact resistance, composites have high strength and stiffness, especially considering their low density, and have good fatigue and corrosion resistance. The inclusion of metals like

aluminium or titanium through this technology almost seems like an expected evolution of composites own concept, fibre/matrix reinforcement.

There are a variety of scenarios that make impact loads likely enough for them to have to be considered in the design process. Impact loads cause localised damage that can compromise the entire structure. The knowledge of how a joint will perform against impact loads is very important to structural designers. This, in turn, allows for a better selection of materials, adhesives and joint configurations with optimised parameters like failure loads, costs and weight.

Impact testing is normally divided into two main subcategories: high-velocity impact and low-velocity impact. High-velocity impact is normally associated in the aeronautical industry with hail and bird strikes or runway debris hitting the lower fuselage of the plane on take-off and landing, and ballistic impacts in military applications or terrorist attacks [7]. Lower velocity impacts can be the result of maintenance trucks and movable stairways colliding with the aircraft or construction/maintenance mishaps like tool dropping [7, 8].

Studying the joint performance to impact is also very important for the automotive industry, where adhesives are used as the only joining method for some structural components and as such have to ensure that during a crash the joint is able to sustain the collision forces, transferring them to the substrates that will deform in order to prolong the collision time and absorb the energy. This would require the adhesive used to be ductile enough to allow the necessary deformation of the substrate without fracturing.

While there have been a number of studies related to low and high-velocity impact properties of FMLs in the last decades, most of them focus on perforation or pendulum tests, and the study of the through thickness properties of the technology alone in its two major parameters: materials and geometry (circular clamps, FML panels, under tensile loading, etc.) [8–12].

After gaining a proper understanding of these materials in a single lap joint subjected to quasi-static conditions, and since experimental testing for high-velocity impact would require the use of an unavailable SHPB (Split-Hopkinson Pressure Bar) setup, this project will focus on low-velocity experimental tests. Although there is no clear limit separating these, it is normally accepted that impact speeds lower than 10 m/s, capable of being reproduced by a drop-weight machine, are low-velocity impact settings.

The results of a combination of numerical models and experimental testing for these two reinforcement approaches, will ultimately be benchmarked against traditional CFRP-only joints.

1.2 Objectives and methodology

The main objective of this thesis is to characterise the quasi-static and impact behaviour of CFRP single lap joints reinforced with metal laminates and adhesive layers.

To achieve these objectives the following research methodology plan was used:

- Characterisation of the adhesives used, determining the mechanical properties of the adhesives under quasi-static and impact conditions, a necessary step for numerical modelling,
- Development of quasi-static and impact numerical models for CFRP, CML and ALR single lap joints,
- Manufacture and experimental testing of CFRP, CML and ALR single lap joints to validate the numerical models and characterise impact behaviour.

1.3 Thesis outline

This thesis is comprised of the following main sections:

- Introductory chapter: the motivation, objectives and research methodology for the dissertation are explained;
- Literature Review: documents the state of the art of adhesive bonding technology, delamination prevention techniques, failure modes and loading conditions, providing a theoretical framework of the study area in which the project is inserted.
- Experimental Procedures: focused on describing experimental tests, methods and equipment used.
- Summary of the appended papers: The main objectives and conclusions reached for each individual paper are laid out;
- Conclusions: The dissertation's concluding remarks are presented and possible future research guidelines are suggested;
- Appended papers: Paper A - Reinforcement of CFRP Single Lap Joints using Metal Laminates, and Paper B - Reinforcement of CFRP Single Lap Joints with Adhesive Layers. Paper A was submitted to the scientific journal Composite Structures and Paper B to the International Journal of Adhesion and Adhesives.

2 Literature Review

2.1 Adhesive bonding

Adhesive bonding is a material joining method in which a material, the adhesive, is applied between two surfaces of a different material and after a chemical process known as curing, forms an adhesive bond that joins them.

There are four classical theories that explain the adhesive bond created. The adsorption, the mechanical, the electrostatic and the diffusion theory. These try to explain which forces create the intimate bond that transmits loads and resists separation [13].

The adsorption theory explains the adhesion for smooth surfaces due to contact at a molecular level, the presence of ionic/covalent bonds between adhesive and substrate as well as weaker secondary forces resultant of dipolar interaction [14]. The mechanical theory tackles the rough or porous, and attributes the bonding forces to a series of singular, localised physical connections in pores and cavities on the surface of the material that anchor the adhesive to the adherend after cure [14].

These were later contested by proponents of the electrostatic theory, that advocate that the binding is the result of the transfer of the electrostatic charge between adhesive and substrate, but support for this theory seems to be diminishing in recent years due to an incongruence in the estimates of the energy of this bond and higher fracture energies observed [14].

Conversely, the diffusion theory is gaining traction, and states that "adhesion is developed through the interdiffusion of molecules in between the adhesive and the adherend" [15], explaining polymer to polymer adhesion. However, the idea that only one of these can be correct should not be fostered, as it is likely that in reality, they all are relevant to the understanding of adhesion on a broader scope.

The term adhesively bonded joints refers to the joining method end result, a design that combines the adherends, the parts that were joined, and the adhesive.

Adhesive joints are an alternative to mechanical joining methods or joining methods that require the melting of materials like welding, or brazing. Despite having a lower strength compared to metals if presented with a big enough bearing area the bond can withstand substantial loads and take on a structural role in engineering applications, making them very suited for one of their main applications - joining thin sheets of materials [13, 16].

The use of adhesives offers several advantages like low weight, high bond stiffness and a uniform distribution of stress along the bonded area. Unlike welding it does not introduce residual thermal stresses due to unwanted changes in the microstructure and avoids the creation of stress concentration zones caused by the use of mechanical fasteners like bolts.

Additionally, they are a good choice when bonding surfaces of dissimilar materials because their flexibility can compensate for different thermal expansion coefficients, have good damping properties beneficial to fatigue resistance and noise/vibrations control, and

since the application method is not very complex it can be automated [13].

However, there are some disadvantages to the use of adhesives. Its mechanical behaviour is very dependent on the load type, so a careful joint design is required to limit peel stresses and encourage shear loadings. Harsh environmental conditions can also have a detrminetal effect on the joint strength and the curing method can be difficult to accurately control in certain conditions as a precise combination of heat/pressure and time may be necessary depending on the adhesive type. A proper surface treatment must also be ensured and after curing the joining is considered permanent and disassemble of parts is very difficult.

Moreover, despite the use of some kind of adhesives for millennia [17], the invention of the first polymeric adhesive during the first decade of the 20th century [18], and a fast development of adhesives ever since, an adequate universal criteria for the dimensioning of joints is yet to be found. Instead, a good understanding of fracture mechanics and analytical/numerical models of joint strength prediction is indispensable for modelling adhesive behaviour and perform a correct joint design [19].

Ultimately, the existence of adhesives in structural applications provides a larger range of possibilities in either the manufacturing methods and the potential viable materials that can be used in the mechanical design process. Thus, we can expect overall better designs, or even new designs that would not be possible without them.

2.1.1 Joint Configurations

An adhesive joint can have several configurations, figure 4 . Depending on the function of the joint, structural or non-structural, the expected loads, available bond area and taking into consideration factors such as complexity, manufacturing time and cost a decision regarding the adhesive joint configuration is taken.

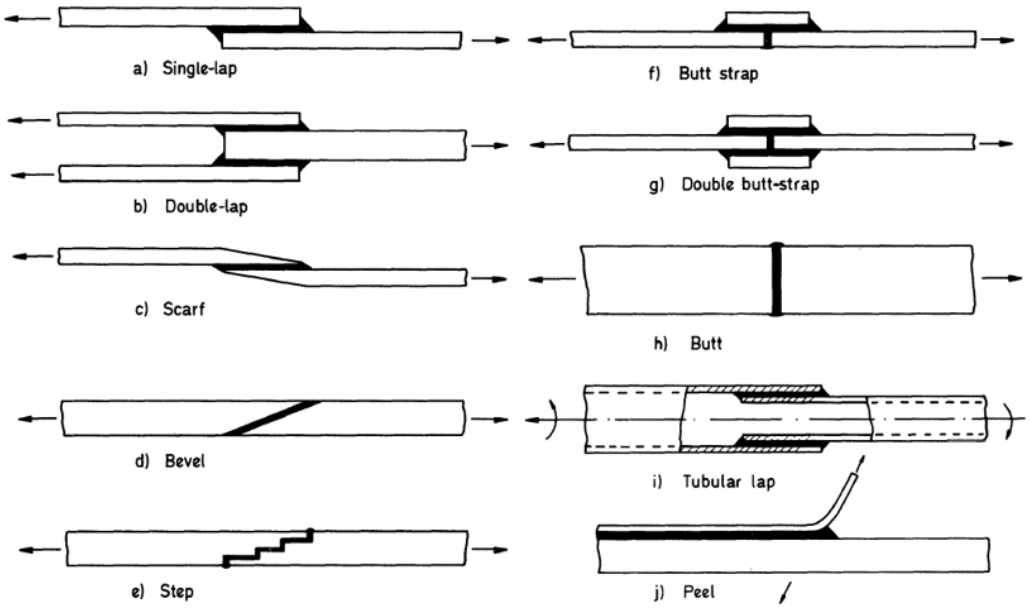

Figure 4: Common joint configurations (Adapted from Adams 1984) [16]

Understanding that different load types cause a different behaviour in the adhesive is extremely important. There are four important stress types: normal (tension and compression), shear, cleavage and peel. Illustrations for these stresses can be seen on figure 5.

Ideally, the joint should be designed to be under shear loading. Peel, more prevalent with flexible adherends, and cleavage stresses are considered the most prejudicial to the joint strength as the stress is concentrated on a "thinner" line and not the whole adhesively bound area.

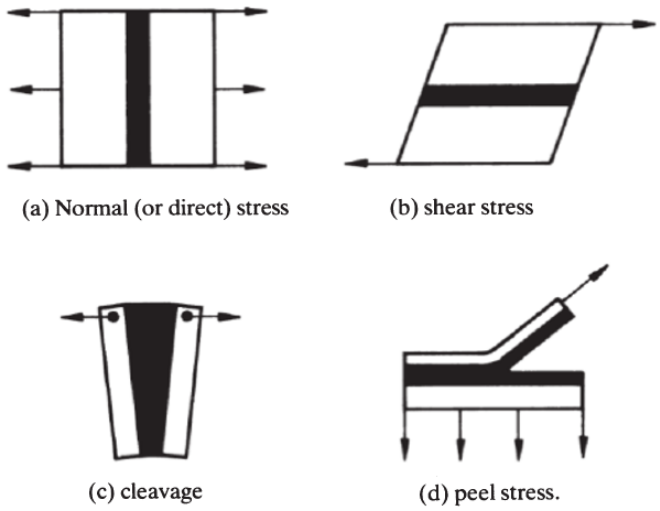

Figure 5: Types of stress on a joint (Adapted from Kinloch 1987) [20]

SLJs are the most common joint design in practical applications due to its simplicity and bond area, but more complex solutions are available to minimise peel stresses that occur after this joint deforms under traction due to the bending moments formed.

Further alterations can be made to the basic designs to optimise their performance like filleting the adhesive or tapering the substrate [21].

2.1.2 Failure Modes

There are three major failure modes in adhesive joints:

- Adhesive failure – caused by poor adhesion. This type of failure can be recognised by the absence of adhesive remains in one of the substrates after rupture. An inadequate surface preparation is in most cases the responsible factor. Although some materials have a lower adherence than others a careful surface treatment can be employed to improve them. Among these treatments are degreasing, grit blasting, plasma surface treatments, anodization and the use of primers – adhesion promoter substances.
- Cohesive failure in the adhesive – adhesive limited failure. This failure is recognised by the presence of a layer of adhesive in each substrate. It is a result of either a bad

joint design or simply due to the fact that the adhesive cannot withstand the applied load.

If a redesign of the joint is not possible then an adhesive with better mechanical properties must be used. Cohesive failures indicate a good adhesion.

- Cohesive failure in the adherend – the ideal failure for adhesive joints. The failure occurs outside of the adhesive damaging the adherend, signifying that the joining method is no longer the weakest spot in the structural design. In this case, given that the adhesive is stronger than the adherend, homologation of the joint can be achieved simply by demonstrating that the substrate is adequate for the function [6].

These failure types are represented on figure 6. A mixed failure can sometimes be observed, normally a combination of adhesive and cohesive failure.

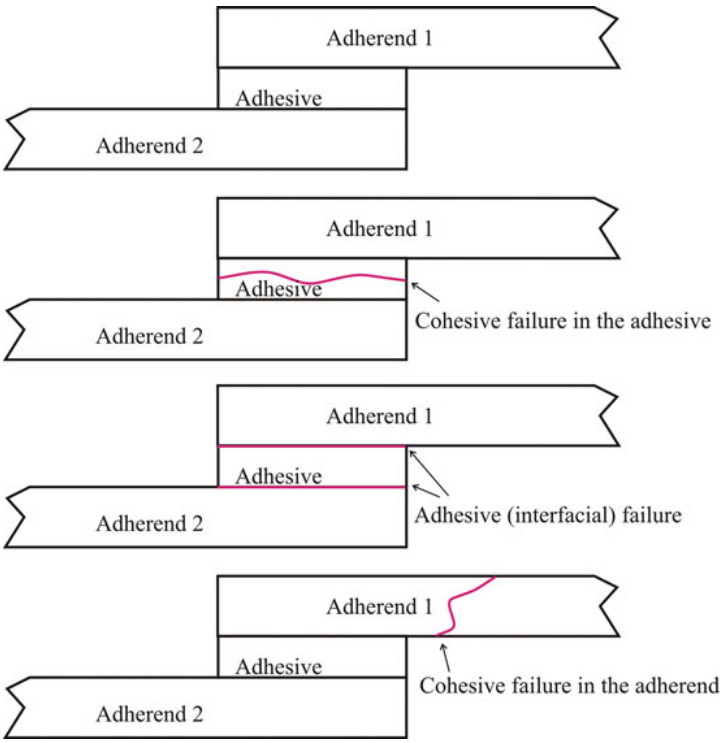

Figure 6: Failure types in adhesive joints [13]

2.2 Fibre Reinforced Plastics

Fibre reinforced plastics (FRP) are a type of composite materials whose polymer matrix is reinforced with fibres. The matrix is usually a thermosetting polymer like epoxy or polyester and the most common fibres are carbon, glass and aramid.

One of the most common examples is carbon fibre reinforced plastic (CFRP), and the carbon fibres provide the matrix with very good properties of strength to weight ratio and specific stiffness. Because of this, fibre reinforced materials are highly anisotropic exhibiting the best mechanical properties in the direction of the fibres and the worse in the

perpendicular direction to them. If a more in-plane isotropic behaviour is necessary, this can be achieved by stacking plies of fibres in different directions. However, engineers can use these exceptional properties in certain directions in applications where the expected loadings are directionally oriented, designing their products in such a way as to cause this type of loading, or study the stress distribution on their product and determine the optimal configuration of the composite layup. This is known as deterministic design and takes into consideration the different failure mechanisms in FRPs like brittle fibre fractures, fibre pull-out, fibre-matrix debonding under tensile loading or matrix cracking for compressive loads [22].

Additionally, for more complex geometries or designs for functions with more unpredictable loads probabilistic design is employed, using statistical methods to quantify risk and support the design process [22]. This extensive process has become easier, faster and more efficient with computer-aided engineering.

Since well-established isotropic design procedures, like the ones used for metallic materials, cannot be easily converted to composites, there is an added difficulty in the design for these materials requiring a multidisciplinary approach with materials engineers working side by side with structural engineers and extensive certification/homologation [22, 23].

Nevertheless, the fact that these materials usage is, despite the cost, steadily increasing in demanding industries like the aeronautic and automotive, seen in figure 7, is a great testament to their unique properties and their importance to weight reduction, for example to meet increasingly challenging emissions standards or performance targets like fuel economy .

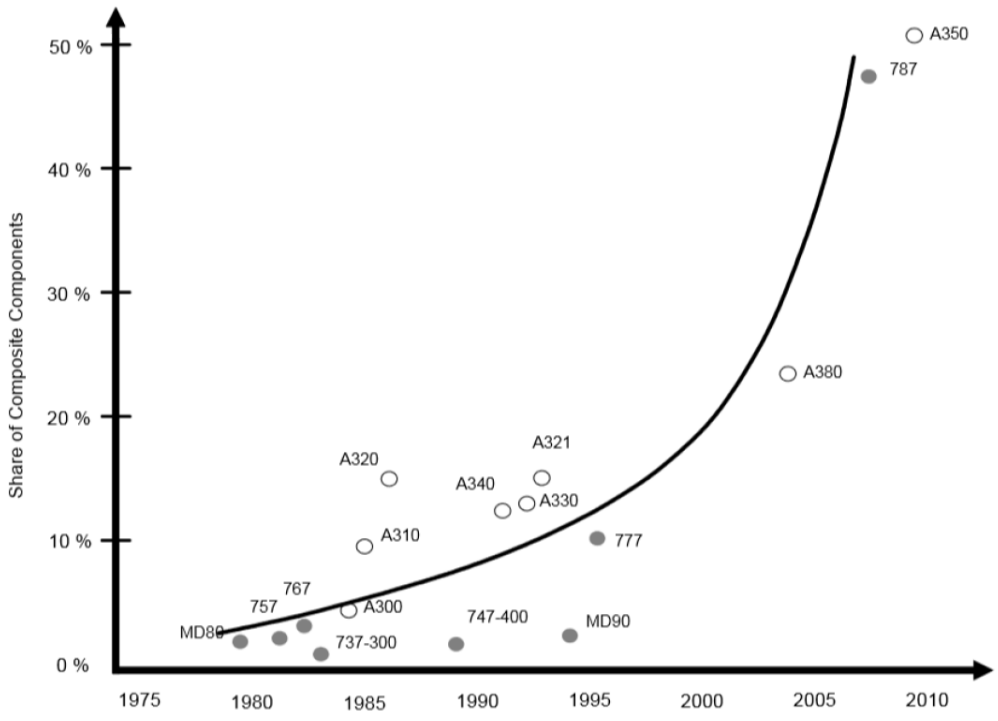

Figure 7: Share of composite materials in commercial aircraft [24]

Other advantageous CFRP properties include excellent fatigue properties, low coefficient of thermal expansion and corrosion resistance [25].

Glass fibre reinforced plastic is also commonly used. It is cheaper than CFRP, more resistant to impact damage and are good thermal and electrical insulators [22]. They do, however, have worse mechanical properties and a higher density.

2.2.1 Failure Modes

In addition to the failure modes presented for adhesively bound joints, there are additional failure sub-types associated with the use of composite materials as adherends, a consequence of a phenomenon known as delamination - a transversal failure mode due to peel stresses and poor bonding between the fibres and the polymeric matrix, figure 8. Environmental degradation can also facilitate delamination.

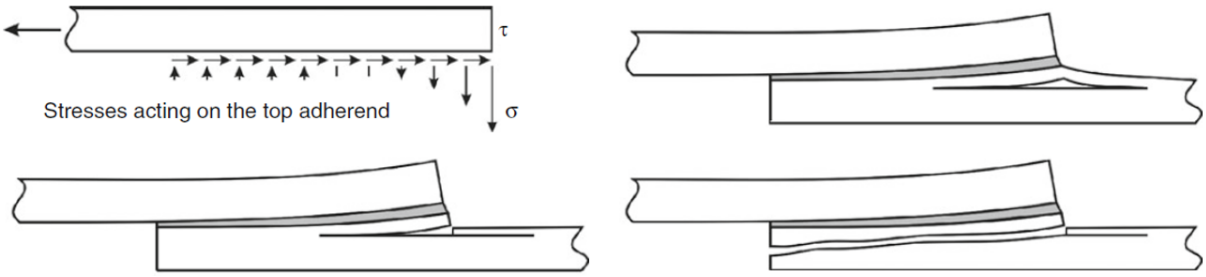

Figure 8: Delamination process illustrated [26]

As a result, the standard D5573 of the American Society for Testing and Materials identifies seven failure modes in FRP joints: adhesive failure, cohesive failure, thin-layer cohesive failure, fibre-tear failure, light-fibre-tear failure, stock-break failure, figure 9, and mixed failure [27].

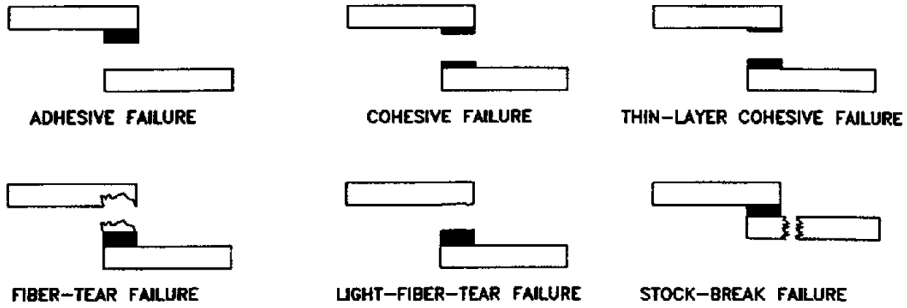

Figure 9: Failure modes in FRP joints [27]

2.2.2 Delamination Prevention

Delamination is seen as a real issue to tackle before a more representative use of composite materials in structural applications, or even the full extent of the advantages of their application can be seen. There are safety concerns about the detection of delamination cracks, and since studies show that the crack growth in CFRP is relatively high for

low stress fatigue cycles this could lead to unpredictable catastrophic failures of composite structures [28, 29].

The initiation of the cracks themselves could be traced back to mechanical fasteners holes or impact damage [29]. In fact, composites higher notch sensitivity and low shear strength is actually one of the reasons to prefer the use of adhesive joints over mechanical connections. The uniform stress distribution observed along the bond translates into good fatigue resistance.

Although, traditionally, and according to Pingkarawat [28] the answer to deal with this problem has been to over-design the structures adding significant weight, several novel methods have been proposed to mitigate the issue, shown in figure 10.

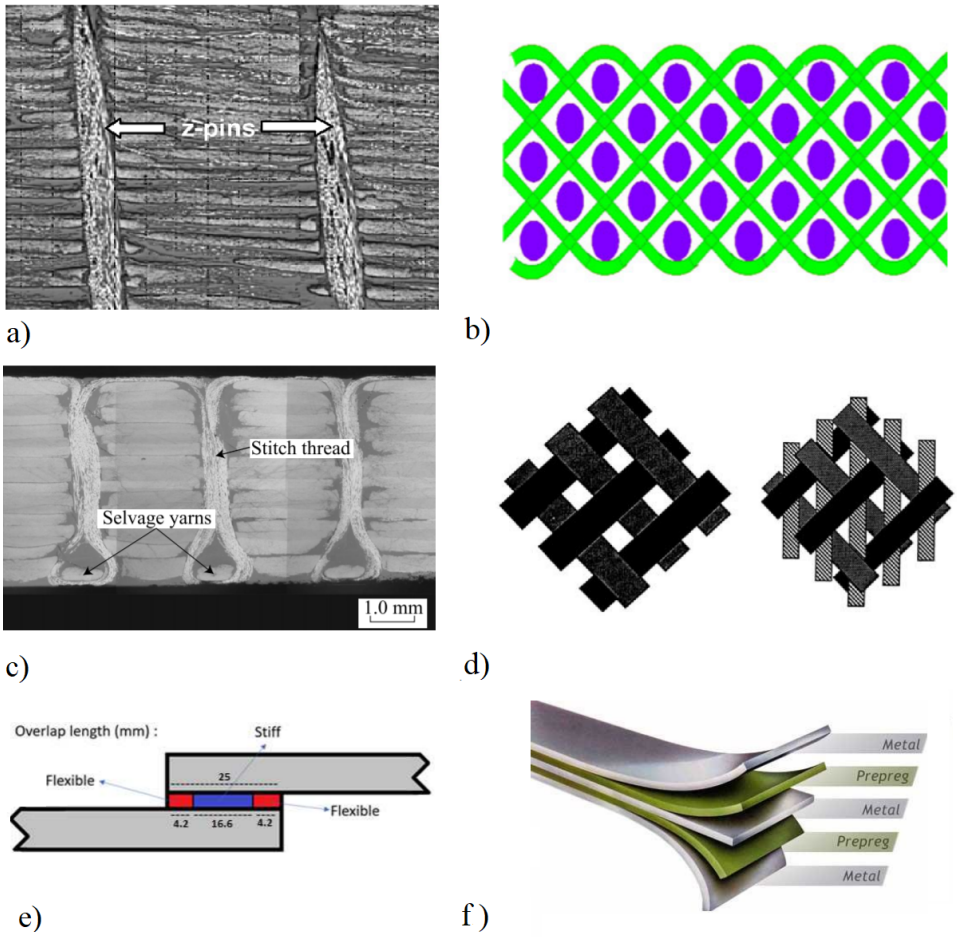

Figure 10: Delamination prevention methods: a)Z-pin [30]; b) 3d Weaving [31]; c) Stitching [32]; d)Braiding [33]; e)Mixed adhesive joint [34]; f) Fibre Metal Laminates [35]

The main delamination prevention methods are:

- Z-pins – this technique introduces small pins, either fibrous or metallic, in the through thickness direction of the composite, holding the laminate plies together by a combination of adhesion and friction [30].
- 3D weaving - reinforcement of the interlaminar properties by creating complex three dimensional dry fibre preforms before applying the resin [31, 33].

- Stitching - embedding of stitch threads in the through-thickness direction, bridging delamination cracks [32].
- Tufting - a single side stitching approach. A needle inserts a tow through the layers of the dry fabric. The loop of yarn is held in place only by the friction of the fibres and the textile [36].
- Braiding - Intertwining multiple fibres by braiding [33].
- Z-anchoring - A variant of the Z-pin method, using vertical or angled pins with flattened ends at the surfaces of the composite, thus increasing pull-out strength [37].
- Mixed Adhesive Joints (or functionally graded adhesive joints) - Using a more flexible adhesive at the ends of the overlap reducing peel stresses in that critical section [21, 34].
- Optimising adhesive joint geometry - adding tapered sections or reducing the adherend thickness near stress critical areas, decreasing overlap etc. [21, 38].
- Inter-plies - use of thermoplastic plies between dissimilar materials like steel and CFRP in hybrid adherends to facilitate adhesion in the interface [39].
- Fibre Metal Laminates - use of metal laminates to reinforce the composite transversal properties

Some techniques, like 3D weaving, stitching, braiding, tufting and z-anchoring, while successful at reducing delamination cannot be applied to prepreg laminates, requiring the reinforcement to occur before the resin is infused in the fibres, thus greatly reducing their real-world applicability, since most Fibre-Reinforced-Plastics used in the industry are in the prepreg format [30]. Furthermore, the complexity of the reinforcement by any of these techniques would significantly increase the cost of the final product parts [38].

Unlike the previous methods, Z-pinning is effective in increasing delamination resistance and can be used in the reinforcement of prepreg laminates. Some automatised insertion methods have already been designed, possibly enabling large scale productions, figure 11. The technique was used in the F/A-18E/FSuperhornet, a Boeing fighter [28,30].

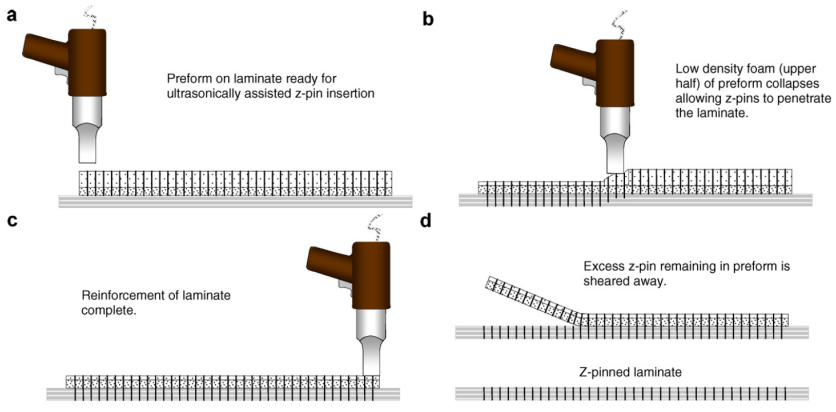

Figure 11: Schematic of the UAZ® process (adapted from Mouritz 2007) [30]

However, the use of Z-pins can have an adverse effect on in-plane mechanical properties like the elastic modulus, strength, and fatigue performance of the materials [30,38], though Mouritz (2007) notes that the worsening of mechanical properties is dependent on a variety of factors like volume content of zpins and the directional orientation of the plies suggesting that the benefits could outweigh the drawbacks in certain applications [30].

The use of Metal Laminates to reinforce the transversal direction of the composite created a hybrid metallic composite material group known as Fiber Metal Laminates (FML), and inspired the configurations studied in this thesis. They can easily be used with prepregs, stacking metal sheets just as they would for a composite prepreg ply. Several studies have shown their potential for delamination prevention for quasi-static conditions [6,40,41] and this study sets out to further develop the concept and characterise its impact behaviour in a single lap joint.

Given the importance of FMLs for the project the next sub-chapter is dedicated to their history, concept, configurations, unique material properties and possible applications.

2.3 Fibre Metal Laminates

Concept

When, after World War II, bonded Aluminium layers used on the dutch aircraft Fokker F-27 wings were found to have good fatigue resistance properties because adjacent intact layers bridged a fatigue crack on a damaged layer, significantly slowing down the crack propagation, the idea of using laminated materials to improve fatigue properties was born [42].

Fibre Metal Laminates were created in the 1980s at the Delft University of Technology attempting to combine properties of both composite materials and metals. The first attempt, known as ARALL - Aramid Reinforced ALuminium Laminates, was produced by alternating thin Aluminium alloy sheets and Aramid prepreg layers [42, 43].

Later, and with a patent submitted, in which the history of FMLs and the intent of using it in structural component of aircrafts is still very noticeable, figure 12, the same principle was used to develop other configurations with reinforcements like glass and carbon fibres, GLARE and CARRALL respectively [42] [44].

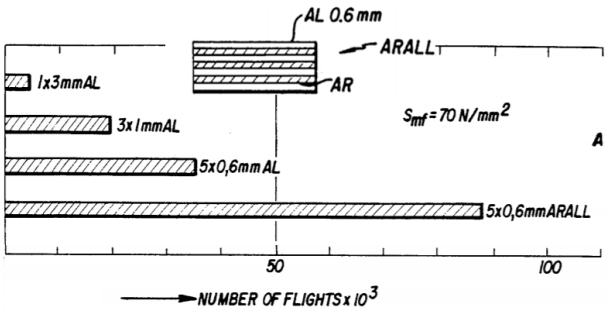

Figure 12: Configuration comparison per flights completed (Adapted from US Patent US4489123A) [44]

Fibre Metal Laminates made a reputation for themselves for being highly damage tolerant while having a high weight saving potential [43]. In addition to the excellent fatigue resistance, figure 13, further research and development of this concept revealed additional advantages like fire and corrosion resistance.

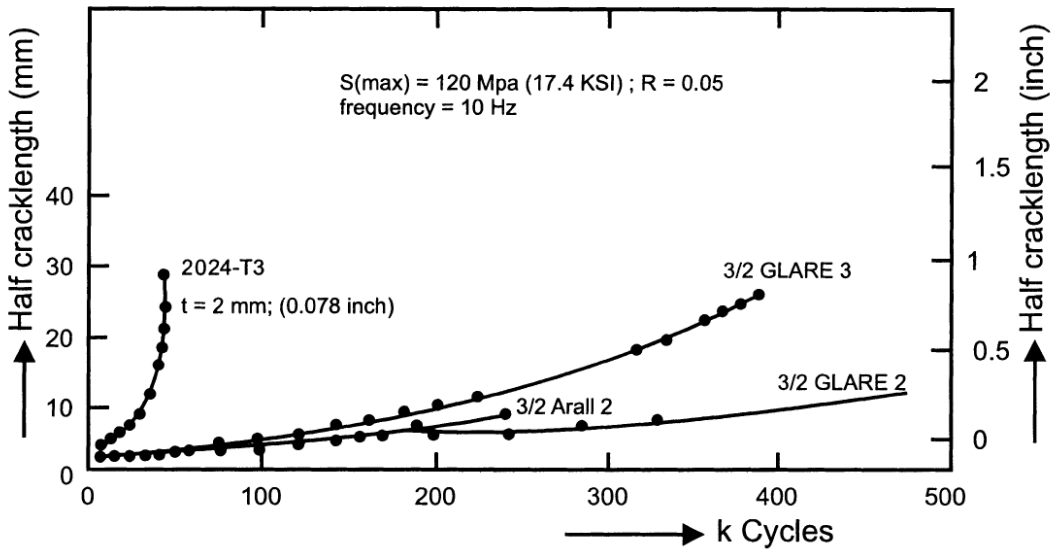

Figure 13: Crack propagation of GLARE vs Al alloy 2024 T3 [43]

In 1988, Aloha Airlines Flight 243, operated on a Boeing 737, suffered an explosive decompression in mid-air. A large section of the roof was torn off, but the crew managed to land the airplane in a nearby airport. The dramatic incident was attributed to an inadequate maintenance program that failed to detect "significant disbonding and metal fatigue damage" that eventually led to structural failure [45].

Asundi (1997) lists three possible solutions to prevent similar incidents: shortening inspection periods which would result in higher maintenance costs and a less effective use of the aircrafts; a decrease of the allowable design stresses which would increase the overall weight of airplanes negatively affecting fuel consumption and the maximum payload weight; and finally the development of "new aircraft materials with a better fatigue resistance and preferably a higher specific strength and lower density" [46].

It is this last suggestion that reflects the desire for materials like Fibre Metal Laminates with their high strength, low density, fatigue resistance and impact damage tolerance to be implemented in the aeronautics industry in possible application areas shown in figure 14 [46].

FML Impact Properties

As a hybrid material, these properties are dependent on several parameters like materials used, the direction of the fibre reinforcement and the metal-composite ratio. A comprehensive diagram of these parameters can be seen in figure 15. The same variables also play a role in the quasi-static properties of the material.

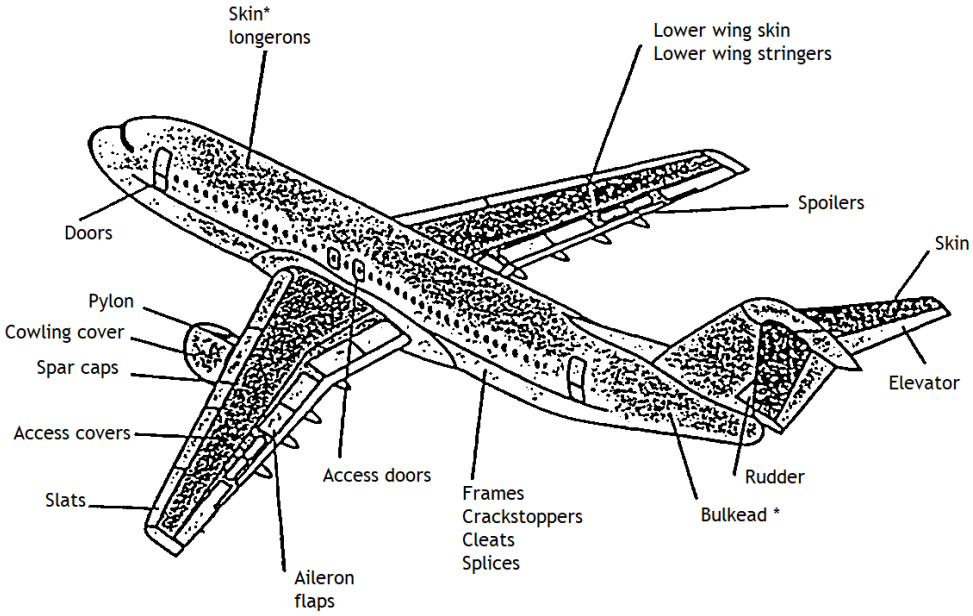

Figure 14: Possible areas of application of FMLs in aircraft construction [46]

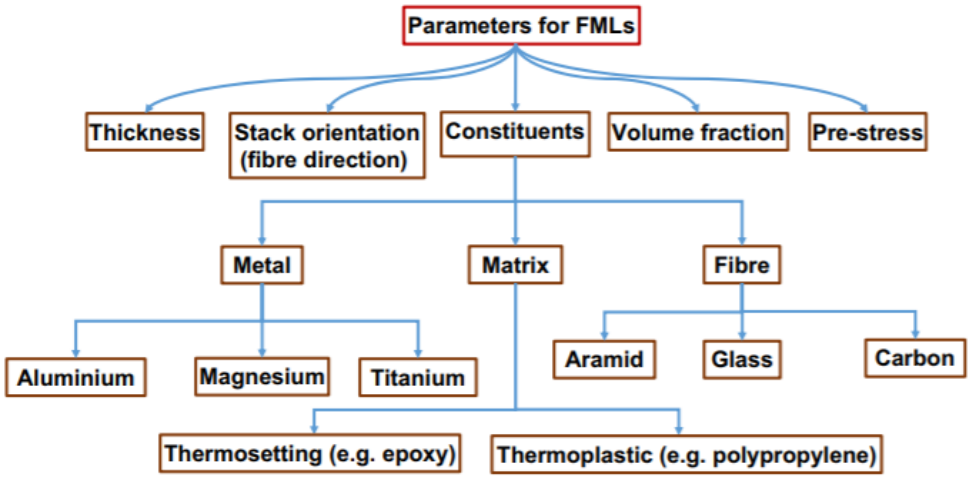

Figure 15: Parameters that influence FMLs mechanical properties [10]

Nevertheless, FML properties have been studied both for low velocity and high-velocity impact testing [8–12, 47–49]. Aluminium alloys like 2024-T3 have been shown to have the best properties under impact due to their stiffness and ductility.

Despite other advantages, titanium and magnesium have been tested but did not surpass the aluminium performance and steel is normally considered too heavy for effective use in aircraft and, as such, there has not been extensive research into its contribution to the impact properties of Fibre Metal Laminates [10]. They could more easily be implemented in the automotive industry, with modern high strength steels.

The fact that these materials use post-stretching of the aluminium sheets, delamination, matrix cracking and fibre-bridging as energy-dissipating mechanisms increases their overall impact resistance [10]. They are considered to have excellent energy-absorption characteristics, especially in high-velocity impact conditions [48].

Some of these mechanisms, for an impact test of a CFRP-Aluminium FML configuration, are shown in Figure 16.

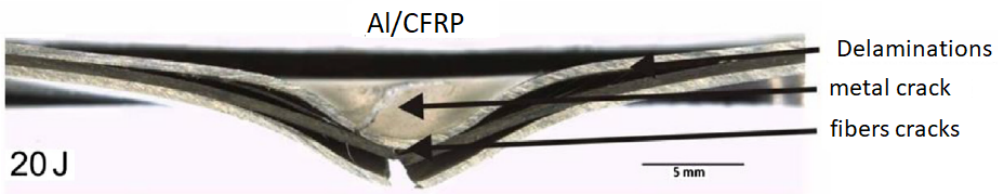

Figure 16: Cross section of an impacted CFRP-AL FML [10]

2.3.1 Adfeup contribution

ADFEUP, the Adhesion Research and Development group at the Faculty of Engineering of the University of Porto (FEUP), has been researching the use of Fibre Metal Laminates in bonded joints since 2015.

Using a combination of numerical modelling and experimental testing, the research was mainly focused on the optimisation of single lap joints for a quasi-static loading, varying parameters like the metal laminate material, laminate thickness, metal to composite percentage volume, configuration of the joint and adhesive used [6, 41, 50, 51].

The culmination of this research resulted in the publication of one published scientific article: "Reinforcement of CFRP joints with fibre metal laminates and additional adhesive layers" and one article under preparation, "Strength of hybrid laminates aluminium carbon-fibre joints with different layup configurations".

With this thesis, the group intends to widen the study of bonded FML joints to low-velocity impact scenarios.

This is especially important because while there have been a number of studies regarding impact properties of FMLs in the last decades, most of them focus on the properties of the material alone, varying parameters like the materials used and geometry [8–12, 47–49], this project aims to analyse its behaviour in a bonded joint, possibly the best joining method for the material in question.

2.4 Joint Strength Prediction

The ability to accurately predict the failure load of a joint when designing it is crucial for the widespread use of adhesives in structural applications. As such various joint strength prediction models both analytical and numerical have been proposed. The applicability of some of these methods is limited to certain scenarios due to specific considerations and simplifications of the model.

While the methods presented here are some of the most used, or historically relevant solutions, there are a multitude of others more complex taking into consideration any combination of material linearity (adhesive and adherend), adherend's properties (isotropic, anisotropic, dissimilar adherend etc) or stresses involved (shear/peel).

2.4.1 Analytical Solutions

Linear elastic

The simplest analysis for a single lap joint. For this analysis, only shear deformations are considered for the adhesive and the adherends are assumed to be rigid. Consequently, for this method, shear stresses are constant along the overlap, which, realistically, is not the case.

The shear stress, τ, is given by the following equation,

$$\tau = \frac{P}{bl} \tag{1}$$

Where P is the load, b the joint width and l the length of the overlap.

Volkersen

In 1938, Volkersen, developed a model considering only shear deformations in the adhesive but allowing for elastic deformation in the adherends, introducing the concept of differential shear seen on figure 17 [52].

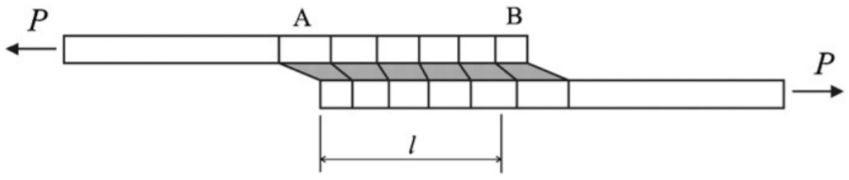

Figure 17: Graphic representation of Volkersen's analysis [53]

Because of the differential deformation along the overlap seen in the previous figure, with maximum deformation for point A and zero for B, assuming continuity of the adhesive/adherend surface, a non-uniform stress distribution along the overlap, with maximum values at the ends of the overlap and the opposite in the middle will develop [53].

Goland-Reissner

Goland and Reissner's method was the first to consider the bending moment and the transverse load caused by an eccentric load path, figure 18. This was especially important for single lap joints in which, for greater overlap lengths a degree of bending deformation of the adherends is very noticeable.

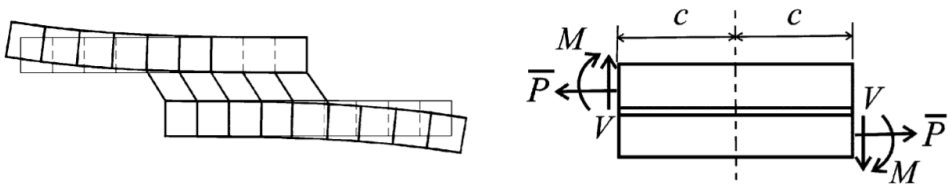

Figure 18: Graphic representation of the Goland-Reissner method [53]

The bending moment will force the joint to rotate in order to align with the direction of loading, creating a nonlinear geometrical problem, forcing the consideration of large deflections of the substrates [53].

The resultant peel-shear stress distributions can be seen in figure 19. Compared to Volkersen's method, Goland-Reissner predicts higher shear stress at the ends of the overlap and a peel component of the adhesive stress distribution.

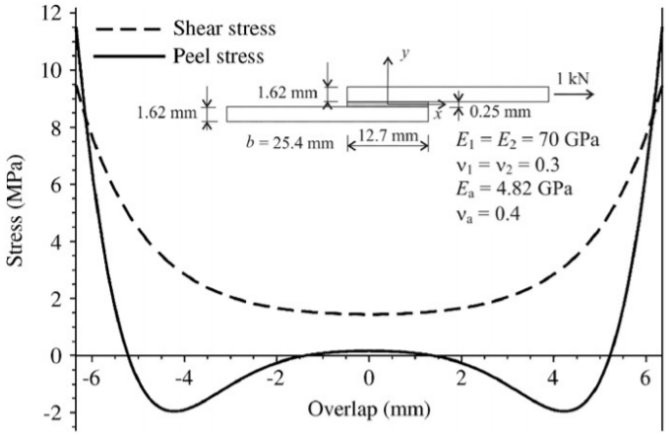

Figure 19: Goland and Reissner's method shear and peel stress distributions [53]

2.4.2 Numerical Solutions

Numerical techniques take advantage of the recent surge in computing processing power available and computational mechanics for engineering aiding purposes.

As previously seen, the analytical models become increasingly complex with attempts to incorporate relevant aspects to the behaviour of adhesive joints. This can be further complicated with the introduction of composite or dissimilar substrates, mixed adhesive joints or other optimisation techniques like adhesive filleting and substrate tapering.

With numerical approaches like the finite element method solutions for complex problems can be calculated, figure 20.

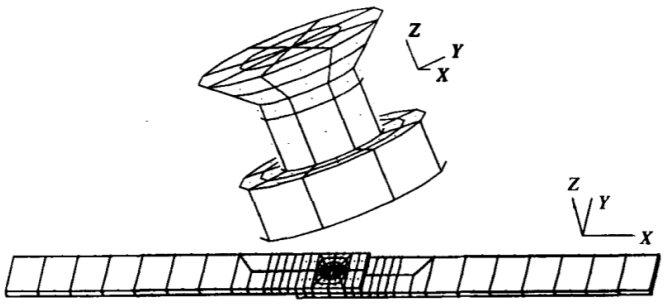

Figure 20: Finite element model of a countersunk riveted joint [54]

Continuum Mechanics vs Fracture Mechanics

Continuum mechanics apply closed-form analytical models to the Finite Element Method, calculating the stresses and strains along the bond. The joint is modelled with continuum elements and assuming a perfect connection between adherends and adhesive [55, 56].

Stresses and strains calculated in the adhesive are then compared to the material mechanical properties to determine if failure has occurred, according to a failure criterion like maximum stress or maximum strain [57]. However, these calculations are very dependent on the mesh and singularity points like the corners of the overlap [56].

Unlike Continuum Mechanics, Fracture Mechanics assumes a non-continuous body and the pre-existence of cracks or other defects like debonding and delamination that will be stress concentration points, likely to result in the failure of the joint [26, 58].

It is only valid under elastic deformations and the crack propagation is said to occur when the strain energy release rate (G), the energy at the tip of the defect, is equal or greater to the critical release rate energy (Gc), the material resistance to crack propagation [56, 57].

Cohesive Zone Modelling

Cohesive Zone Models (CZM) combines continuum mechanics, for damage initiation, and fracture mechanics, for crack propagation purposes. As such, a cohesive zone numerical model does not require the introduction of an initial crack or any user intervention for crack propagation. Instead, the user only needs to assign cohesive elements to areas deemed critical, where failure is likely to occur [59].

Hillerborg et al. established laws of traction-separation, describing the material's behaviour in two distinct stages: the first is based on the elastic properties of the material and reflects the loading of the element up to a maximum critical load, and the second is related to damage simulation, the degradation of the ability of the adhesive to resist separation, eventually leading to complete failure and element deletion [57, 60]. The evolution of the damage process zone, and its relation to a traction-separation law is represented in figure 21.

Cohesive laws can have various shapes, the most common being triangular and trape-

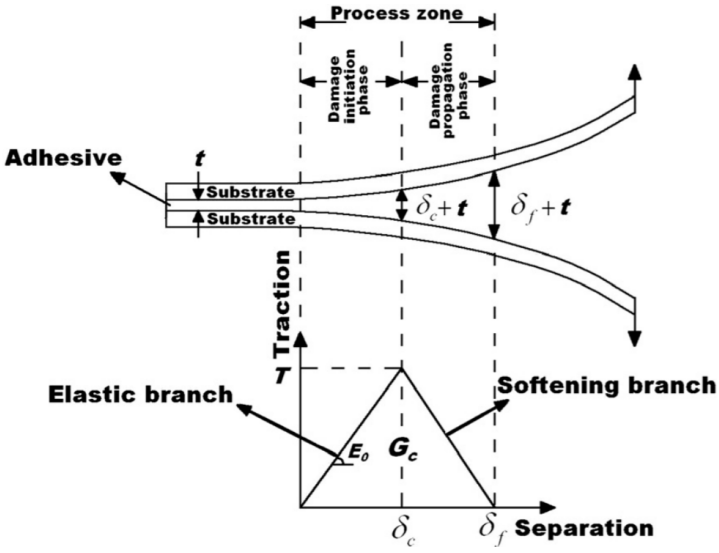

Figure 21: Damage process zone of a triangular traction-separation law [61]

zoidal laws, figure 22. To achieve a traction-separation law that accurately predicts the adhesive behaviour, material properties like stiffness, strength and fracture energies in mode I and mode II must be obtained by experimental fracture tests.

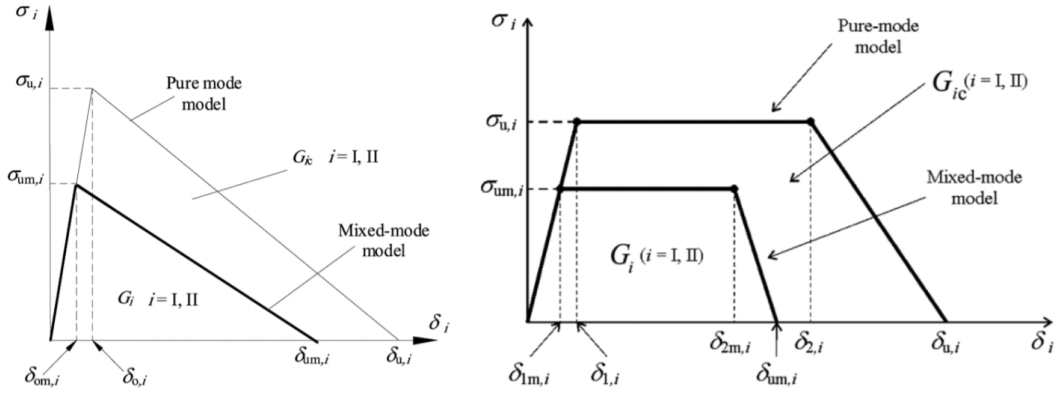

Figure 22: Triangular and Trapezoidal Traction-Separation laws [58]

This approach results in a progressive gradual failure typical of damage mechanics. CZM is currently seen as the most adequate numerical technique to study adhesive joints [57] .

Additionally, for adhesive joints with composite adherends CZM can be used to simulate delamination. There are some “independent” failure criteria for Fibre-Reinforced Plastics like Maximum Stress, Maximum Strain, Tsai-Hill, Tsai-Wu, Hashin etc., but although they are successful for some failure modes like fibre fracture or matrix cracking there is no criterion applicable to delamination [62].

Delamination in composites can be simulated numerically by the placement of cohesive elements, with the FRP material cohesive properties, between composite elastic layers, treating the bonding between plies similarly to an adhesive joint of two solid materials [62].

2.5 Impact Loadings

The strength of adhesive joints under impact loading is extremely important because of the interest that industries like the aeronautics, aerospace and automotive have taken in the technology.

For these applications impact loading scenarios are abundant and, consequently, the manufacturers must have sufficient theoretical and experimental knowledge on the behaviour of adhesives and adhesive joints for the different impact loading conditions, in order to consider them for their projects.

Even though impact loads are seen as exceptional, sporadic, unpredictable and out of normal service conditions for the majority of the projects there can be situations in which the impact is part of the normal functioning of the structure. As a result, while for the first case there is a bigger emphasis on minimising damage and absorbing energy, and the joint could be designed to fail a certain way under impact, for the latter case the design requirement may be that no damage should be observed in a singular occurrence, and that the joint has sufficient impact fatigue resistance to perform throughout its service life.

Because adhesives are very strain rate dependent, the impact study of adhesives is normally divided into three subcategories – low-velocity, medium velocity and high-velocity impact. A concrete defined speed limit to these categories does not exist but since the test procedures and machines used for each of them are very different it is common to associate them to the machine used.

For example, low velocity impact is associated with tests performed by a pendulum under 10 m/s, medium velocity with speeds up to 10 m/s using drop-weight machines and high-velocity tests can reach testing speeds 100 m/s by using a Split-Hopkinson-Pressure-Bar tester.

Low to mid velocity impact can replicate instances of tool dropping during manufacture/maintenance, hits to aircraft fuselage by maintenance trucks or movable stairways and low-velocity car collisions while high velocity impact testing can simulate bird/hail strikes in aircrafts, figure 23, or high-speed crashing in automobiles [7, 8].

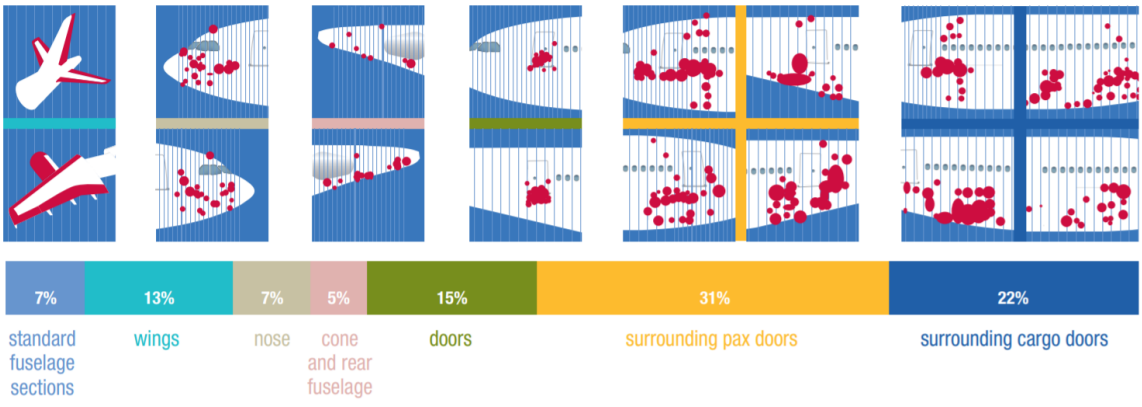

Figure 23: Global percentage of impacts by zones on an Airbus A320 [63]

Impact tests can be also divided in relation to the type of solicitation: compression, tension or torsion.

Finally, Harris and Adams [64] demonstrated in 1985, that the performance of a joint, especially regarding energy absorption, is more dependent on the choice of the substrate than the adhesive. In fact, he argued, that it is mostly the plasticity behaviour of the adherend that determines the failure load and energy absorbed, if a strong ductile adhesive is used. The study goes on to conclude that from the use of high strength substrates result high failure loads with low energy absorption while ductile substrates deliver lower failure loads with higher energy absorption [64].

3 Experimental Procedures

3.1 Adhesives

The two adhesives used in this study were: the 3M Scotch Weld AF 163 2K and Nagase Denatite XNR6852E-3. Although they are both epoxy-based structural adhesives, they are very different substances in respect to their use and mechanical properties.

3M Scotch Weld AF 163-2k is a "thermosetting modified epoxy structural adhesives in film form" [65]. The film form with knit-supporting made it ideal for application in ALR joints, with a clean manufacturing process and easy control of the bondline thickness. This adhesive was used for both CML and ALR joints.

The Nagase Denatite XNR 6852 E-3 is an adhesive from the Denatite^{TM} Epoxy Resin Series by Nagase-ChemteX designed for CFRP-CFRP and CFRP-Metal interfaces. It is marketed for the automotive and aerospace industry, and was used only for CML joints.

The cure cycles for both adhesives are presented in figures 24 and 25.

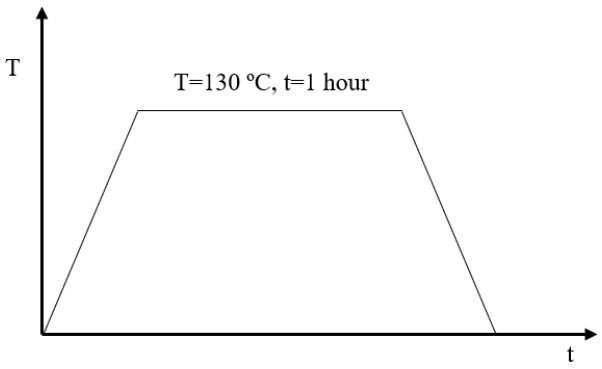

Figure 24: Cure cycle for adhesive 3M^{TM} Scotch-Weld^{TM} AF 163-2K

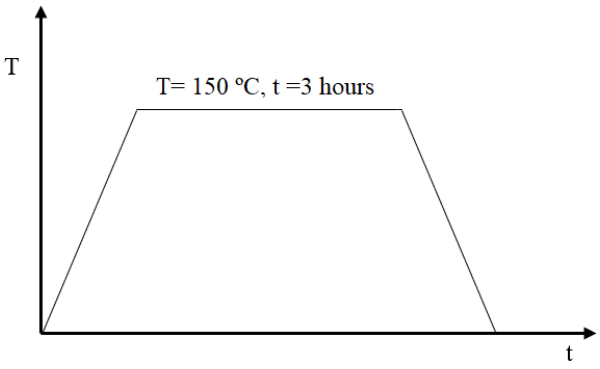

Figure 25: Cure cycle for adhesive Nagase Denatite^{TM} XNR 6852E-3

For the Nagase Denatite XNR 6852 E-3, having previously been used extensively by ADFEUP, the properties, for both quasi-static and impact conditions, were already determined.

However, for the adhesive AF 163-2K, only the adhesive properties for quasi-static conditions were previously determined by Palmares (2016) [41] and Santos (2018) [6].

The impact properties had to be obtained for the traction-separation law of the cohesive sections of the numerical study. To characterise the adhesive for a low-velocity impact testing speed of 3m/s Thick Adherend Shear Test (TAST), Double Cantilever Beam (DCB)and End Notched Flexure (ENF) tests were performed. The DCB and the TAST were performed at the required velocity, but excessive deformation of the adherends prevented the direct characterization of the fracture energy in mode II for that speed. Instead, ENF tests were done for an intermediate crosshead velocity of 100mm/min and logarithmically extrapolated for 3m/s. The extrapolation of fracture energies using a logarithmic relation was first proposed by Zgoul and Crocombe [66] and later validated by Avendaño et al. [67].

3.1.1 TAST

TAST specimens were manufactured in accordance to the ISO 11003-2 standard [68], concerning test methods of an adhesive shear behaviour. The specimen geometry, which can be seen in figure 26, creates an adhesive bond area of 162.5 mm^2.

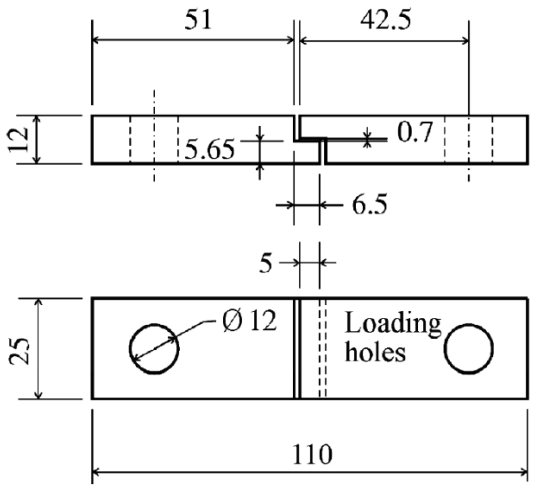

Figure 26: TAST specimen geometry [69]

The calculation of the shear modulus and maximum strain was not possible to be obtained because the linear-elastic behaviour was not captured in a satisfactory manner by the data acquisition system.

3.1.2 DCB

The geometry of the DCB specimen is shown in figure 27. Steel adherends are used to minimise the effect of plastic deformation during the test loading.

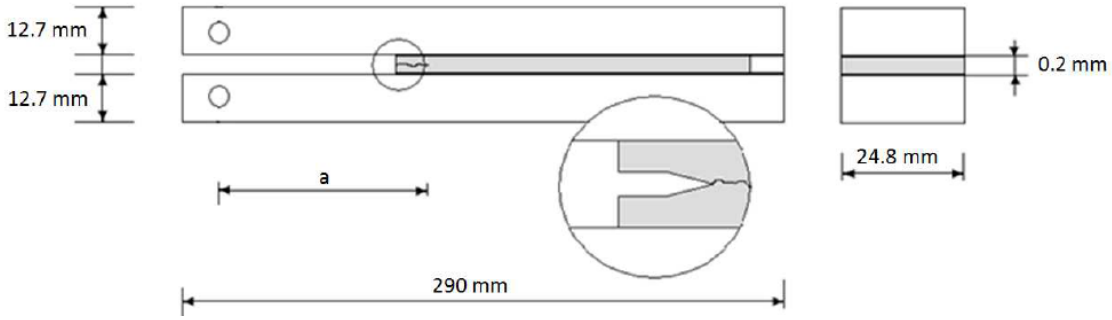

Figure 27: DCB and ENF specimen geometry [40]

To promote a good adhesion the surface of the adherends the surface was grit blasted and de-greased with acetone.

To control the thickness of the adhesive layer, even though the adhesive being tested had knit supporting capabilities, additional precautionary measures were taken by adding calibrated steel spacers at the ends of the bonded area.

At the crack initiation zone, and in between the steel spacers a sharp blade was placed, introducing a pre-crack in the adhesive layer at mid adhesive thickness. The specimen was then pre-loaded for a short period of time until crack propagation occurred. With this procedure, the effect of a blunt crack is minimized. The length of the crack initial length was then measured.

The difference between DCB and ENF tests is the load application method. To replicate pure peel mode I loading the specimen is loaded in the direction perpendicular to the adhesive layer for DCB testing, as shown in figure 28

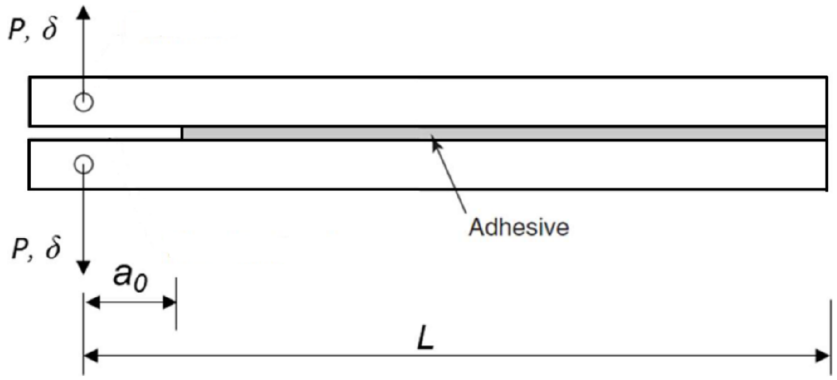

Figure 28: Schematic representation of a DCB test

For the low velocity impact testing speed of 3m/s, 3 specimens were tested using a drop-weight machine. A cohesive failure was obtained.

During crack propagation, the values of the load (P) and displacement (δ) were recorded, the first by the machine's load cell and the second indirectly by the integration of the loads obtained. The displacement data was further validated with the help of high-speed camera footage, 29.

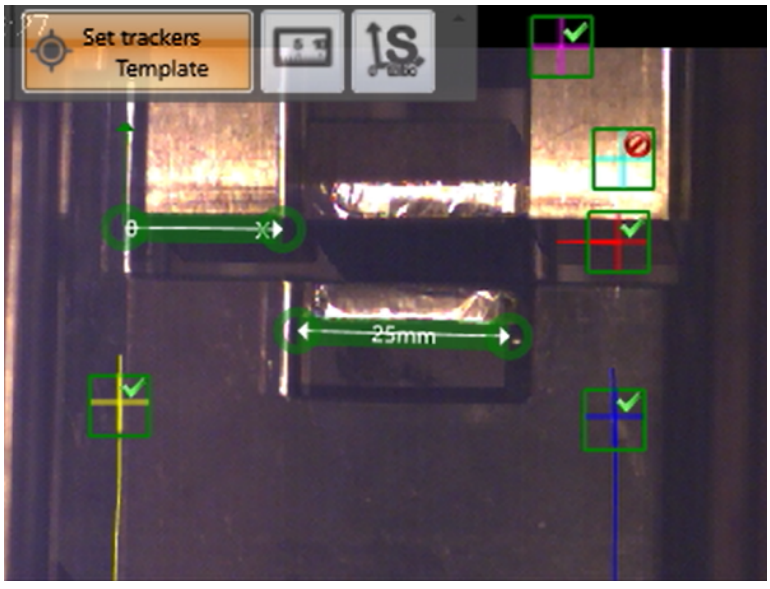

Figure 29: High-Speed Camera footage of DCB testing

Using the Compliance Based Beam Method (CBBM) data reduction scheme developed by de Moura et al. (2008) [70], that introduced a crack equivalent concept to DCB testing, the fracture energy in mode I could be calculated without measuring the crack length throughout the test duration, something impossible to do for impact testing. G_{IC} was obtained using the following expression

$$G_{\mathrm{Ic}} = \frac{6P^2}{B^2 h}\left(\frac{2a_{\mathrm{e}}^2}{h^2 E_{\mathrm{f}}} + \frac{1}{5G_{13}}\right) \tag{2}$$

where, E_f and G_{13} are, respectively, the corrected bending modulus and shear modulus of the specimens and a_{eq} is the equivalent crack length, estimated from the specimen compliance. B and h are specimen geometry parameters, the width of the specimen and the height of the adhesive layer respectively. P is the load obtained from the load-displacement curve.

3.1.3 ENF

ENF tests use the same specimen geometry as DCB. To induce shear stresses in the adhesive layer, three point bending loading is applied. A schematic representation of the test can be seen in figure 30. However, this test was not possible to be performed for the velocity required, 3m/s, due to excess plastic deformation of the steel specimens.

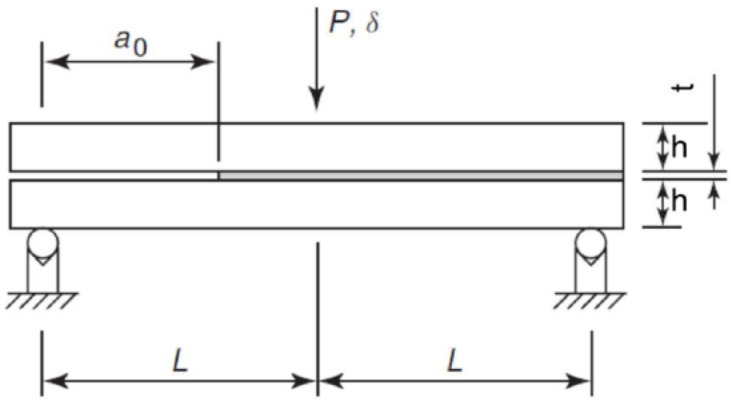

Figure 30: Schematic representation of an ENF test

The fracture energy in mode II of 3 specimens was determined for a crosshead test speed of 100mm/min for, which in conjunction with the previously determined fracture toughness for quasi-static conditions, enables the logarithmic extrapolation of the G_{IIC} for 3m/s. The extrapolation of fracture energies using a logarithmic relation was first proposed by Zgoul and Crocombe and later [66] validated by Avendaño et al. [67].

The CBBM method for ENF specimens [71] was used. Just like for mode I, CBBM for ENF testing also does not require the measurement of the crack length. The fracture energy in mode II was calculated using the following expression

$$G_{IIc} = \frac{9P^2 a_{eq}^2}{16B^2 E_f h^3} \tag{3}$$

Despite the choice of an intermediate speed to reduce the plastic deformation of the adherends, the complete elimination of the phenomenon was not possible.

3.2 Adherends

The materials used in the adherends for the studied joint configurations were chosen for their common use in applicable industries.

For the composite parts of the joints, Carbon Fibre Reinforced Plastic supplied by CIT Composite Materials from Italy in a prepreg roll of 600 mm by 15m was used. The product is sold under the name HS 160 T700 and is a 0° oriented carbon-epoxy composite.

The CFRP elastic orthotropic properties were previously determined by Campilho et al. 2005 [72] and can be found on table 1.

Table 1: CFRP elastic orthotropic properties [72]

Ex (MPa)	**Ey (MPa)**	**Ez (MPa)**	**νxy**	**νyz**	**νxz**	**Gxy (MPa)**	**Gyz (MPa)**	**Gxz (MPa)**
109000	8819	8819	0.342	0.342	0.38	4315	4315	3200

The Aluminium alloy used for the metal laminates in CML joints was from the 2024-T3 Alclad series, obtained in sheets of a thickness of 0.4 and 0.8 mm from AMI Metals in Belgium. The specific series was chosen for its use in aircraft construction for instance in the skin of aircraft, due to its tensile strength [73, 74].

The mechanical properties of this alloy are shown in table 2, obtained from stress-strain curves from tensile tests performed by Structures and Materials Laboratory of the Delft University of Technology, when they researched this alloy suitability for integration in GLARE, a type of metal laminates of glass fibre and a metal laminates.

Table 2: Mechanical properties of Al-2024-T3 Alclad Series [75]

Young's Modulus (GPa)	**Yield Stress (MPa)**	**Ultimate Stress (MPa)**	**Poisson's Ratio**	**Elongation (%)**
66	350	440	0.3	12

3.3 Single Lap Joints Manufacturing

The manufactured Single lap joints were based on the geometry shown in figure 31.

To study the performance of CML joints two adhesives were used: the 3M Scotch AF 163-2k and the Nagase Denatite XNR 6852 E3. For the second adhesive, 25 mm width

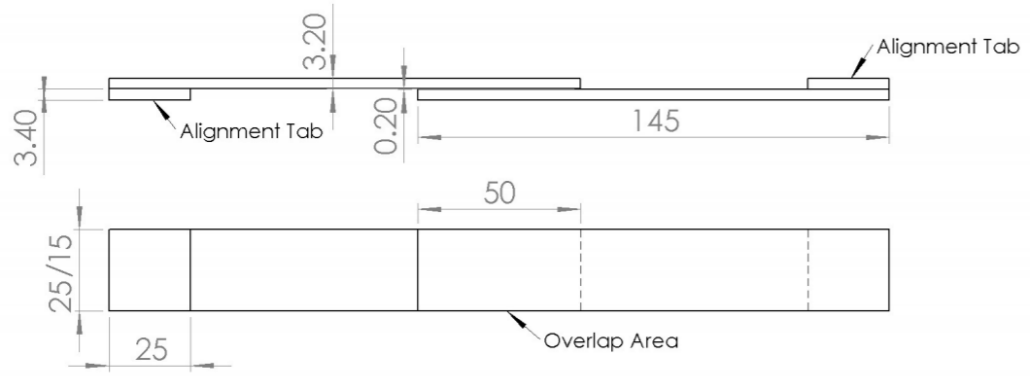

Figure 31: Single Lap Joint Geometry

specimens resulted in failure loads that were too high for the machine gripping system to test without slipping, figure 32, and thus it was decided that a reduction of the width to 15 mm was needed to bring down its strength in order to obtain a failure load level and mode. As such, single lap joints with 15 mm width were used for paper A [76], "Reinforcement of CFRP SLJs using Metal Laminates", on the use of metal laminates for CFRP single lap joint reinforcement.

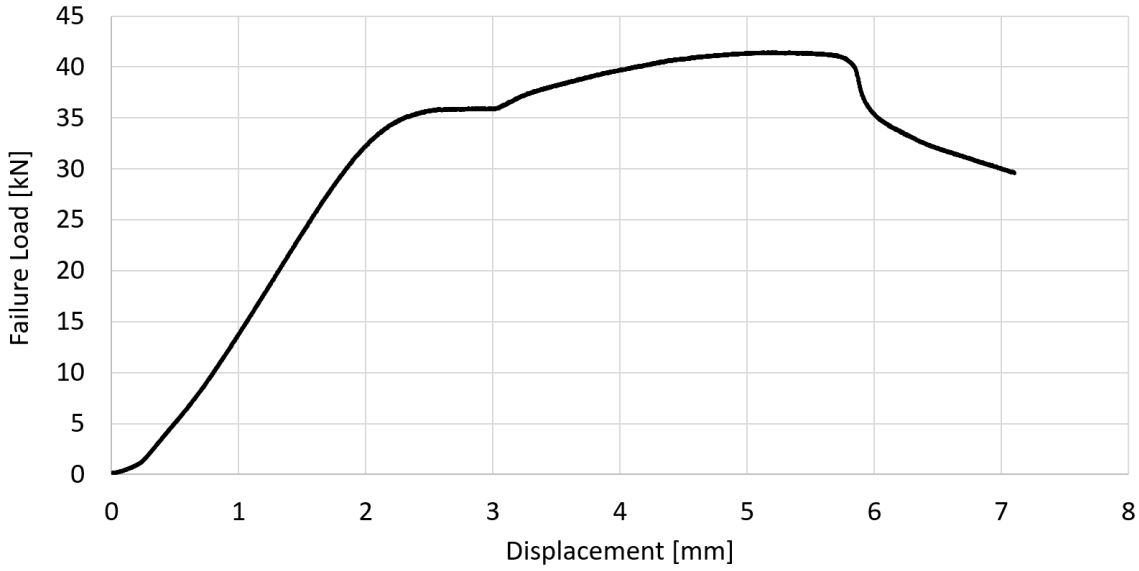

Figure 32: Nagase XNR6852 E-3 25 mm SLJ slipping

In paper B [77],"Reinforcement of CFRP Single Lap joints using Adhesive layers", the adhesively reinforced single lap joints the used adhesive AF 163-2k. Since this adhesive is not as strong as the Nagase XNR6852 E-3, joints with 25 mm width could be tested without problems.

Because of the knit-supporting capability of the film adhesive, the control of the adhesive layer thickness did not have to be very precise, production of the SLJs was done using a manufacturing mould based on the design presented in figure 33, with the specimens being cut later to their desired width.

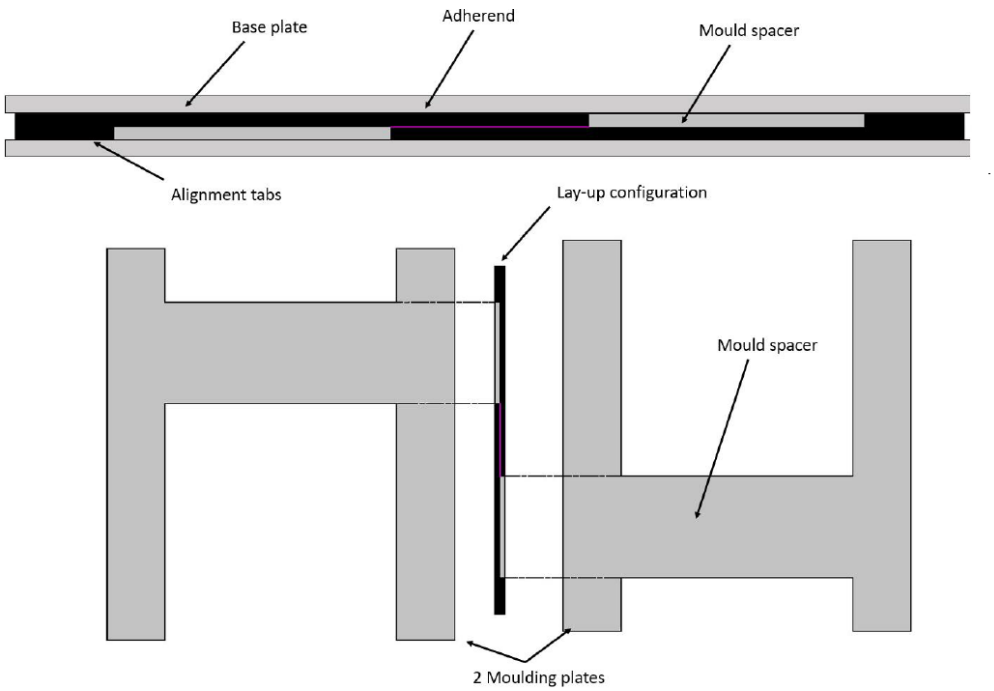

Figure 33: Manufacturing mould scheme [6]

Because XNR6852 E-3 is a paste adhesive without knit-support, and the cure temperature of this adhesive and the CFRP are more dissimilar, its joint substrates were manufactured first in one cure and then the single lap joints were assembled and cured in a second time (for the adhesive).

It was observed that the manufacturing method, i.e. curing the adhesive and substrate composite plies in one cure, or in two separate cures, had no significant effect on the mechanical properties of the CML joint for the AF163-2k adhesive. As such, for adhesives that offer knit supporting capabilities, the first manufacturing method is preferred, reducing manufacturing times and energy use.

The CML and CFRP-only SLJ configurations differ only in the through thickness direction, where two laminates of Aluminium occupy the tops of the adherends, reducing the number of CFRP plies used in order to maintain a comparable overall adherend thickness of 3.2 mm.

The joints with adherends superficially reinforced with adhesive layers were manufactured very similarly to CML joints. A single configuration with a layer of AF 163-2k adhesive (0.2 mm thickness) replacing a layer of CFRP composite ply (0.15 mm thickness) in the tops of the adherend was developed.

The other two configurations of interlaminar adhesive layer reinforced SLJs present in Paper B were developed by Gomes [6] in his master thesis. The experimental data used in the article for these was also a product of his work.

Since the newly suggested adhesively reinforced configuration, ALR, was the best performing out of the three, only this one was analysed for impact conditions and no manufacture of additional configurations proposed by Gomes took place.

3.4 Surface treatments

The process for the manufacture of the CML joints required some additional steps for the surface preparation of the Aluminium sheets. A previous study by Palmares (2016) [41], found that grit blasting and degreasing with acetone was insufficient to ensure a correct adhesion to the Aluminium laminates, resulting in a mixed cohesive-adhesive failure type for the quasi-static loading condition tested. As such, experimental tests between two Aluminium adherends were performed to find an improved surface treatment that would result on a good bond for this Al-Adhesive-Al interface.

The following procedures were studied:

- Phosporic Acid Anodising the surface according to the ASTM D 3933 standard,
- applying a sol-gel anodising replacement, the 3M^{TM} Surface Pre-Treatment AC-130-2,
- applying a primer, the Structural Adhesive Primer EW – 5000 AS.

The results can be seen in figure 34.

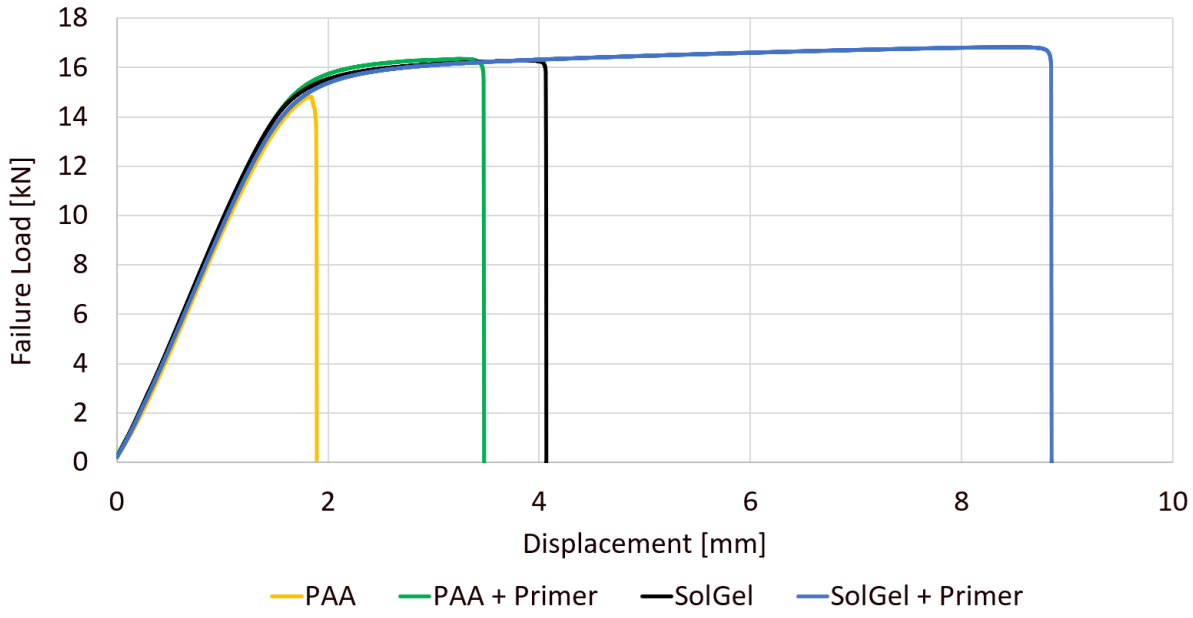

Figure 34: Al-Adhesive-Al Surface treatment study

Although the difference in surface treatments did not result in an increase in the failure load, this can be explained by the fact that the Aluminium substrates were being plastically deformed. The solution that provides the best bonding results for this Aluminium alloy will consequently be the one that produces the largest increase of the maximum displacement before failure. This was found to be the treatment of the surface with the sol-gel Phosphoric Acid Anodising Replacement Solution (3M^{TM} Surface Pre-Treatment AC-130-2), followed by the application of the Structural Adhesive Primer EW – 5000 AS by manually brushing it unto the surface.

3.5 Tensile Testing

For quasi-static conditions the single lap joints were tested using an Instron 8801 servo-hydraulic testing machine with a load cell of 100 kN at a constant crosshead speed of 1mm/min, according to the standard ASTM D5868 - 01(2014) "Standard Test Method for Lap Shear Adhesion for Fiber Reinforced Plastic (FRP) Bonding" [78].

The fixturing of the specimens was ensured using clamps that hold the free extremities of each specimen, using 4 bolts manually tightened with torque wrench. The torque was applied progressively, up to 108 N.m, ensuring an even clamping force. Dowel pins aligned the sample and the clamps.

After correcting the displacement measured by the machine, to take into consideration the compliance of the gripping system, the load-displacement curves could be plotted.

3.6 Impact Testing

For impact conditions, a drop-weight impact machine developed by ADFEUP was used [79]. This machine is capable of dropping a 56 kg mass off a maximum height of 1.27 m, achieving an impact speed of 5 m/s.

The impact speed used was 3m/s for a weight of 31.3 kg, resulting in an impact energy of 140.85 J.

The displacements were indirectly obtained by trapezoidal time integration of the load data, and further validated by using slow-motion footage obtained with a high-speed camera.

4 Summary of appended papers

4.1 Paper A

Paper A focus on the reinforcement of CFRP single lap joints using metal laminates as a delamination prevention technique. In this paper the performance of aluminium reinforced joints using two different epoxy-based adhesives is analysed for quasi-static and impact conditions. Numerical models are developed and validated against experimental data.

Paper A shows that using metal laminates to reinforce CFRP single lap joints is a viable method to reduce, and even avoid delamination. It is also demonstrated that a positive Composite Metal Laminate (CML) joint performance relies on a correct selection of the reinforcement thickness, which is dependent on the mechanical properties of the adhesive used.

4.2 Paper B

Paper B studies the possible role of additional adhesive layers as a reinforcement technique for delamination prevention in CFRP single lap joints. Several suggested configurations are experimentally tested for quasi-static conditions, and the reinforced joint with the best performance is impact tested. A numerical model is developed to study the behaviour of the best suggested joint in both quasi-static and impact conditions.

The adhesive reinforcement technique is shown to be advantageous in limiting delamination, and, depending on the loading condition, avoiding it altogether.

4.3 Thesis Summary

In addition to the conclusions reached in each paper , the combination of the findings of both independent papers allows the comparison of the two distinct approaches to the reinforcement of CFRP single lap joints.

This direct comparison is possible because the two methods were experimentally tested for the same joint geometry, 25 mm width, adhesive and loading conditions.

Paper A used smaller specimens, with 15 mm width, because 25 mm wide single lap joints would not fail for the second adhesive (XNR6852 E-3). In order to compare CML joints with ALR, without resorting to a joint strength analysis, additional 25 mm specimens of CML joints with 0.4 mm aluminium reinforcements using AF163-2K were manufactured and tested.

The performance of both reinforcement methods when compared to the reference single lap joint of carbon fibre reinforced plastic can be visualised in figure 35.

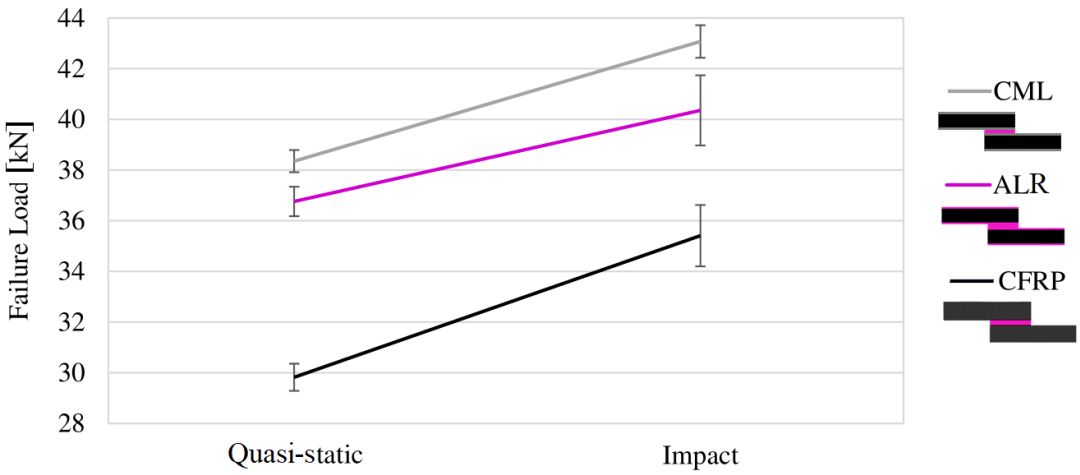

Figure 35: Reference CFRP vs CML vs ALR for the adhesive 3M Sotch Weld AF 163-2K

The use of a CML reinforced CFRP single lap joint saw the biggest improvement in the failure loads. The static failure load increased by 28.6% while the impact failure load increased 21.7%.

For the ALR single lap joints, the static and impact failure loads were increased by 23.27 % and 13.97 % respectively. Despite performing worse than CML joints, this technique could still be very interesting for the industry, as using the adhesive itself as reinforcement is logistically simpler, faster to manufacture and adds less weight to the reinforced joint.

Lastly, a good correlation between the numerical models and the experimental results was achieved for both loading conditions, not only regarding failure load prediction, as seen on figures 36 and 37, but also in respect to failure modes and load displacement curves.

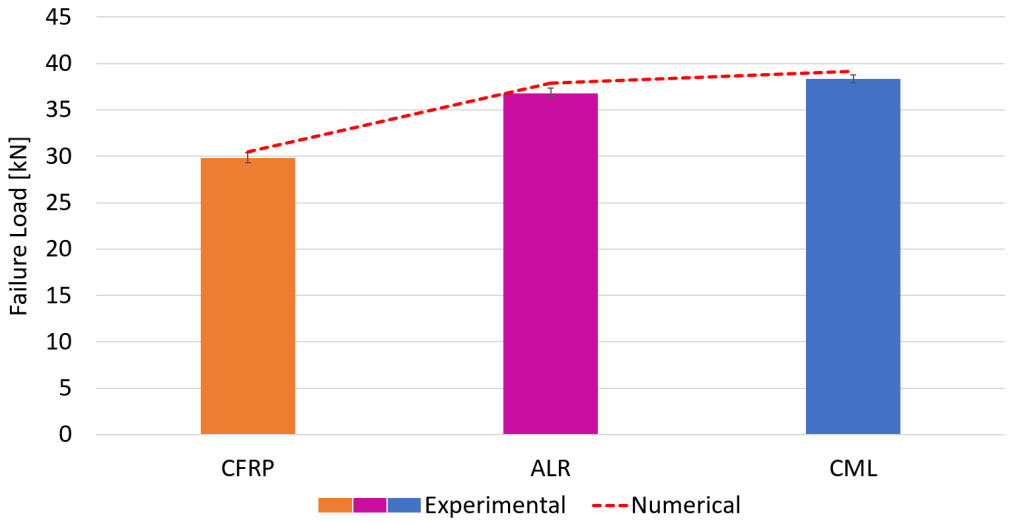

Figure 36: Comparison between FEA predictions and experimental results for quasi-static conditions

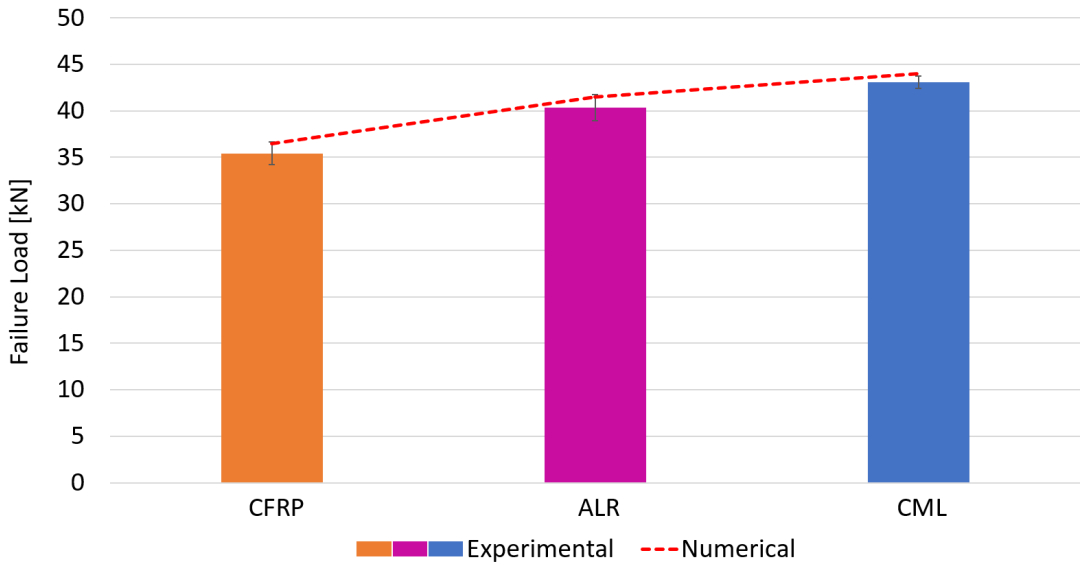

Figure 37: Comparison between FEA predictions and experimental results for impact conditions

5 Conclusions

The performance of two CFRP single lap joints reinforcement techniques as delamination prevention techniques was analysed for quasi-static (1mm/min) and impact (3m/s) conditions.

Numerical models using the finite element method were developed for the configurations studied. Cohesive zone modelling was used to simulate the behaviour of the adhesive and delamination in the CFRP adherends. The numerical models were later validated by experimental tests.

The first method used aluminium metal laminates as reinforcement. Two adhesives were used and it was demonstrated that the performance of this technique was heavily dependent on the mechanical properties of the adhesives used. A reinforcement configuration that successfully eliminated delamination for one adhesive, presented worse results than the CFRP-only reference joint for the other.

The effect of laminate thickness on the peel stresses at the interface was studied and a new configuration was proposed. A new joint configuration, with thicker metallic reinforcements, performed satisfactorily for both adhesives, completely eliminating delamination in one, and delaying its onset on the second, increasing the joint strength. Reinforced joints were also shown to have better energy absorption capabilities under impact loadings, with higher failure loads and maximum displacements.

The second technique used additional layers of adhesive used in the bonding of the joints to reinforce the composite substrates in the through thickness direction. For the best configuration of adhesively reinforced joints, known as ALR, the adhesive layers were placed on the tops of the adherends. The concept was very similar to that of a CML joint, instead of the stress concentration being formed near the overlap endings and then directly transmitted to a small area of the CFRP matrix the reinforcement would instead distribute them over a greater area.

As reinforcement, the AF163-2K adhesive was used, as more flexible adhesives behave better than stronger yet stiffer adhesives in delamination prevention.

Even though for quasi-static conditions ALR joints avoided delamination, the same did not happen for impact conditions, where delamination occurred. However, ALR joints still outperformed the reference CFRP-only joints in any other analysed criteria, with higher failure loads and increased maximum displacement.

For the same adhesive and conditions using CML joints as reinforcement appeared the more beneficial technique, but ALR has several advantages over CFRP like lower added weight and logistic ease of use, as the material used as reinforcement is already being used for non-reinforced standard joints. Ultimately, any of these reinforcement techniques would result in an improvement of the delamination resistance properties of a joint.

Lastly, a good correlation between the numerical models and the experimental results

was achieved for all configurations tested and loading conditions. The failure loads determined numerically were validated experimentally with minimal errors and the numerical failure modes correctly depicted the experimentally obtained failures.

6 Future Work

The work contained in this thesis could be improved by additional study into the following topics:

- Study the identified weak spot in CML reinforced joints, the Al-CFRP interface. An additional adhesive layer between the two could be implemented as both the Adhesive-CFRP and the Adhesive-Al interfaces are producing a stronger bond than the direct transition that uses only the resin of the CFRP matrix.
- Study the dynamic behaviour of both CML and ALR joints for higher velocity impact loadings, up to 100 m/s, using Split-Hopkinson Pressure Bar tests.
- Study the fatigue properties of both CML and ALR joints when compared to a CFRP-only SLJ
- Study the performance of CML and ALR joints for a different fibre reinforced plastic, for example glass fibres or aramid fibres.
- Analyse the effect of environmental degradation of CML and ALR joints

References

[1] The new-technology boeing 787 dreamliner, which makes extensive use of composite materials, promises to revolutionize commercial air travel. Technical report, Aviation Week & Space Technology Market Supplement, 2005.

[2] Airbus. Experience and lessons learned of a composite aircraft. ICAS2016, 30th Congress of the International Council of the Aeronatuical Sciences, 2016.

[3] Mrazova Maria. Advanced composite materials of the future in aerospace industry. *Incas Bulletin*, 5:139–150, 09 2013.

[4] Dow Automotive Systems. Structural Bonding of Lightweight Cars: Crash durable, safe and economical. https://www.dupont.com/transportation/structural-adhesives.html, 2019. [Online; accessed 28-May-2019].

[5] Aluminum, structural adhesive help boost cadillac performance and quietness, May 2013.

[6] Daniel dos Santos. Optimization of cfrp joints with fibre metal laminates. Master Thesis, Faculdade de Engenharia da Universidade do Porto, 2018.

[7] A. Vlot. Impact properties of fibre metal laminates. *Composites Engineering*, 3(10):911 – 927, 1993.

[8] Freddy Moriniere. *Low-velocity impact on fibre-metal laminates*. PhD thesis, Technische Universiteit Delft, 2012.

[9] A. Vlot. Impact loading on fibre metal laminates. *International Journal of Impact Engineering*, 18(3):291 – 307, 1996.

[10] Raj Das, Avishek Chanda, J Brechou, and Arnab Banerjee. Impact behaviour of fibre-metal laminates. pages 491–542, 02 2016.

[11] Ankush P. Sharma, Sanan H. Khan, Rajesh Kitey, and Venkitanarayanan Parameswaran. Effect of through thickness metal layer distribution on the low velocity impact response of fiber metal laminates. *Polymer Testing*, 65:301 – 312, 2018.

[12] Patryk Jakubczak, Jarosław Bieniaś, and Barbara Surowska. 12 - impact resistance and damage of fiber metal laminates. In Vijay Kumar Thakur, Manju Kumari Thakur, and Asokan Pappu, editors, *Hybrid Polymer Composite Materials*, pages 279 – 309. Woodhead Publishing, 2017.

[13] L.F.M. Silva, Andreas Öchsner, and R Adams. *Handbook of Adhesion Technology*, pages 1–7. 01 2011.

[14] David E. Packham. *Theories of Fundamental Adhesion*, pages 1–31. Springer International Publishing, Cham, 2017.

[15] Chapter 1 - introduction and adhesion theories. In Sina Ebnesajjad, editor, *Adhesives Technology Handbook (Second Edition)*, pages 1 – 19. William Andrew Publishing, Norwich, NY, second edition edition, 2009.

[16] R Adams and William C. Wake. Structural adhesive joints in engineering. 01 1984.

[17] Paul Peter Anthony Mazza, Fabio Martini, Benedetto Sala, Maurizio Magi, Maria Perla Colombini, Gianna Giachi, Francesco Landucci, Cristina Lemorini, Francesca Modugno, and Erika Ribechini. A new palaeolithic discovery: tar-hafted stone tools in a european mid-pleistocene bone-bearing bed. *Journal of Archaeological Science*, 33(9):1310 – 1318, 2006.

[18] Carraher C.E., Jr. *Introduction to polymer chemistry fourth edition.* 01 2017.

[19] F Chaves, L.F.M. Silva, Marcelo De Moura, David Dillard, and V H. C. Esteves. Fracture mechanics tests in adhesively bonded joints: A literature review. *The Journal of Adhesion*, 90:955–992, 11 2014.

[20] Anthony Kinloch. *Adhesion And Adhesives: Science And Technology.* Springer International Publishing, 1987.

[21] Lucas F M da Silva and R D Adams. Techniques to reduce the peel stresses in adhesive joints with composites. *International Journal of Adhesion and Adhesives*, 27(3):227 – 235, 2007.

[22] K.V.N. Gopal. 14 - product design for advanced composite materials in aerospace engineering. In Sohel Rana and Raul Fangueiro, editors, *Advanced Composite Materials for Aerospace Engineering*, pages 413 – 428. Woodhead Publishing, 2016.

[23] J.R. Fekete and J.N. Hall. 1 - design of auto body: Materials perspective. In Radhakanta Rana and Shiv Brat Singh, editors, *Automotive Steels*, pages 1 – 18. Woodhead Publishing, 2017.

[24] Corporate Research Centre EADS Deutschland GmbH. The research requirements of the transport sectors to facilitate an increased usage of composite materials. part i: The composite material research requirements of the aerospace industry, 2004.

[25] Tamer Sinmazçelik, Egemen Avcu, Mustafa Özgür Bora, and Onur Çoban. A review: Fibre metal laminates, background, bonding types and applied test methods. *Materials & Design*, 32(7):3671 – 3685, 2011.

[26] M Banea and L.F.M. Silva. Adhesively bonded joints in composite materials: An overview. *Proceedings of The Institution of Mechanical Engineers Part L-journal of Materials-design and Applications - Proc Inst Mech Eng L-J Mater*, 223:1–18, 01 2009.

[27] ASTM D5573-99(2012). Standard practice for classifying failure modes in fiber-reinforced-plastic (frp) joints. Technical report, ASTM, 2012.

[28] K. Pingkarawat and A.P. Mouritz. Improving the mode i delamination fatigue resistance of composites using z-pins. *Composites Science and Technology*, 92:70 – 76, 2014.

[29] Masaki Hojo, Keisuke Tanaka, Claes Göran Gustafson, and Ryuichi Hayashi. Effect of stress ratio on near-threshold propagation of delimination fatigue cracks in unidirectional cfrp. *Composites Science and Technology*, 29(4):273 – 292, 1987.

[30] A.P. Mouritz. Review of z-pinned composite laminates. *Composites Part A: Applied Science and Manufacturing*, 38(12):2383 – 2397, 2007.

[31] Prasad Potluri, Paul Hogg, Mubeen Arshad, Dhaval Jetavat, and Peiman Jamshidi. Influence of fibre architecture on impact damage tolerance in 3d woven composites. *Applied Composite Materials*, 19, 10 2012.

[32] Akinori Yoshimura, Tomoaki Nakao, Shigeki Yashiro, and Nobuo Takeda. Improvement on out-of-plane impact resistance of cfrp laminates due to through-the-thickness stitching. *Composites Part A: Applied Science and Manufacturing*, 39(9):1370 – 1379, 2008.

[33] P. Potluri, A. Rawal, M. Rivaldi, and I. Porat. Geometrical modelling and control of a triaxial braiding machine for producing 3d preforms. *Composites Part A: Applied Science and Manufacturing*, 34(6):481 – 492, 2003. ICMAC 2001 - International Conference for Manufacturing of Advanced Composites.

[34] J.J.M. Machado, P.M.-R. Gamarra, E.A.S. Marques, and Lucas F.M. da Silva. Improvement in impact strength of composite joints for the automotive industry. *Composites Part B: Engineering*, 138:243 – 255, 2018.

[35] Jia Xue. *Tensile strength and thermal residual stress of CARALL and UACS/AL laminates*. PhD thesis, 09 2012.

[36] G. Dell'Anno, J.W.G. Treiber, and I.K. Partridge. Manufacturing of composite parts reinforced through-thickness by tufting. *Robotics and Computer-Integrated Manufacturing*, 37:262 – 272, 2016.

[37] Ananth Virakthi, S Kwon, Sung Lee, and Mark Robeson. Delamination resistance of composite laminated structures reinforced with angled, threaded, and anchored z-pins. *Journal of Composite Materials*, 53:002199831880520, 10 2018.

[38] X Shang, EAS Marques, JJM Machado, RJC Carbas, D Jiang, and LFM da Silva. A strategy to reduce delamination of adhesive joints with composite substrates. *Proceedings of the Institution of Mechanical Engineers, Part L: Journal of Materials: Design and Applications*, 233(3):521–530, 2019.

[39] Laura Hader-Kregl, Gernot M. Wallner, Christoph Kralovec, and Carola Eyßell. Effect of inter-plies on the short beam shear delamination of steel/composite hybrid laminates. *The Journal of Adhesion*, 0(0):1–13, 2018.

[40] D.G. dos Santos, R.J.C. Carbas, E.A.S. Marques, and L.F.M. da Silva. Reinforcement of cfrp joints with fibre metal laminates and additional adhesive layers. *Composites Part B: Engineering*, 165:386 – 396, 2019.

[41] Miguel Palmares. Strength of hybrid laminates aluminium carbon-fibre joints with different lay-up configurations. Master Thesis, Faculdade de Engenharia da Universidade do Porto, 2016.

[42] A Vlot and J W Gunnink. *Fibre metal laminates: An introduction*. 01 2001.

[43] L.B Vogelesang and A Vlot. Development of fibre metal laminates for advanced aerospace structures. *Journal of Materials Processing Technology*, 103(1):1 – 5, 2000.

[44] Jacobus Schijve, Laurens B. Vogelesang, and Roelof Marissen. Laminate of metal sheet material and threads bonded thereto, as well as process for the manufacture thereof, Dec 1984.

[45] National Transportation Safety Board. Aircraft accident report, aloha airlines flight 243, boeing 737-100, n73711, near maui, hawaii, april 28, 1998, 1989.

[46] A. Asundi and Alta Y.N. Choi. Fiber metal laminates: An advanced material for future aircraft. *Journal of Materials Processing Technology*, 63(1):384 – 394, 1997.

[47] Shengqing Zhu and Gin Boay Chai. Low-velocity impact response of fibre–metal laminates – experimental and finite element analysis. *Composites Science and Technology*, 72(15):1793 – 1802, 2012.

[48] A.A. Ramadhan, Abdul Rahim Abu Talib, Azmin Shakrine Mohd Rafie, and R. Zahari. The behaviour of fibre-metal laminates under high velocity impact loading with different stacking sequences of al alloy. In *AEROTECH IV*, volume 225 of *Applied Mechanics and Materials*, pages 213–218. Trans Tech Publications Ltd, 11 2012.

[49] E. Sitnikova, Z.W. Guan, G.K. Schleyer, and W.J. Cantwell. Modelling of perforation failure in fibre metal laminates subjected to high impulsive blast loading. *International Journal of Solids and Structures*, 51(18):3135 – 3146, 2014.

[50] Radu Cristian Dumbravă. Optimization of cfrp joints with fibre metal laminates. Master Thesis, Faculdade de Engenharia da Universidade do Porto, 2015.

[51] João Martins. Cfrp joints with hybrid laminates metal-carbon fibre. Master Thesis, Faculdade de Engenharia da Universidade do Porto, 2018.

[52] Olaf Volkersen. Die nietkraftverteilung in zugbeanspruchten nietverbindungen mit konstanten laschenquerschnitten, 1938.

[53] Lucas F.M. da Silva, Paulo J.C. das Neves, R.D. Adams, and J.K. Spelt. Analytical models of adhesively bonded joints—part i: Literature survey. *International Journal of Adhesion and Adhesives*, 29(3):319 – 330, 2009.

[54] C-P Fung and J Smart. An experimental and numerical analysis of riveted single lap joints. *Proceedings of the Institution of Mechanical Engineers, Part G: Journal of Aerospace Engineering*, 208(2):79–90, 1994.

[55] L.F.M. Silva and Raul Campilho. Advances in numerical modelling of adhesive joints, 01 2012.

[56] Felipe Chaves. *Fracture Mechanics Applied to the Design of Adhesively Bonded Joints*. PhD thesis, Faculdade de Engenharia da Universidade do Porto, 2013.

[57] CCRG de Sousa, Raul Campilho, EAS Marques, Marcelo Costa, and L.F.M. Silva. Overview of different strength prediction techniques for single-lap bonded joints. *Proceedings of the Institution of Mechanical Engineers, Part L: Journal of Materials: Design and Applications*, 231, 11 2016.

[58] Filipe J. P. Chaves, L. F. M. da Silva, M. F. S. F. de Moura, D. A. Dillard, and V. H. C. Esteves. Fracture mechanics tests in adhesively bonded joints: A literature review. *The Journal of Adhesion*, 90(12):955–992, 2014.

[59] M.F.S.F. De Moura, J.P.M. Gonçalves, J.A.G. Chousal, and R.D.S.G. Campilho. Cohesive and continuum mixed-mode damage models applied to the simulation of the mechanical behaviour of bonded joints. *International Journal of Adhesion and Adhesives*, 28(8):419 – 426, 2008. Special Topic Issue on Structural Adhesive Joints.

[60] A. Hillerborg, M. Modéer, and P.-E. Petersson. Analysis of crack formation and crack growth in concrete by means of fracture mechanics and finite elements. *Cement and Concrete Research*, 6(6):773 – 781, 1976.

[61] Ping Hu, Xiao Han, L.F.M. Silva, and W.D. Li. Strength prediction of adhesively bonded joints under cyclic thermal loading using a cohesive zone model. *International Journal of Adhesion and Adhesives*, 41:6–15, 03 2013.

[62] Pedro Camanho. Failure criteria for fibre-reinforced polymer composites. Technical report, Departamento de Engenharia Mecânica e Gestão Industrial, 2002.

[63] Airbus. Fast #48. Airbus Technical Magazine - Flight Airworthiness Support Technology, 2011.

[64] J A Harris and R Adams. An assessment of the impact performance of bonded joints for use in high energy absorbing structures. *Proceedings of The Institution of Mechanical Engineers Part C-journal of Mechanical Engineering Science - Proc Inst Mech Eng C-J Mech E*, 199:121–131, 04 1985.

[65] 3M. 3m scotch-weld structural adhesive film af 163-2k technical datasheet. Technical report, 3M, 2009.

[66] M. Zgoul and A.D. Crocombe. Numerical modelling of lap joints bonded with a rate-dependent adhesive. *International Journal of Adhesion and Adhesives*, 24(4):355 – 366, 2004.

[67] R. Avendaño, R.J.C. Carbas, E.A.S. Marques, L.F.M. da Silva, and A.A. Fernandes. Effect of temperature and strain rate on single lap joints with dissimilar lightweight adherends bonded with an acrylic adhesive. *Composite Structures*, 152:34 – 44, 2016.

[68] ISO 11003 2 International Standard. Adhesives determination of shear behaviour of structural adhesives part 2 tensile test method using thick adherends. ISO, 2001.

[69] M Banea, L.F.M. Silva, and Raul Campilho. Mode ii fracture toughness of adhesively bonded joints as a function of temperature: Experimental and numerical study. *The Journal of Adhesion*, 88:534–551, 04 2012.

[70] Marcelo De Moura, Raul Campilho, and J P. M. Goncalves. Crack equivalent concept applied to the fracture characterization of bonded joints under pure mode i loading. *Composites Science and Technology*, 68:2224–2230, 08 2008.

[71] M.F.S.F. de Moura, R.D.S.G. Campilho, and J.P.M. Gonçalves. Pure mode ii fracture characterization of composite bonded joints. *International Journal of Solids and Structures*, 46:1589–1595, 2008.

[72] R.D.S.G. Campilho, M.F.S.F. de Moura, and J.J.M.S. Domingues. Modelling single and double-lap repairs on composite materials. *Composites Science and Technology*, 65(13):1948 – 1958, 2005.

[73] Zainul Huda, Iskandar Taib, and Tuan Zaharinie. Characterization of 2024-t3: An aerospace aluminum alloy. *Materials Chemistry and Physics*, 113:515–517, 02 2009.

[74] W. Brockmann, O.D. Hennemann, H. Kollek, and C. Matz. Adhesion in bonded aluminium joints for aircraft construction. *International Journal of Adhesion and Adhesives*, 6(3):115 – IN1, 1986.

[75] T.J. De Vries and C.A.J.R. Vermeeren. R-curve testdata: 2024-t3, 7075-t6, glare 2 and glare 3. Delft University of Technology, 1995.

[76] M. A. Morgado, R.J.C. Carbas, E. A. S. Marques, and L.F.M. da Silva. Reinforcement of cfrp single lap joints using metal laminates. 2019.

[77] M. A. Morgado, R.J.C. Carbas, D.G. dos Santos, and L.F.M. da Silva. Reinforcement of cfrp single lap joints using adhesive layers. 2019.

[78] ASTM D5868 01(2014). Standard test method for lap shear adhesion for fiber reinforced plastic (frp) bonding. Technical report, ASTM, 2014.

[79] Diogo P.C. Antunes, António M. Lopes, Carlos M.S. Moreira da Silva, Lucas F.M. da Silva, Paulo D.P. Nunes, Eduardo A.S. Marques, and Ricardo J.C. Carbas. Development of a drop weight machine for adhesive joint testing. Accepted for publication, 2019.

Appendices

Paper A

Reinforcement of CFRP Single Lap Joints using Metal Laminates

M. A. Morgado[1], R.J.C Carbas[1,2], E. A. S Marques, [2] L.F.M da Silva[1]

[1]Department of Mechanical Engineering, Faculty of Engineering, University of Porto, Portugal

[2]Institute of Science and Innovation in Mechanical and Industrial Engineering (INEGI), Faculty of Engineering, University of Porto, Portugal

Abstract: Despite the increase of composite usage in recent years for structural applications, the susceptibility to delamination failure of these materials is seen as a big limitation for a more widespread and efficient use of the materials. A technique aiming to reduce delamination by reinforcing composite adherends with aluminium laminates, inspired by the concept of Fibre Metal Laminates (FMLs), is analysed for single lap joints using two different epoxy-based adhesives. Unlike FMLs, the suggested reinforced joints known as Composite Metal Laminates (CML), are not reinforced throughout the transverse direction but only at the adherends edges. An adequate performance is displayed for quasi-static (1mm/min) and impact conditions (3m/s). Delamination could not be avoided, but was delayed for the reinforced configurations, substantially increasing the failure loads. A numerical model using a finite element analysis is developed, and numerical and experimental results are compared. Additionally, since the performance of the technique is dependent on the mechanical properties of the adhesive used, a method is proposed to determine the minimum metal laminate thickness required for a positive performance of the reinforced joints when compared to a basic CFRP-only single lap joint (SLJ).

Keywords: Fibre Metal Laminates; CFRP; Single Lap Joint; Delamination; Adhesive Bonding; Impact; Numerical.

1 Introduction

Composite usage has seen a surge in use in recent years for structural applications, replacing traditional materials like steel and aluminium alloys in applications in which weight is a significant constraint.

Composite materials like Fibre reinforced plastics (FRP) with their unique properties such as high specific stiffness and excellent strength to weight ratio have been used in the aeronautics/aerospace industries for some time now, but recent models like the Airbus A350 and the Boeing 787 Dreamliner have shown that these materials can account for more than 50% of the structural weight. [1–3].

Structural adhesives are commonly used to join composites, as their higher notch sensitivity and low shear stress properties makes them unsuitable for being joined with mechanical fasteners. Additionally, adhesive bonding is also a joining method with low added weight. However, hybrid joints, using fasteners and adhesive can still be useful for applications with expected high stress loads.

Delamination of composites in adhesive joints is seen as a real issue to tackle. Caused by de-bonding of the fibres and the polymeric matrix due to peel stresses, it is a phenomenon that leads to premature joint failure, precluding the full use of the joint potential.

Several novel methods have been suggested to mitigate this transversal failure mode without overdesigning components, like Z-pinning [4], weaving/stitching/tufting [5–7], or using interplies [8]. The objective of this study is to study the performance of a concept influenced by the material technology of FMLs in a delamination prevention role, as some of the referred methods can not be used with prepregs, the most common application method in the industry (weaving, stitching, tufting) [4], or have some negative effects on other properties like the elastic modulus, strength and fatigue properties of the materials [4, 9].

FMLs reinforce the through thickness direction of FRP materials by adding metal sheets, typically aluminium or titanium, in between composite plies. As a technology of its own, FMLs have several advantages like high damage tolerance and excellent fatigue resistance, while preserving the low weight enthusiasm of FRPs [10].

As a result, GLARE a specific type of FML has already been used in the fuselage and the tail of the Airbus A380 airliner [11]. Previously, aluminium strips have been added in composite aircraft frames to ensure electrical continuity, with the purpose of dissipating lightning strikes [12].

FMLs have previously been studied both for low velocity and high velocity impact testing [13–20] and aluminium alloys like 2024-T3 have been shown to have the best properties under impact due to their stiffness and ductility, however most of the literature refer to the properties of the material alone, varying parameters like the materials used and geometry.

This study aims to, numerically and experimentally analyse the performance of metal laminates as reinforcement in SLJs for both quasi-static and impact conditions, using an aluminium alloy commonly used in FMLs and two epoxy-based adhesives. Additionally, a guide for standardisation of a reinforced joint design is suggested, as the performance of a configuration is heavily dependent on the adhesive used. The numerical models use finite element analysis and cohesive zone models to simulate the behaviour of the studied

configurations.

A SLJ was chosen as the test joint, due to its well-established common use in the industry for its simplicity. The failure load, failure mode and energy absorption capabilities of the joints will be studied. The reinforced joints, known as composite metal laminates (CML) are benchmarked against traditional CFRP-only SLJs.

2 Experimental Details

2.1 Adherend

The materials used in the adherends for the studied CML configurations were chosen for their common use in previous FML configurations [21].

The composite material utilised was Carbon Fibre Reinforced Plastic supplied by CIT Composite Materials from Italy in a prepreg roll, a product sold under the name HS 160 T700 and is a 0° oriented carbon-epoxy composite.

The CFRP elastic orthotropic properties were previously determined by Campilho et al. 2005 [22] and can be found in Table A.1.

Table A.1: CFRP elastic orthotropic properties [22]

Ex **(MPa)**	***Ey*** **(MPa)**	***Ez*** **(MPa)**	ν**xy**	ν**yz**	ν**xz**	***Gxy*** **(MPa)**	***Gyz*** **(MPa)**	***Gxz*** **(MPa)**
109000	8819	8819	0.342	0.342	0.38	4315	4315	3200

Machado et al. (2017) studied the fracture toughness in mode I [23], and mode II [24], of CFRP as a function of temperature and strain rate. The fracture energies for quasi-static conditions were experimentally obtained and, using a logarithmic trend function the same properties were then extrapolated for low velocity impact conditions. The tensile and shear strength of CFRP were taken from a study by Shang et al. (2018) [9].

The relevant cohesive properties of CFRP for the numerical models are summarized in Table A.2

Table A.2: Quasi-static and impact cohesive properties of CFRP [9, 23, 24]

CFRP Cohesive Properties	**Quasi-static**	**Impact**
${t_n}^0$ [MPa]	40	40
${t_s}^0$ [MPa]	35	35
G_{IC} [N/mm]	0.59	0.39
G_{IIC} [N/mm]	1.2	0.82

The aluminium alloy used for the metal laminates was the 2024-T3 Alclad series, obtained in sheets of thickness of 0.4 and 0.8 mm from AMI Metals in Belgium. The specific series was chosen for its use in aircraft construction for instance in the skin of aircrafts, due to its tensile strength [25, 26].

The mechanical properties of this alloy, obtained from stress-strain curves from tensile tests performed by Structures and Materials Laboratory of the Delft University of Technology, are shown in Table A.3 [27].

Table A.3: Mechanical properties of Al-2024-T3 Alclad Series [27]

Young's Modulus (GPa)	**Yield Stress (MPa)**	**Ultimate Stress (MPa)**	**Poisson's Ratio**	**Elongation (%)**
66	350	440	0.3	12

Surface treatments of the aluminium included gritblasting, de-greasing, the application of a Sol-Gel anodising replacement solution (3M^{TM} Surface Pre-Treatment AC-130-2), and a primer (Adhesive Primer EW – 5000 AS).

2.2 Adhesives

Two epoxy-based adhesives were used in this study: the 3M Scotch Weld AF 163 2K, a "epoxy structural adhesives in film form" [28] and the Nagase Denatite XNR6852E-3 by Nagase-ChemteX, a paste adhesive designed for CFRP-CFRP and CFRP-Metal interfaces and marketed for the automotive and aerospace industry.

The adhesive were cured following manufacturer's recommendations, at 130°C for 1 hour for the AF163-2K, and 150°C for the XNR6852 E-3.

For quasi-static conditions, the mechanical properties of the AF163-2K adhesive were determined in previous studies by Palmares (2016) and Gomes et al. (2019) [29, 30].

Morgado et al. (2019) [31], in order to study the behaviour of the adhesive in SLJs under low-velocity impact, determined the fracture energies and shear strength of the adhesive for 3m/s.

A summary of the determined mechanical properties for each condition are presented in Table A.4.

Table A.4: AF163-2k quasi-static and impact properties [29–31]

AF 163-2k Cohesive Properties	**Quasi-static**	**Impact**
$t_s{}^0$ [MPa]	46.86 ± 2.57	41.40 ± 4.21
G_{IC} [N/mm]	4.05 ± 0.07	6.06 ± 0.30
G_{IIC} [N/mm]	9.77 ± 0.21	18.73*

*logarithmically extrapolated

The remaining elastic properties, necessary for the numerical modelling of a SLJ under impact, were assumed to remain constant and are shown in A.5

Table A.5: AF163-2k mechanical properties assumed constant [29, 30]

E [MPa]	G [MPa]	$t_n{}^0$
1520	565	46.93

Table A.6: Nagase Denatite XNR 6852 E-3 mechanical properties [32, 33]

Nagase Denatite XNR 6852 E-3 Properties	**Quasi-static**	**Impact**
E [MPa]	1728	3600
G [MPa]	665	603
$t_n{}^0$ [MPa]	51.5	77.7
$t_s{}^0$ [MPa]	44.9	42.9
G_{IC} [N/mm]	9.2	13.3
G_{IIC} [N/mm]	51	64.1

2.3 Singe Lap Joint: Geometry and Manufacture

The manufactured SLJs were based on the geometry shown in Figure A.1.

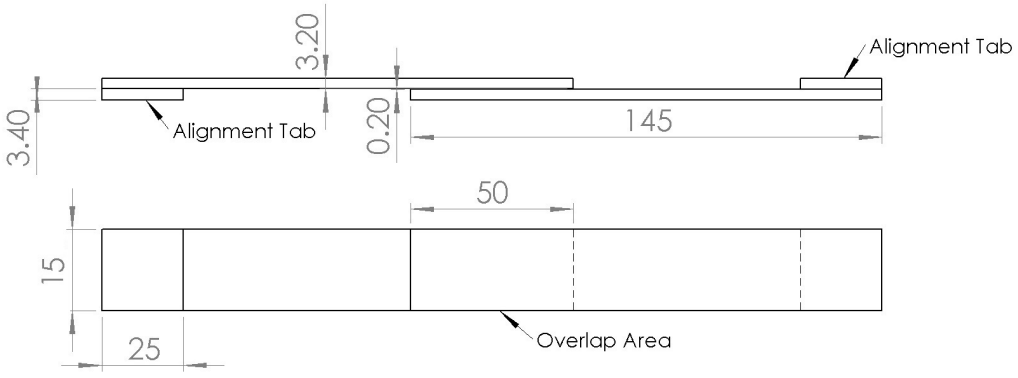

Figure A.1: Single Lap Joint Geometry (dimensions in mm)

The CML and CFRP-only SLJ configurations differ only in the through thickness direction, where two sheets of aluminium occupy the tops of the adherends, reducing the number of CFRP plies used in order to maintain a comparable overall thickness of 3.2 mm. CML configurations using 0.4 and 0.8 mm thick aluminium sheets for the two adhesives tested were manufactured and tested. The configuration for a CML adherend with 0.4 mm aluminium sheet reinforcement can be seen in Figure A.2.

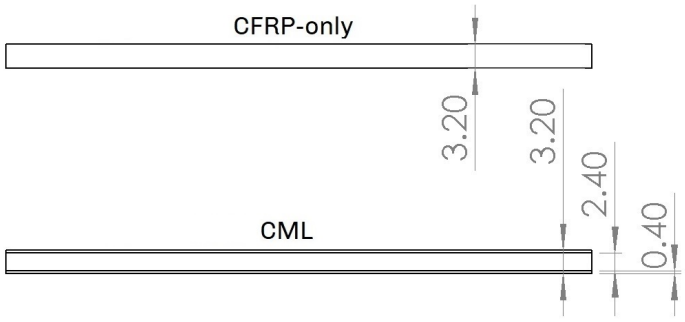

Figure A.2: Example of an adherend's through thickness geometry (dimensions in mm)

The thickness of the metal reinforcement is a variable to be optimised, a compromise between the weight of the finished joint and its mechanical properties.

2.4 Testing Conditions

At least 5 different specimens were tested for each configuration and loading scenario under study.

For quasi-static conditions the SLJs were tested using an Instron 8801 servo-hydraulic testing machine with a load cell of 100 kN at a constant crosshead speed of 1mm/min, according to the standard ASTM D5868 - 01(2014) [34].

For impact conditions, a drop-weight impact machine developed in-house was used [35]. This machine is capable of dropping a 56 kg mass off a maximum height of 1.27 m, achieving an impact speed of 5 m/s.

The displacements were indirectly obtained by trapezoidal integration of the load against time, and further validated by using an high speed camera slow-motion footage captured with an high speed camera..

The impact speed used was 3m/s for a weight of 31.3 kg, resulting in an impact energy of 140.85 J.

All tests were performed at laboratory ambient conditions (room temperature of 24°C, relative humidity of 55%).

3 Numerical Models

The numerical models were developed using ABAQUS. The FE analysis analysis was performed with the objective of predicting both the failure load and failure mode of the modelled joints.

Two models were used, one for quasi-static conditions and one for impact loading. Both were based on a 2D planar deformable shell part and differed only in boundary conditions and the step-type analysis used.

The boundary conditions used are shown in Figure A.3. An encastre is used in one of the extremities to replicate the gripping system. For the other end of the SLJ, for

quasi-static conditions (tensile testing), a displacement of 5 mm was imposed, and for impact conditions (drop-weight) a mass with the same weight as the one dropped on the specimen was modelled and given the same velocity as the impactor in the experimental test, 3 m/s. This 3 m/s velocity predefined field was created on the initial step and propagated to the subsequent analysis step.

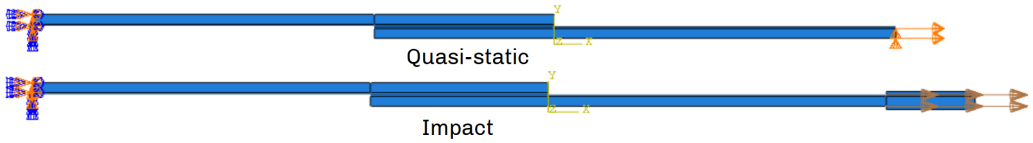

Figure A.3: Modelled boundary conditions

Regarding the step type itself, a static general analysis was used for quasi-static conditions while for impact conditions a dynamic explicit step was used.

The material properties previously shown in the experimental details section were used for the numerical modelling.

3.1 Elastic modelling

The selection of the best performing reinforcement laminate thickness is a complex process. In this study, Al sheets with 0.4 mm and 0.8 mm thickness were available for use. To maximise the weight advantage of CFRP the metallic laminates should be as thin as possible. The concept of CML joints uses the metal sheet component to avoid stresses from being concentrated directly on the CFRP matrix, on a small area at the ends of the overlap, spreading them instead over a larger surface area, the CFRP-Aluminium interface.

However, because no adhesive is used to join the metal reinforcement and the composite, and only the resin of the composite prepreg is used as bonding agent, delamination could still occur in this interface. Therefore, the choice of the metal laminate thickness plays a major role to prevent this from happening, as its thickness will move this weak spot further away from the overlap, decreasing the magnitude of the stresses, in particular peel stresses, acting on it. Increasing the thickness will also increase the stiffness of the reinforcement, minimising transversal plastic deformation and transmitting less peel stresses to the Al-CFRP transition. The material choice, due to different material elastic properties, can influence this design process in the same way, but since this study focused on the use of an aluminium alloy the joint design will necessarily be a compromise between the weight added to the CFRP joint and the stiffness needed to prevent delamination in the metal-composite interface.

Finally, the mechanical properties of the adhesive used in the overlap are also key to the behaviour of the SLJ and the stresses observed throughout the transverse direction.

In order to study this multi-variable problem, and help standardise the design of CML joints, a numerical procedure is proposed. A fully elastic model, i.e. without cohesive

damage modelling, was developed. Using the path tool, Figure A.4, and a loading boundary condition of 20 kN, the peel stresses in the Aluminium-CFRP interface were obtained along the overlap.

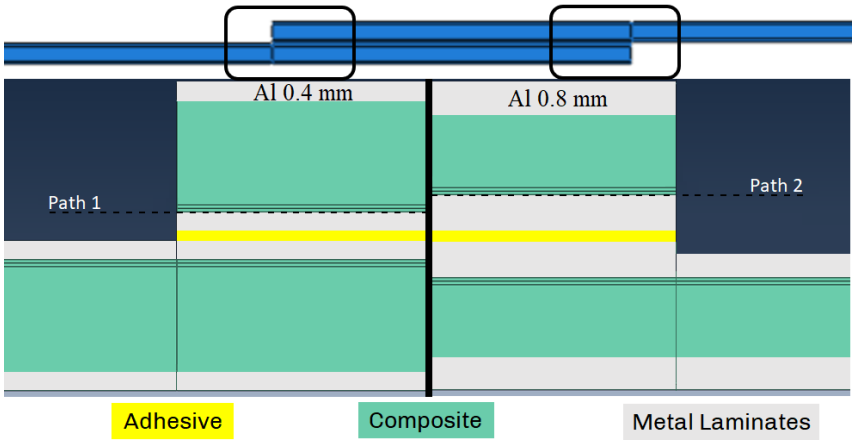

Figure A.4: Paths on the Al-CFRP interfaces (0.4 and 0.8 mm configuration)

The maximum peel stresses, obtained at the ends of the overlap, can be seen in Figure A.5

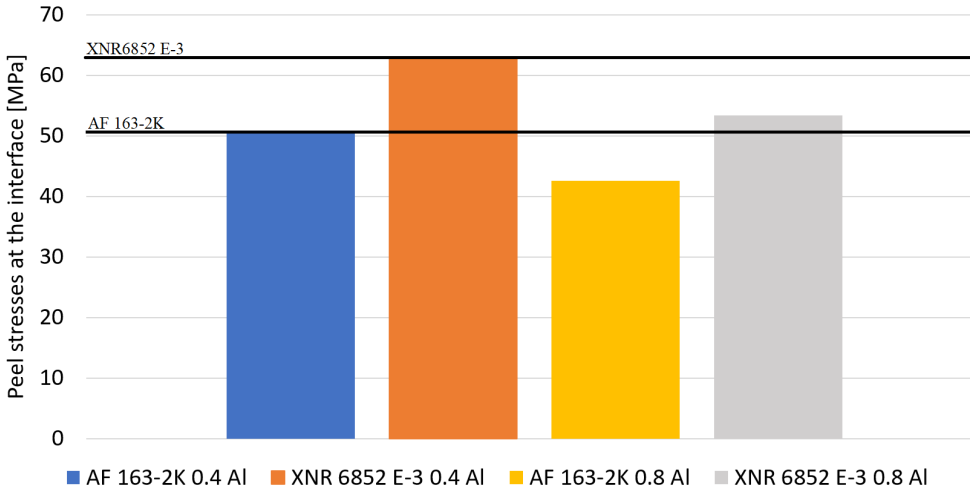

Figure A.5: Maximum peel stresses along the interface

Increasing the thickness of the Al laminate from 0.4 to 0.8 mm has the disadvantage of increasing the weight of the joint by 15.6%, but this new configuration of 50% CFRP and 50% aluminium doubles the distance between the weaker Al-CFRP interface and the adhesive bondline, decreasing the magnitude of the peel stresses transmitted to it.

The peel stress chart also shows that that peel loadings are greater for joints using XNR 6852 E-3, as a result avoiding delamination will be harder for this adhesive. Its higher Young's modulus and shear modulus force the substrates to rotate and bend more, which in turn increases the peel stresses.

3.2 Cohesive Zone Modelling

A cohesive zone model (CZM) was used to model the adhesive behaviour. Triangular traction-separation laws were applied to the adhesive layers of the model to simulate damage evolution. Additionally, a similar CZM was introduced in the CFRP material to model delamination. These interlaminar cohesive element layers were placed in between elastic homogeneous CFRP sections.

Situated on top of an elastic layer of homogeneous CFRP with a thickness of half one composite ply for the AF-163 2k (0.075 mm) and one full composite ply layer for the XNR6852 E-3 models (0.15 mm), the cohesive sections were given a thickness of half a layer of CFRP (0.075mm). The model's sections can be seen in Figure A.6.

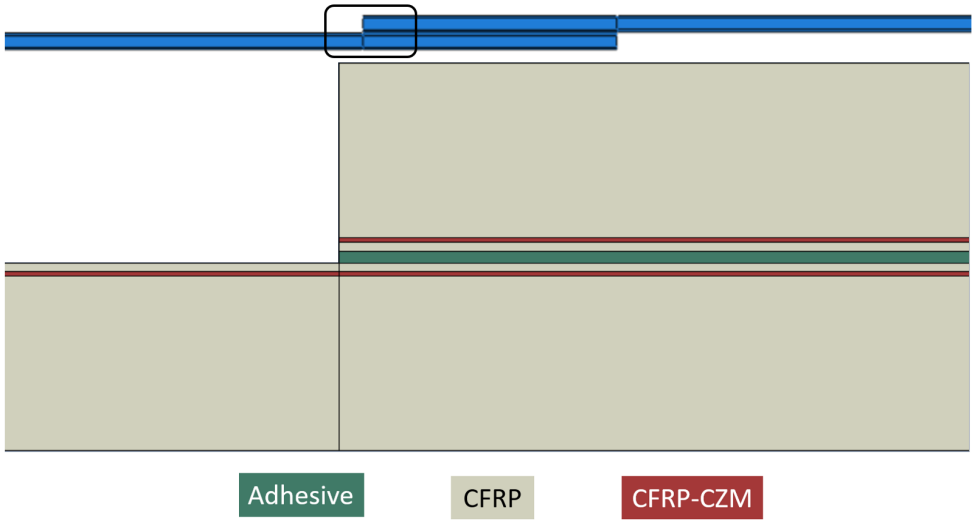

Figure A.6: CFRP-only model (XNR6852 E-3)

Effectively, the cohesive layer simulates the possible de-bonding between the plies of CFRP. The different height for the adhesive elastic layers for each adhesive was implemented after the one used for AF163-2k with satisfactory results was found to be underestimating the failure load for the XNR6852 E-3 adhesive, initiating delamination too soon.

For the CML configurations instead of modelling CFRP delamination in the adhesive-composite interface, it was moved to the aluminium-CFRP bond.

The elastoplastic behaviour of the aluminium was also modelled. For CML models a Johnson-Cook failure criterion was added to reproduce metal cracking and failure.

The Johnson-Cook damage constants used are shown in Table A.7 [36].

Table A.7: Johnson-Cook Damage parameters of Al-2024-T3 alloy [36]

Material	**A**	**B**	**C**	**n**	**m**	**d1**	**d2**	**d3**	**d4**	**d5**
Al-2024-T3	265	426	0.018	0.34	1	0.13	0.13	-1.5	0.011	0

A (yield stress), B (hardening modulus), C (dimensionless strain-rate dependency coefficient), n (power exponent of strain work-hardening) and m (power exponent of the thermal softening coefficient) are material properties obtained through torsion tests [36].

The parameters d1 to d5 are damage constants: D1, d2 and d3 concern pressure dependence/quasi-static conditions, d4 strain rate dependence and d5 is temperature related. [37, 38]

After damage is introduced, and given that for maximum degradation D equals to 1, the residual stiffness of damaged elements can be calculated by the following equation [36]:

$$E_d = (1 - D) \cdot E \tag{4}$$

Figure A.7 shows the numerical model used for CML joints with different sections highlighted in distinct colours.

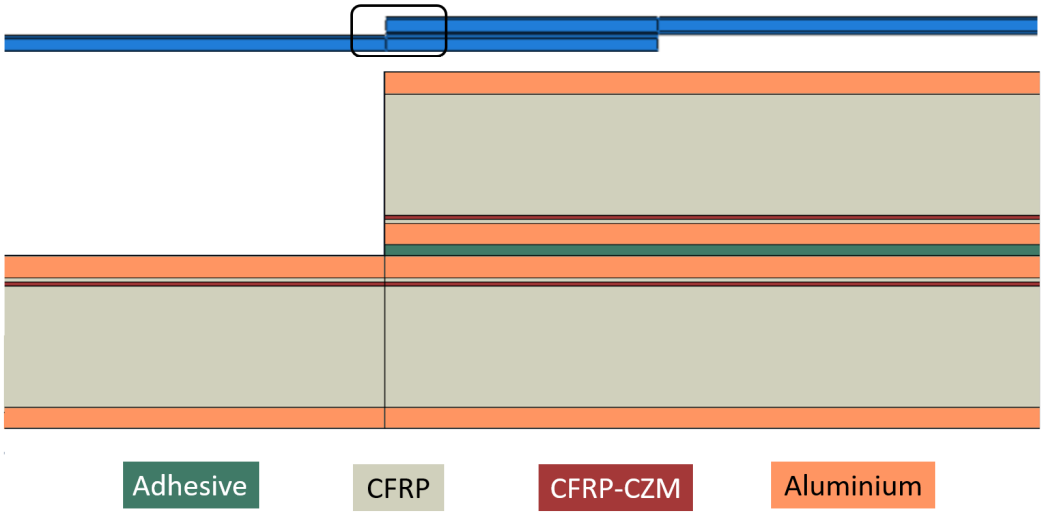

Figure A.7: CML model (XNR6852 E-3)

For the aluminium and elastic sections of CFRP, four-node plane stress (CPS4R) and four-node plane strain elements (CPE4R) were used. For the cohesive sections, adhesive and CFRP, COH2D4, a 4-node two-dimensional cohesive element was used.

4 Results

4.1 AF 163-2K - 0.4 mm Al

A typical quasi-static experimental load displacement curve for each configuration and the corresponding numerical can be seen in Figure A.8. The CML reinforcement was able to improve the failure load of a standard CFRP-only joint by almost 30%, increasing the average failure load of a CFRP SLJ from 17.89 ± 0.54 kN to 23.1 ± 0.43 kN with the use of a 0.4 mm aluminium sheet reinforcement.

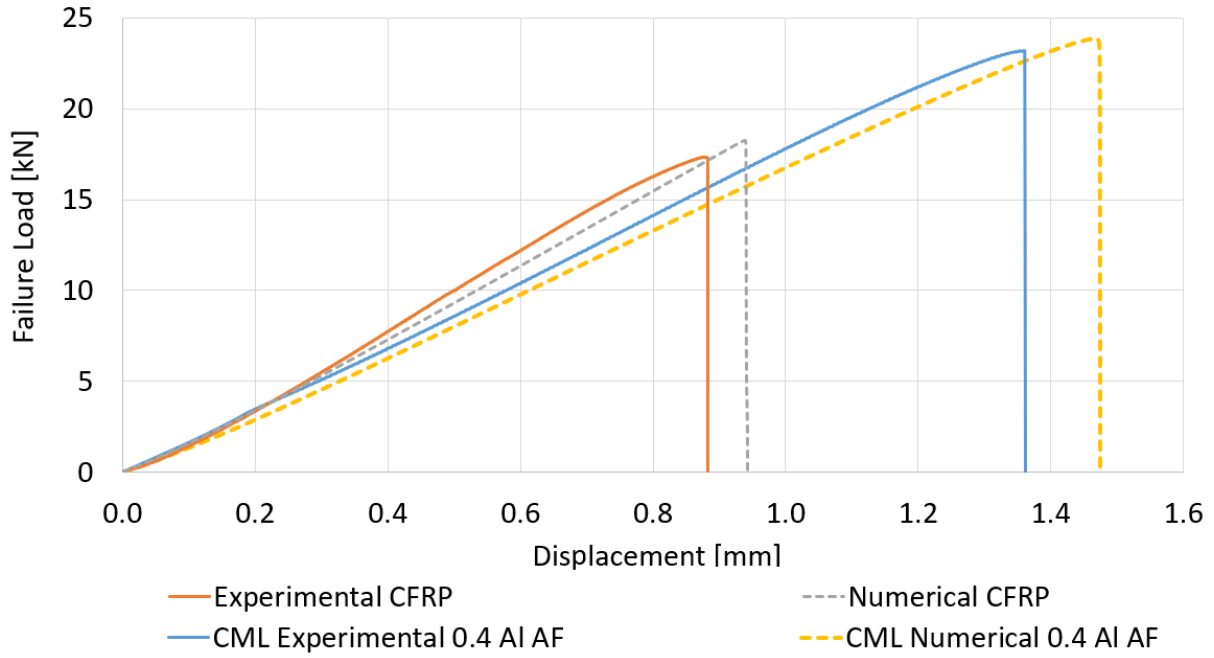

Figure A.8: Numerical vs Experimental P-δ curves under quasi-static conditions (AF163-2K)

The failure mode for the CFRP reference joint was delamination. For the CML joint delamination was successively eliminated and a cohesive failure was observed. The failure modes of both joints were correctly reproduced in the numerical model, Figure A.9.

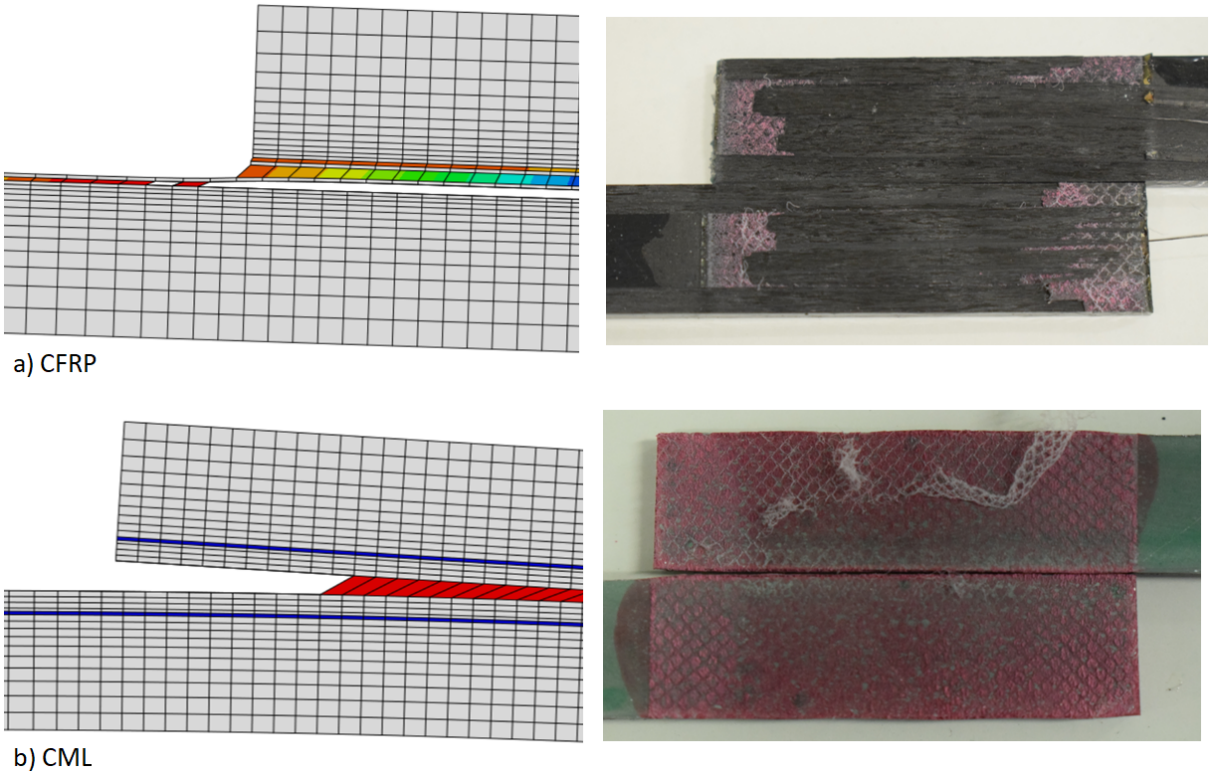

Figure A.9: Comparison between quasi-static numerical and experimental failure modes obtained (AF163-2k): a)CFRP; b)CML

Regarding the impact performance of CML joints, an average failure load of 26.02 ± 1.44 kN represents a percentage increase of 22.5% when compared to the failure load for CFRP-only joints (21.24 ± 1.21 kN). Most interestingly, a significantly larger displacement for the reinforced joint was also observed. As a consequence of the multiple failure mechanisms like delayed delamination, aluminium fracture and fibre-tear working together, both improvements increase the energy absorbed by approximately 105%, Figure A.10.

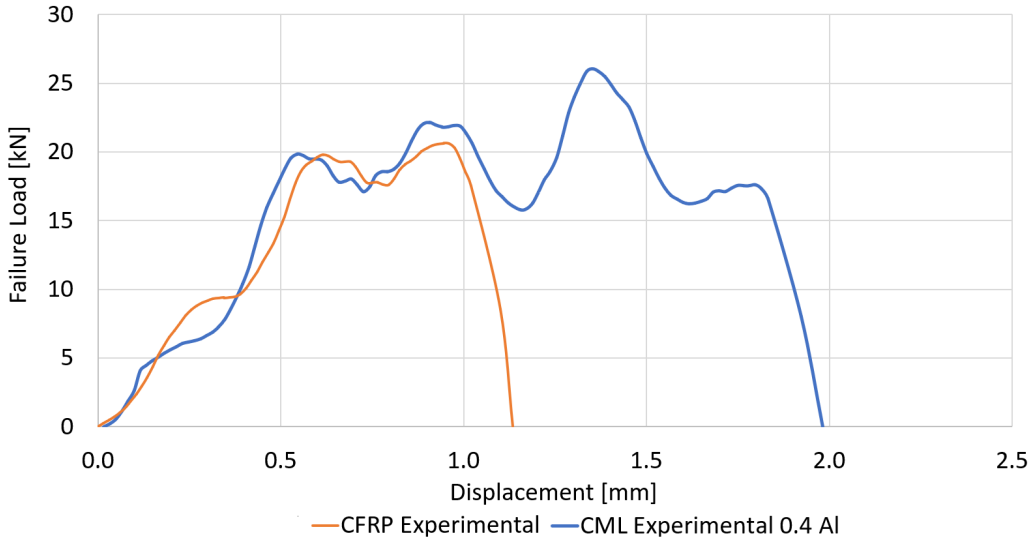

Figure A.10: Typical Impact P-δ curves for CFRP and CML specimens (AF 163-2K)

The numerical models load-displacement curves correlated very well with the experimental results, Figures A.11 and A.12, while correctly predicting the failure types.

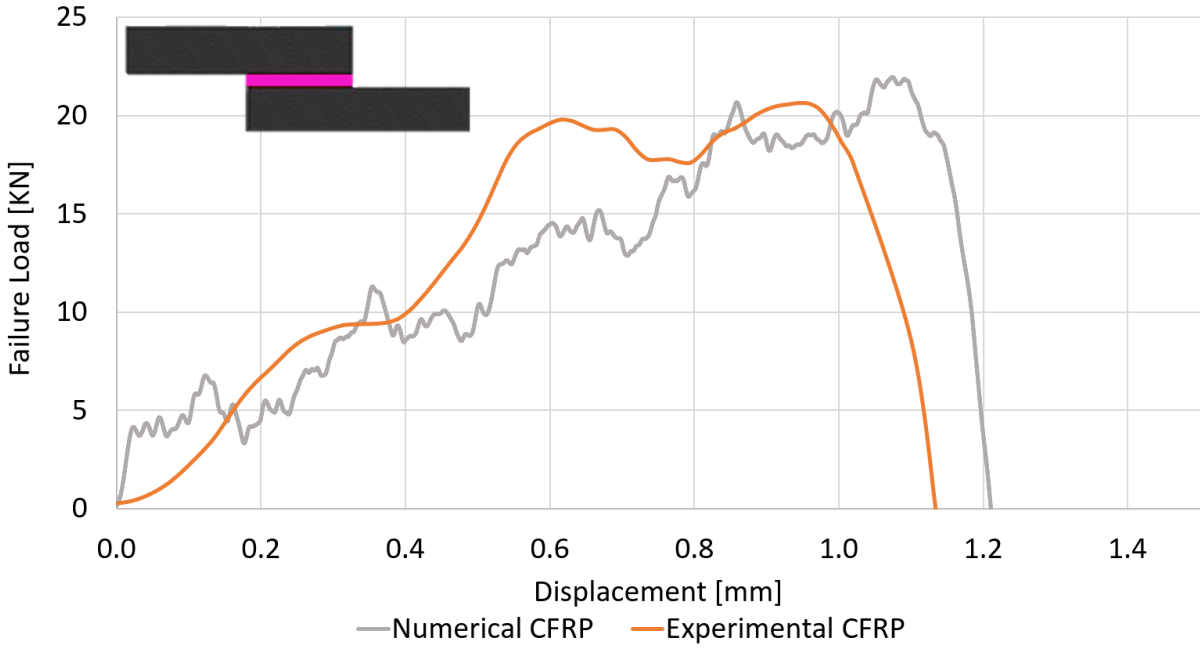

Figure A.11: Numerical vs Experimental P-δ curves for CFRP under impact conditions

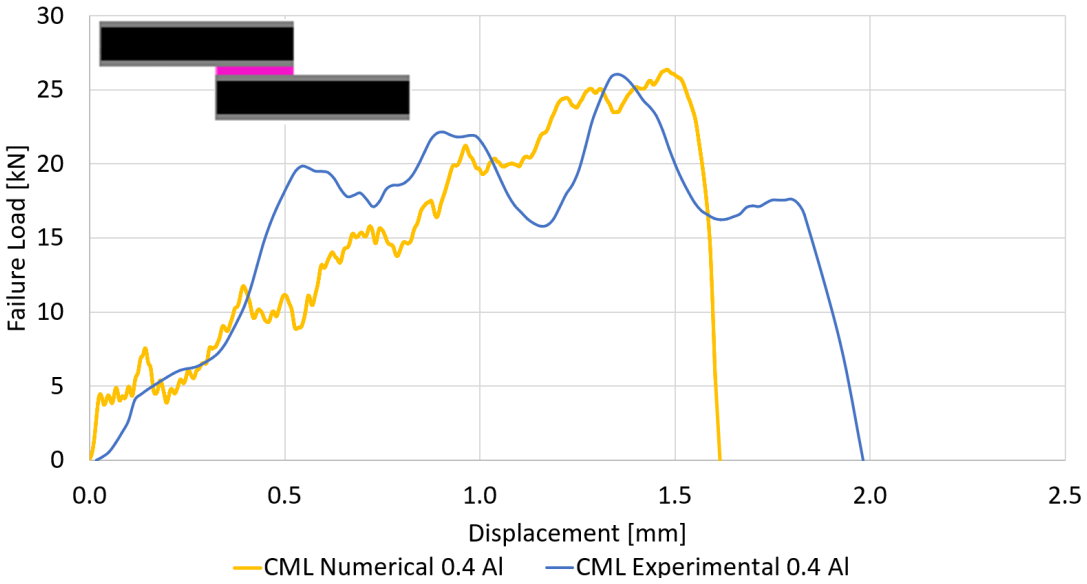

Figure A.12: Numerical vs Experimental P-δ curves for CML under impact conditions

A side by side comparison of the failure modes obtained numerically and experimentally can be seen in Figure A.13. The fracture of the aluminium was perfectly simulated by the Johnson-Cook damage model introduced for impact conditions.

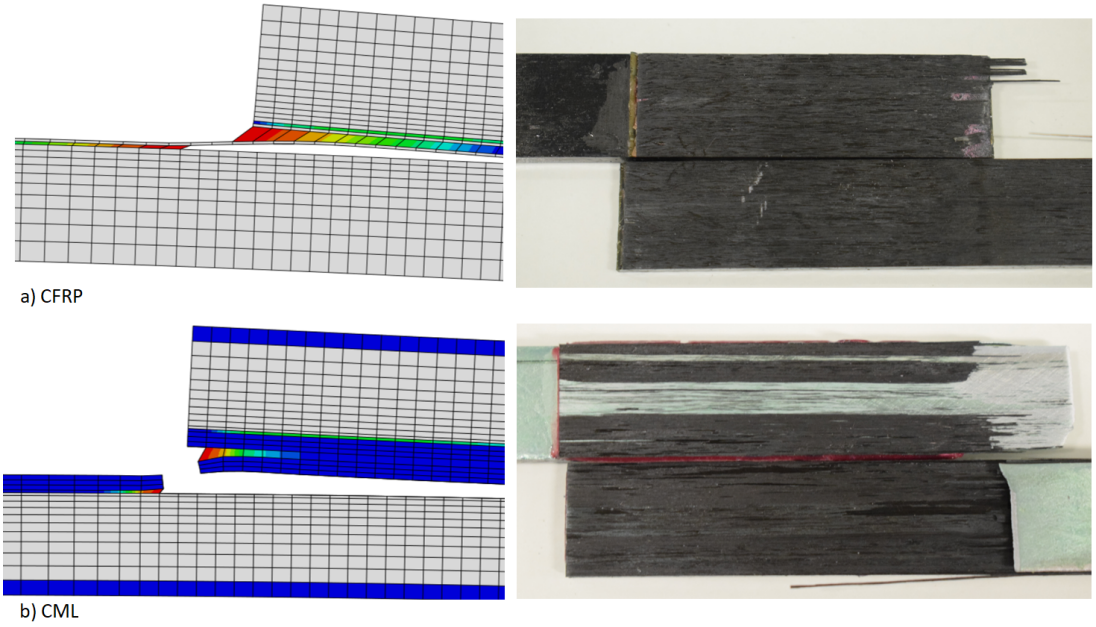

Figure A.13: Comparison between impact numerical and experimental failure modes obtained (AF163-2k): a)CFRP; b)CML

The performance of this CML joint configuration against the CFRP-only reference using this AF163-2k adhesive is very encouraging and can be seen in Figure A.14. The increase of the failure loads for both configurations when the loading condition changes from quasi-static to impact is related to the strain rate dependency of polymers, and in particular adhesives.

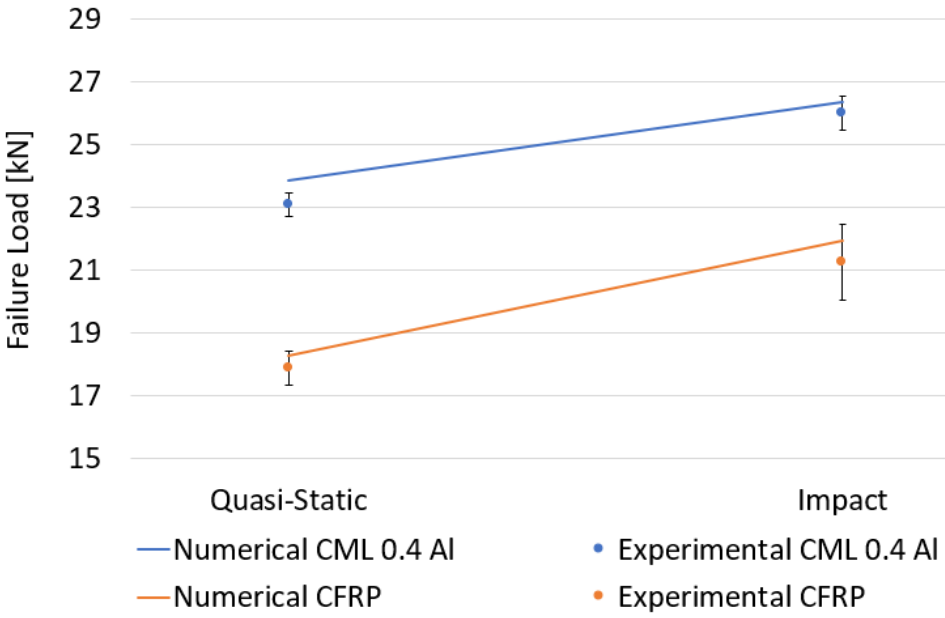

Figure A.14: Summary of CFRP vs CML (AF 163-2K)

4.2 AF 163-2K - 0.8 mm Al

Subsequently, a new joint configuration, using 0.8 mm aluminium sheets as reinforcement, was tested. The new geometry has an equal volume of Al and CFRP, since a total thickness of approximately 3.2 mm per adherend was maintained.

The quasi-static performance of the new configuration, when compared to the previous 0.4 Al geometry, remained practically constant for the same adhesive, with a cohesive failure for the CML joint being once again experimentally obtained.

However, a small decrease in the average failure load, now 21.945 $\pm$ 0.65 kN was registered. This 5% decrease could be due to the lesser rigidity of this new adherend, composed of more aluminium and less carbon fibre. This would result in more bending during tensile testing and the presence of more peel loading in the adhesive layer. Figure A.15 shows plastic deformation due to bending loads present for this configuration, which was never seen to such an extent in preceding tests.

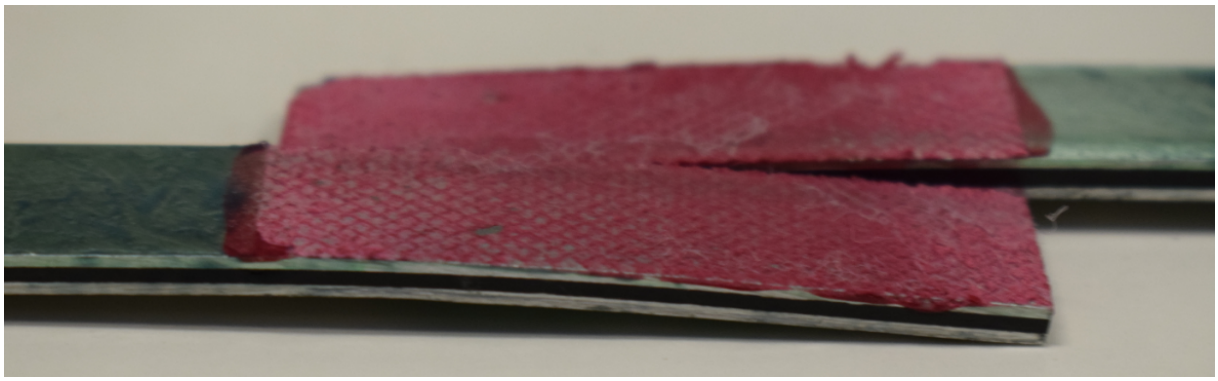

Figure A.15: Plastic deformation due to bending on CML joints (AF163-2K 0.8 mm Al)

A numerical/experimental load displacement curve comparison for this configuration and the CFRP reference are shown in Figure A.16, with the numerical model continuing to approximate well the experimental results.

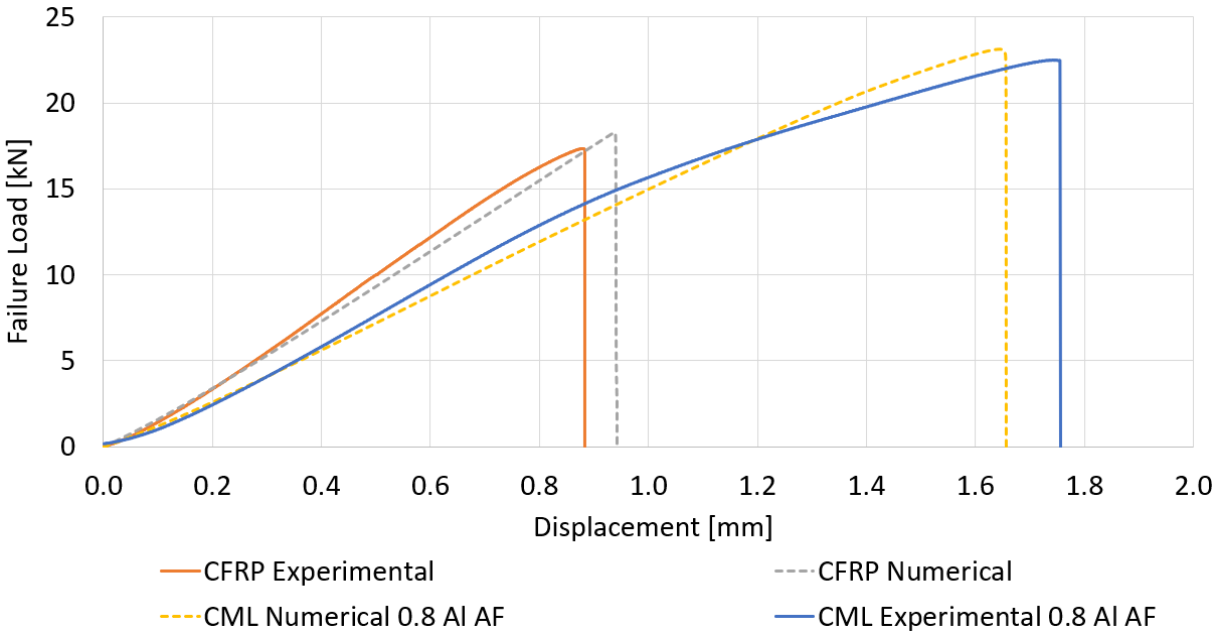

Figure A.16: Numerical vs Experimental P-δ curves under quasi-static conditions (AF163-2K 0.8 mm Al)

The numerical/experimental failure mode comparison for quasi-static conditions is shown in Figure A.17.

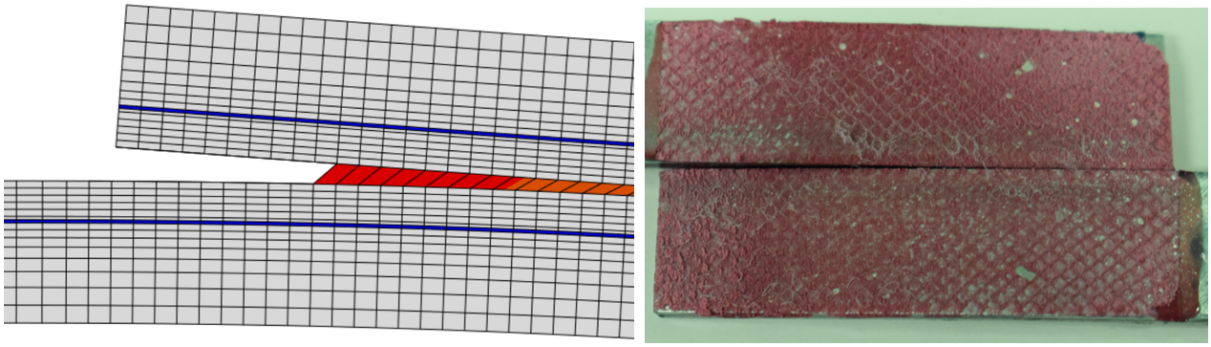

Figure A.17: Numerical vs Experimental P-δ curves under quasi-static conditions (AF163-2K 0.8 mm Al)

Typical experimental impact load-displacement curves of the CML with 0.8 Al reinforcements and the reference CFRP are shown in Figure A.18, where a similar behaviour to the previous 0.4 mm CML configuration is observed.

A comparison of the impact load-displacement curves for both CML configurations is shown in Figure A.19, better demonstrating the differences between the two.

The specimens with the 0.8 mm reinforcements show a smaller slope, something already expected due to their decreased rigidity.

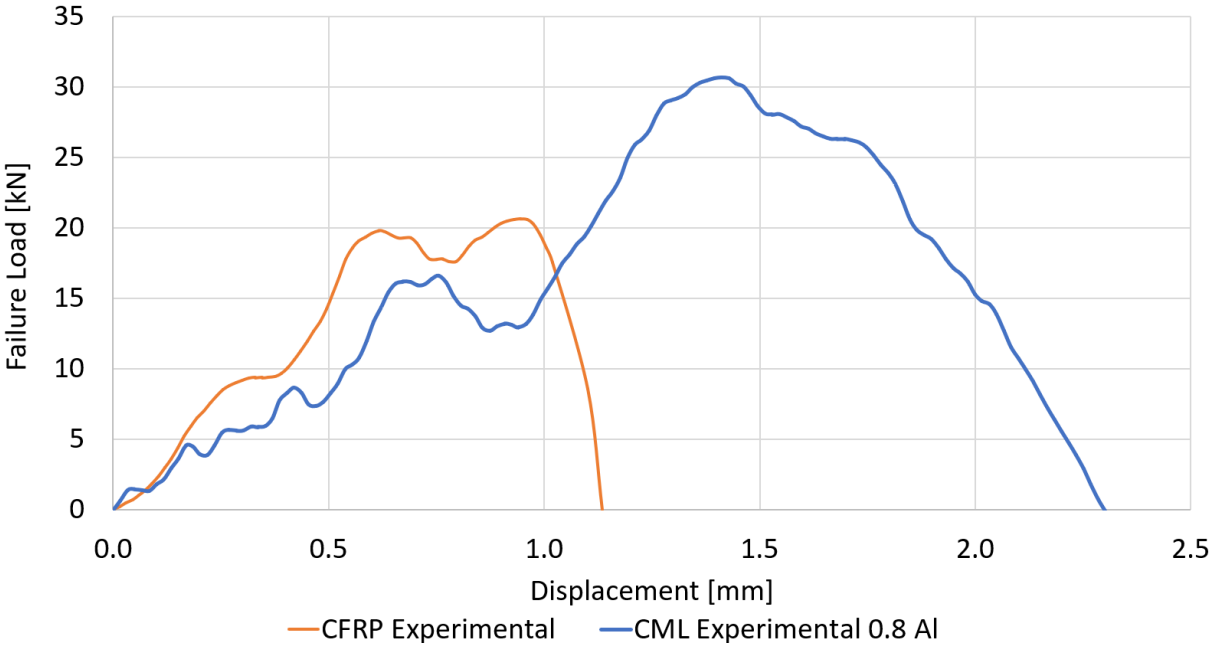

Figure A.18: Typical impact P-δ curves for CML and CFRP specimens impact conditions (AF163-2K 0.8 mm Al)

The higher load and displacement for the new configuration is attributed to a change in the failure mode.

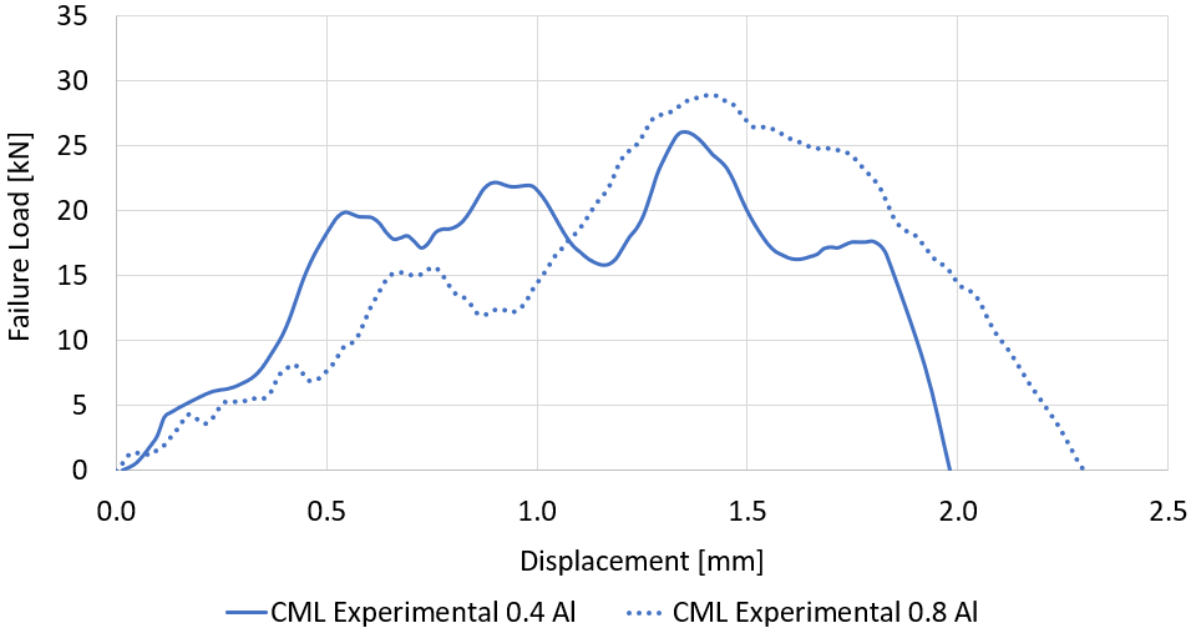

Figure A.19: CML 0.4 vs CML 0.8 typical impact P-δ curves (AF163-2K)

While for the 0.4 mm Al reinforced joint, the failure was caused by delamination followed by aluminium fracture, for the new 0.8 mm Al specimens a cohesive failure was observed. This elimination of premature delamination under impact allowed the SLJ to use the full strength of the adhesive until its failure.

The new failure modes, accompanied by the corresponding numerical simulations, can be seen in Figure A.20.

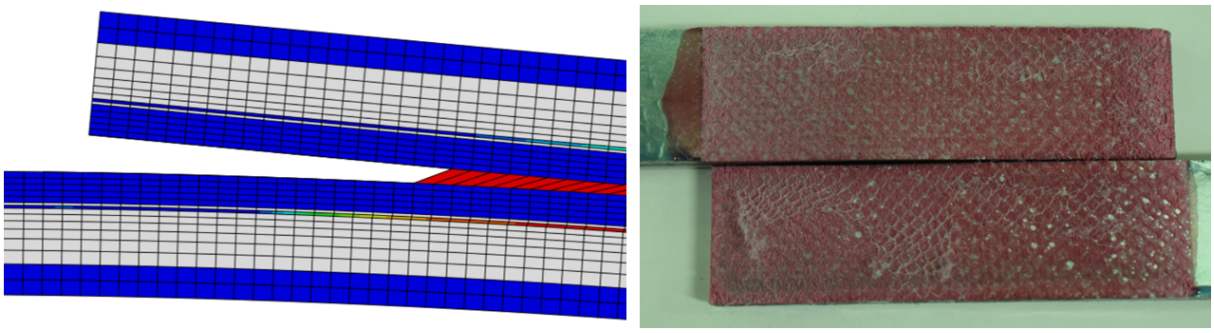

Figure A.20: Comparison between impact numerical and experimental failures obtained (AF163-2k) 0.8 mm Al

The numerical and experimental load-displacement curves under impact for this configuration are compared in Figure A.21. The numerical model accurately predicts the failure load, but overestimates the displacement.

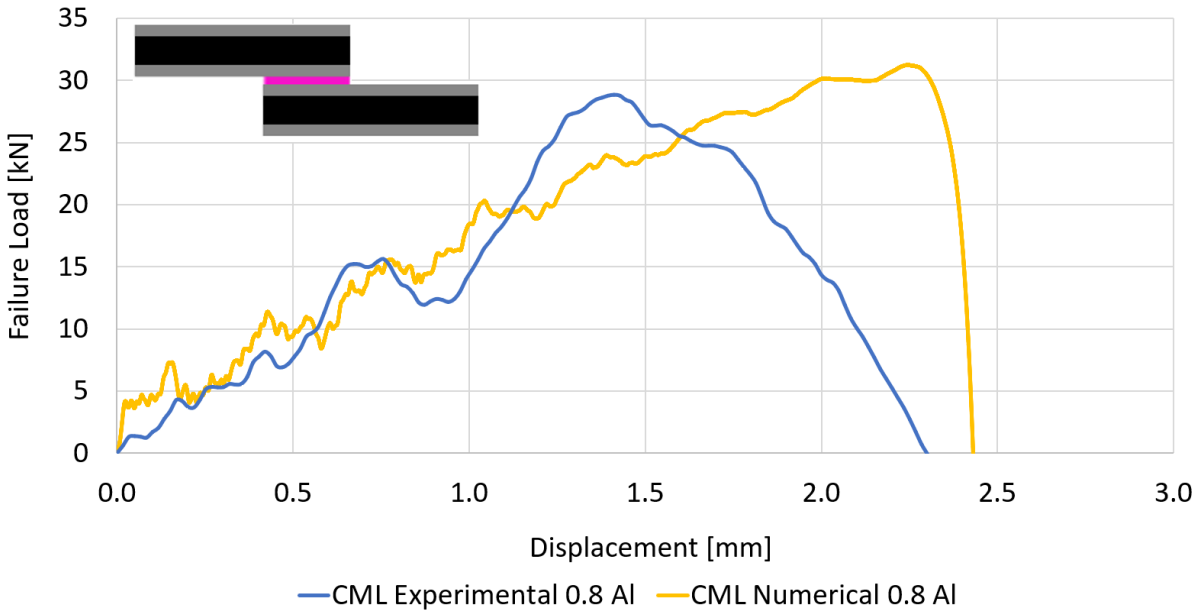

Figure A.21: Numerical vs Experimental P-δ curves under impact conditions (AF163-2K 0.8 mm Al)

A summary of the performance of the CML configuration using 0.8 mm Aluminium laminates and adhesive AF163-2K can be seen in Figure A.22. As previously stated, the main difference to the previous 0.4 mm configuration is the elimination of delamination for impact conditions, and the increase in impact failure load associated with it.

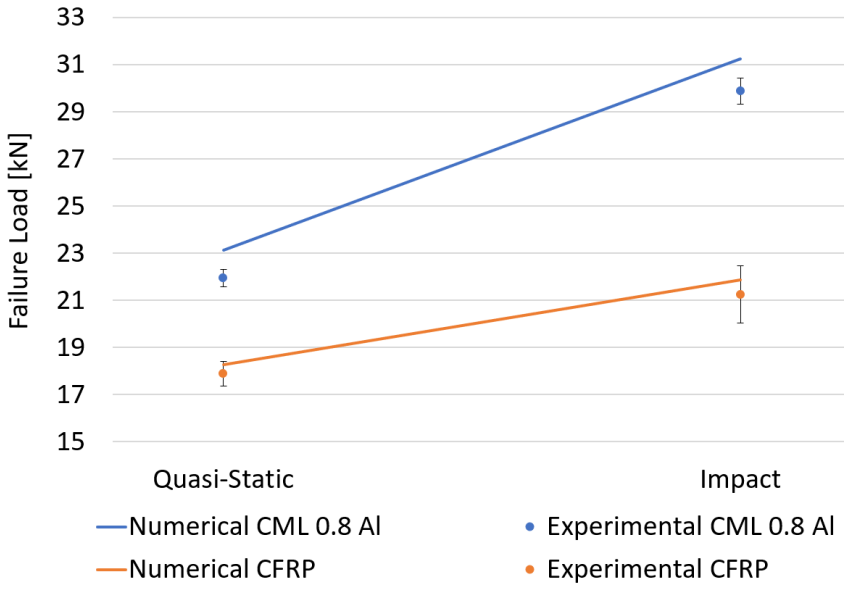

Figure A.22: Summary of CFRP vs CML 0.8 Al (AF 163-2K)

4.3 XNR6852 E-3 - 0.4 Al mm

The same reinforcement configurations were then studied using another adhesive, the Nagase Denatite XNR6852 E-3. It was important to test the reinforcement method to its limits, and a stronger adhesive like the XNR6852 E-3 with a theoretical higher ceiling for improvements provided additional difficulties.

Starting with the lightest reinforcement of 0.4 mm, the use of this configuration with this adhesive registered the highest peel stresses on the fully elastic peel model analysis.

When this configuration of CML was tested, for the first time, the reinforced specimens actually performed worse than the CFRP-only reference joint, Figure A.23, experimentally confirming that CML reinforcement solutions are not universal, and are dependent on the adhesive used.

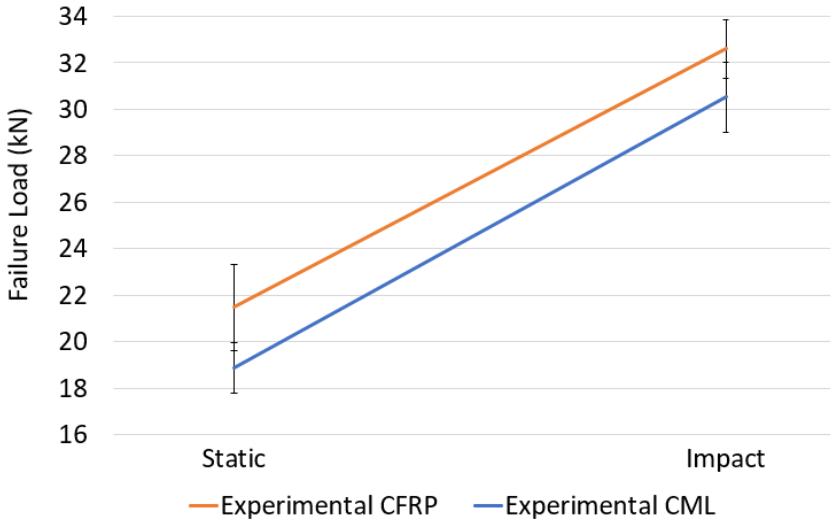

Figure A.23: CFRP vs CML 0.4 Al (XNR6852 E-3)

The CML failure load was 12% lower than the reference joint for quasi-static conditions. In fact this previously successful configuration that had delayed delamination for the AF163-2k adhesive was now seemingly promoting it in a lower load level than its initiation for the composite only joint.

4.4 XNR6852 E-3 - 0.8 Al mm

Finally, the 0.8 mm version of the CML joints was then tested using XNR6852 E-3 adhesive. The 0.4 configuration performed very poorly for this adhesive but the numerical model that calculated the peel stresses at the Al-CFRP interface predicted that for this second, thicker metallic reinforcement, the critical stresses would be decreased almost to a similar level that produced positive performance in the first configuration tested with AF163-2k.

This new configuration achieved a positive performance for this adhesive. The reference CFRP-only joints had an average failure load of 21.47 ± 1.84 kN, while the reinforced joints registered an average failure load of 27.77 ± 0.76 kN. This improvement represents a 29.3% increase for quasi-static conditions, a similar turnover to the other successful results consistently obtained for the other adhesive, showing that ultimately the concept will work. Its applicability in real applications, however, can be limited by the thickness of the adherends and the available margin for the introduction of the metal laminates.

Although the failure loads were increased by the reinforcement of the SLJs, delamination was still the failure mode for CML joints.

For quasi-static conditions, the numerical models predicted failure by delamination for both configurations, occurring at a higher failure load for CML. The failure load level predicted numerically correlated well with the experimental results. The quasi-static experimental and numerical load displacement curves can be seen in Figure A.24.

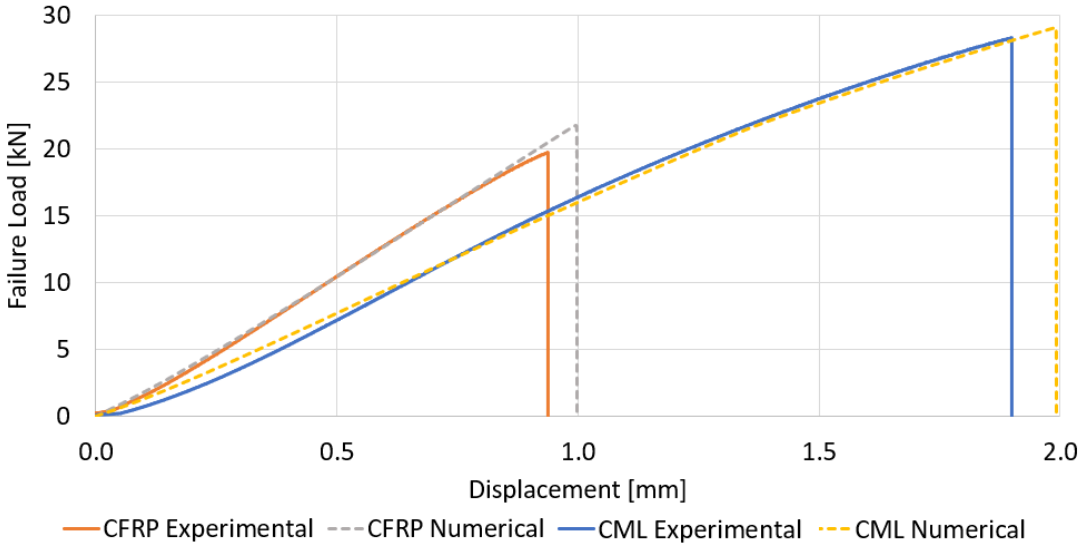

Figure A.24: Numerical vs Experimental P-δ curves of CFRP and CML under quasi-static conditions (XNR6852 E-3)

The failure modes are shown in Figure A.25 showing a good correlation between the two. For some specimens, the beginning of a failure in the adhesive layer could be seen, indicating that a cohesive failure was narrowly missed by this configuration.

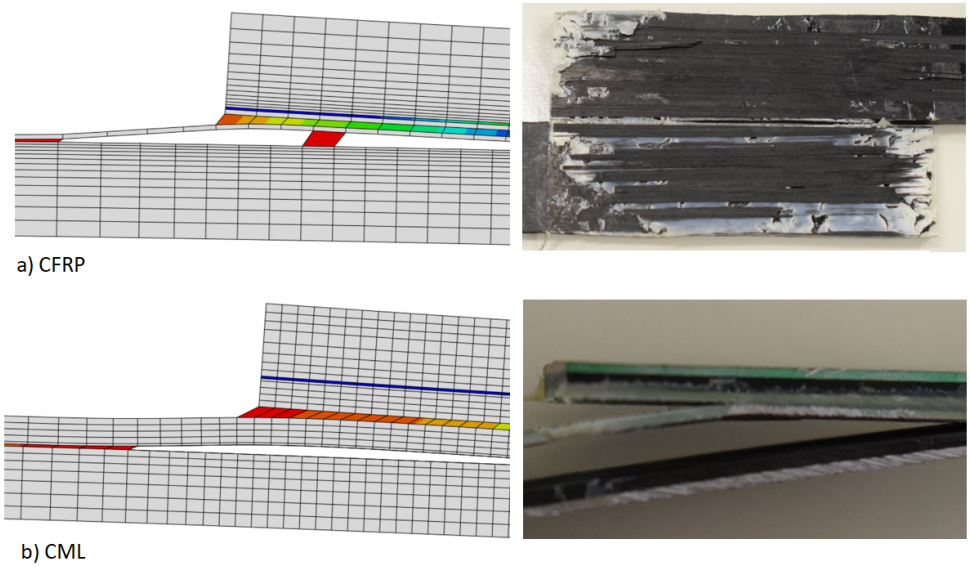

Figure A.25: Comparison between quasi-static numerical and experimental failure modes obtained (XNR6852 E-3): a)CFRP; b)CML

As was the case for quasi-static loading, once the geometry was re-designed the impact performance of CML joints using the XNR6852 E-3 adhesive was very positive. The failure load increased by 22%, a significant increase, from an average failure load of 31.38 $\pm$ 1.25 kN for the reference CFRP joint to 38.27 $\pm$ 1.40 kN for the reinforced CML joints.

Additionally, figure A.26, showing the comparison between experimental CML and CFRP impact load displacement curves, also indicates an increase in the displacement of the reinforced joint. The energy absorbed by the CML configuration is up to 2.5 times greater than the energy absorbed by the reference CFRP-only joint.

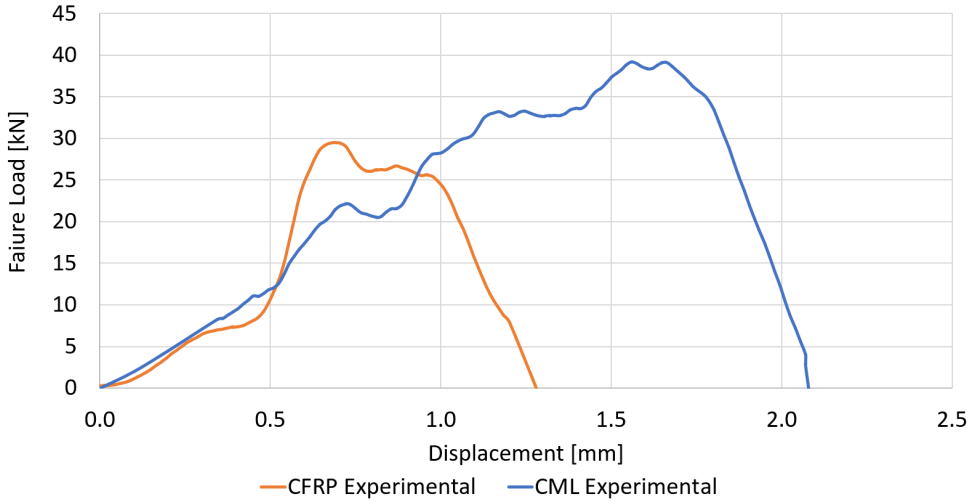

Figure A.26: Typical Impact P-δ curves for CML and CFRP specimens (XNR6852 E-3)

The reason for these improvements, is once again thought to be the result of the delayed onset of delamination and the multi-material layers and interfacial obstacles that the crack has to overcome in the through thickness direction throughout its propagation.

The numerical models predict the failure loads of both the CFRP and CML configuration within a error smaller than 5% , but the displacement was for both configurations overestimated by the numerical model. Superposed numerical and experimental load displacement curves for the CFRP-only joint can be seen on figure A.27 and in figure A.28 for CML joints.

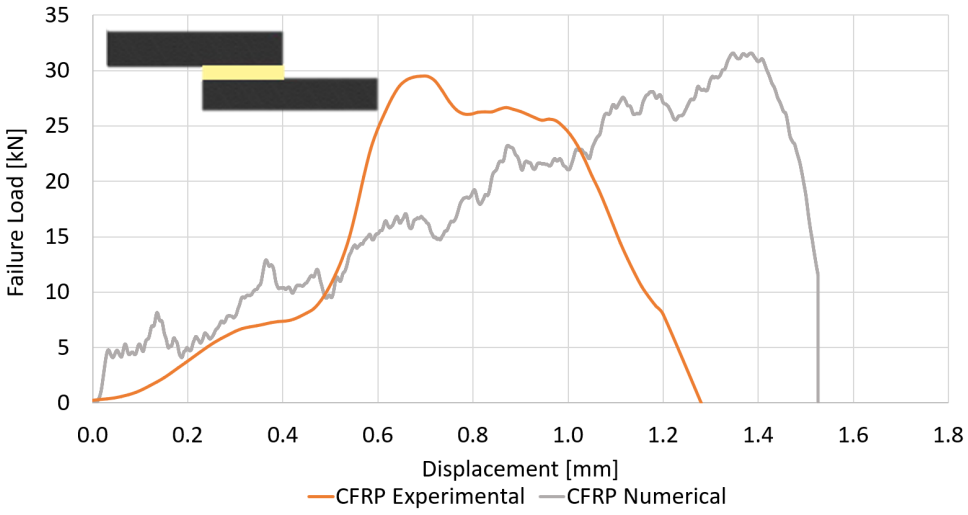

Figure A.27: Numerical vs Experimental P-δ curves for CFRP under impact conditions (XNR6852 E-3)

For the first time in this study, the experimental average failure load for impact conditions exceeded the failure load predicted by the numerical model. This can be explained by the difficulties experienced in the characterisation of the XNR6852 E-3 adhesive, that led to the extrapolation and even estimation of some of its properties for the test speed of 3m/s.

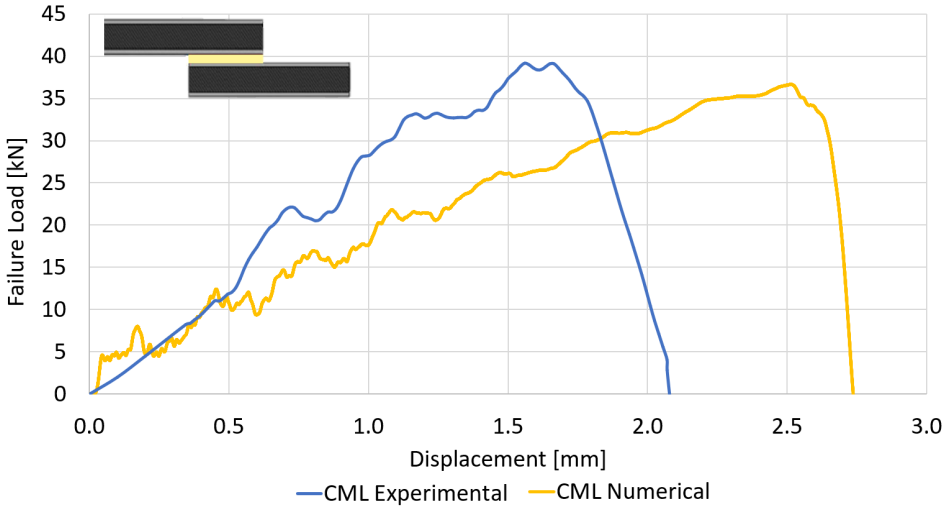

Figure A.28: Numerical vs Experimental P-δ curves for CML under impact conditions (XNR6852 E-3)

Impact testing is notoriously difficult, with very short test window times, sensitivity to the data acquisition frequency, shock waves, vibrations and deformations of the fixing system. Taking all this into consideration, as well as previous very good correlations of the same model it can be said that the numerical model correctly predicted the behaviour of the tested joints under impact.

Moreover, the numerical model accurately depicts the failure mode for each of the studied configuration: delamination for CFRP and delamination with the aluminium reinforcement fractured for CML, figure A.29

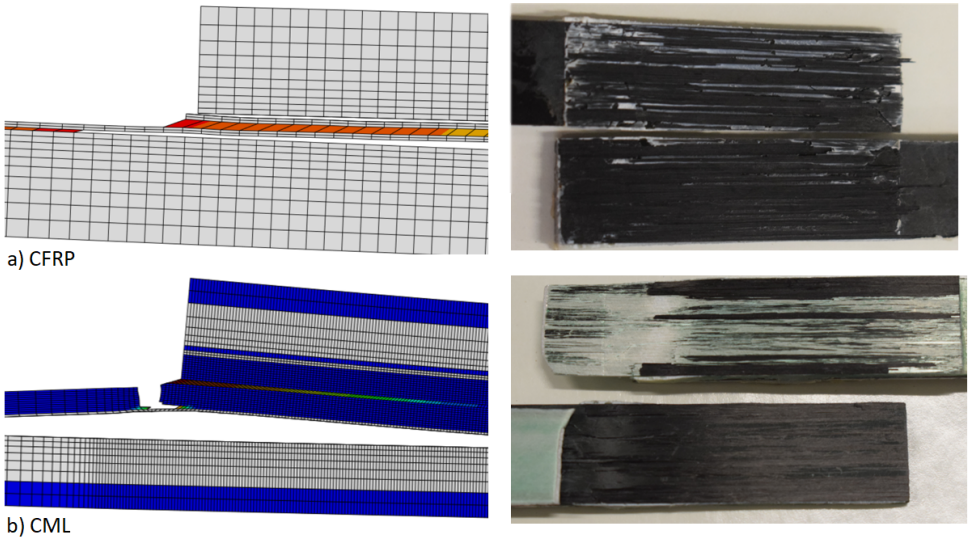

Figure A.29: Comparison between impact numerical and experimental failure modes obtained (XNR6852 E-3): a)CFRP; b)CML

Figure A.30 shows a summary of the performance of CML compared to CFRP joints for quasi-static and impact conditions, as well as the predictions of the numerical models.

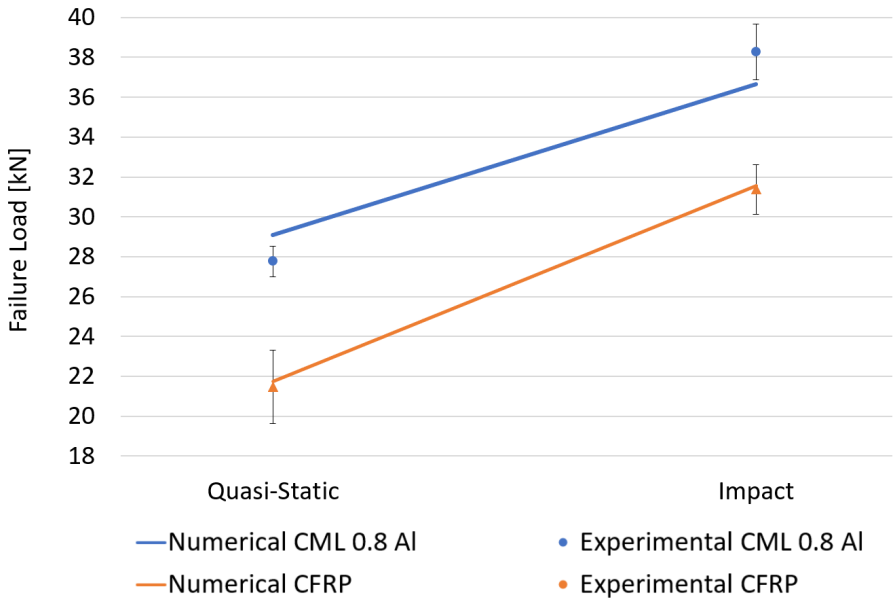

Figure A.30: Summary of CFRP vs CML 0.8 Al (XNR6852 E-3)

Unfortunately, this study was unable to confirm a study by Harris and Adams in 1985 [64], regarding the influence of the rigidity of adherends in impact scenarios . The study demonstrated that if a strong ductile adhesive was used, as is the case of the adhesives used, especially the XNR6852 E-3, the use of high strength substrates would result in high failure loads and low energy absorption, while using more ductile substrates would lower failure loads but increasing the energy absorbed during impact. With the two different configurations of CML joints being tested, the chance to observe this behaviour was theoretically possible, but since the failure type was different for the different configurations, delamination with aluminium fracture and cohesive failures, a comparison could not properly be made.

4.5 Summary of results

Table A.8 presents a concise summary of the quasi-static performance of all configurations tested, in respect to the failure load and mode. The performance of the reinforced joints is compared against the reference CFRP SLJ using the same adhesive.

Table A.8: Summary table of the experimental quasi-static results

Configuration	**Adhesive**	**Average Failure Load**	**Percentage change to CFRP**	**Failure Mode**
CFRP	AF 163-2K	17.89 ± 0.54	-	Delamination
CML 0.4 mm Al	AF 163-2K	23.10 ± 0.44	+29.15	Cohesive
CML 0.8 mm Al	AF 163-2K	21.94 ± 0.65	+22.69	Cohesive
CFRP	XNR 6852 E-3	21.47 ± 1.84	-	Delamination
CML 0.4 mm Al	XNR 6852 E-3	18.90 ± 1.25	-11.99	Delamination
CML 0.8 mm Al	XNR 6852 E-3	27.77 ± 0.76	+29.34	Delamination

The necessity of increasing the laminate thickness when using stiffer adhesives is well illustrated by the contrasting performance of the 0.4 mm thick aluminium reinforced configuration for the AF163-2k and the XNR6852 E-3.

Likewise, table A.9 presents the same information for impact conditions. Under impact, all configurations increased their failure loads when compared to their previous performance for quasi-static conditions, as was expected due to the strain-rate dependent behaviour of the adhesives. It can also be concluded that adhesive XNR6852 E-3 is more strain rate-dependent than the AF163-2k

Table A.9: Summary table of the experimental impact results

Configuration	**Adhesive**	**Average Failure Load**	**Percentage change to CFRP**	**Failure Mode**
CFRP	AF 163-2K	21.24 ± 1.21	-	Delamination
CML 0.4 mm Al	AF 163-2K	26.02 ± 1.44	+22.5	Delamination with Al fracture
CML 0.8 mm Al	AF 163-2K	29.89 ± 1.34	+40.73	Cohesive
CFRP	XNR 6852 E-3	31.38 ± 1.25	-	Delamination
CML 0.4 mm Al	XNR 6852 E-3	30.52 ± 2.23	-2.74	Delamination with Al fracture
CML 0.8 mm Al	XNR 6852 E-3	38.27 ± 1.40	+21.95	Delamination with Al fracture

5 Conclusions

The performance of metallic reinforcements of CFRP SLJs was analysed for two different epoxy-based adhesives and two loading conditions: quasi-static (1mm/min) and impact (3m/s).

The study shows that delamination could be limited by the use of aluminium metal laminates as reinforcement. The performance of the reinforced joints was shown to be very dependent on the adhesive used, and a correct selection of the thickness of the metallic laminates.

For the AF163-2k adhesive, a reinforcement with a 0.4 mm thick metal laminate was enough for satisfying improvements to be obtained. Compared to the CFRP-reference, the quasi-static failure load increased by almost 30 %, and delamination was avoided. Under impact, the increase in the failure load by 22.5 % was coupled with the doubling of the energy absorbed.

However, when a stronger and stiffer adhesive was used, the XNR 6852 E-3, the addition of the metallic reinforcement worsened the joint strength by delaminating earlier than the CFRP-only joint.

A numerical model able to analyse the peel stresses at the CFRP-Al interface was created, the weak spot in the reinforced joints. This analysis was carried out in order to guide the choice of aluminium sheet thickness to ensure an improvement of the SLJ strength. This model suggested that the use of 0.8 mm Al would fix the early delamination seen for XNR6852 E-3. This was experimentally validated, with the new geometry achieving

a similar positive performance for the new adhesive as the one observed previously for AF163-2K in terms of the increases observed for the failure loads.

The same configuration with 0.8 mm thick aluminium sheets using adhesive AF163-2K was the best performing for impact. This was the only configuration able to completely eliminate delamination for these conditions, increasing the failure load by 40%.

Finally, a good correlation between the numerical models and the experimental results was achieved for all configurations tested and different loading conditions. The failure loads determined numerically were validated experimentally with minimal errors and the numerical failure modes correctly depicted the experimentally obtained failures.

References

[1] The new-technology boeing 787 dreamliner, which makes extensive use of composite materials, promises to revolutionize commercial air travel. Technical report, Aviation Week & Space Technology Market Supplement, 2005.

[2] Mrazova Maria. Advanced composite materials of the future in aerospace industry. *Incas Bulletin*, 5:139–150, 09 2013.

[3] Airbus. Experience and lessons learned of a composite aircraft. ICAS2016, 30th Congress of the International Council of the Aeronatuical Sciences, 2016.

[4] A.P. Mouritz. Review of z-pinned composite laminates. *Composites Part A: Applied Science and Manufacturing*, 38(12):2383 – 2397, 2007.

[5] Prasad Potluri, Paul Hogg, Mubeen Arshad, Dhaval Jetavat, and Peiman Jamshidi. Influence of fibre architecture on impact damage tolerance in 3d woven composites. *Applied Composite Materials*, 19, 10 2012.

[6] P. Potluri, A. Rawal, M. Rivaldi, and I. Porat. Geometrical modelling and control of a triaxial braiding machine for producing 3d preforms. *Composites Part A: Applied Science and Manufacturing*, 34(6):481 – 492, 2003. ICMAC 2001 - International Conference for Manufacturing of Advanced Composites.

[7] Akinori Yoshimura, Tomoaki Nakao, Shigeki Yashiro, and Nobuo Takeda. Improvement on out-of-plane impact resistance of cfrp laminates due to through-the-thickness stitching. *Composites Part A: Applied Science and Manufacturing*, 39(9):1370 – 1379, 2008.

[8] Laura Hader-Kregl, Gernot M. Wallner, Christoph Kralovec, and Carola Eyßell. Effect of inter-plies on the short beam shear delamination of steel/composite hybrid laminates. *The Journal of Adhesion*, 0(0):1–13, 2018.

[9] X Shang, EAS Marques, JJM Machado, RJC Carbas, D Jiang, and LFM da Silva. A strategy to reduce delamination of adhesive joints with composite substrates. *Proceedings of the Institution of Mechanical Engineers, Part L: Journal of Materials: Design and Applications*, 233(3):521–530, 2019.

[10] L.B Vogelesang and A Vlot. Development of fibre metal laminates for advanced aerospace structures. *Journal of Materials Processing Technology*, 103(1):1 – 5, 2000.

[11] D. F. Silva, E. C. Botelho, A. C. Ancelotti JR, and C. A. Damato. Environmental conditioning effects on the mechanical properties of titanium fiber-metal laminates. *Composite Materials, 19th International Conference on, July 28eAugust 2, 2013*, 2013.

[12] Y. Liu and M. Ehrhardt. *Frontiers in Aerospace Science: Aerospace Structures and Materials*. Frontiers in Aerospace Science, Volume 1 Series. Bentham Science Publishers, 2016.

[13] Freddy Moriniere. *Low-velocity impact on fibre-metal laminates*. PhD thesis, Technische Universiteit Delft, 2012.

[14] A. Vlot. Impact loading on fibre metal laminates. *International Journal of Impact Engineering*, 18(3):291 – 307, 1996.

[15] Raj Das, Avishek Chanda, J Brechou, and Arnab Banerjee. Impact behaviour of fibre-metal laminates. pages 491–542, 02 2016.

[16] Ankush P. Sharma, Sanan H. Khan, Rajesh Kitey, and Venkitanarayanan Parameswaran. Effect of through thickness metal layer distribution on the low velocity impact response of fiber metal laminates. *Polymer Testing*, 65:301 – 312, 2018.

[17] Patryk Jakubczak, Jarosław Bieniaś, and Barbara Surowska. 12 - impact resistance and damage of fiber metal laminates. In Vijay Kumar Thakur, Manju Kumari Thakur, and Asokan Pappu, editors, *Hybrid Polymer Composite Materials*, pages 279 – 309. Woodhead Publishing, 2017.

[18] Shengqing Zhu and Gin Boay Chai. Low-velocity impact response of fibre–metal laminates – experimental and finite element analysis. *Composites Science and Technology*, 72(15):1793 – 1802, 2012.

[19] A.A. Ramadhan, Abdul Rahim Abu Talib, Azmin Shakrine Mohd Rafie, and R. Zahari. The behaviour of fibre-metal laminates under high velocity impact loading with different stacking sequences of al alloy. In *AEROTECH IV*, volume 225 of *Applied Mechanics and Materials*, pages 213–218. Trans Tech Publications Ltd, 11 2012.

[20] E. Sitnikova, Z.W. Guan, G.K. Schleyer, and W.J. Cantwell. Modelling of perforation failure in fibre metal laminates subjected to high impulsive blast loading. *International Journal of Solids and Structures*, 51(18):3135 – 3146, 2014.

[21] A. Vlot. Impact properties of fibre metal laminates. *Composites Engineering*, 3(10):911 – 927, 1993.

[22] R.D.S.G. Campilho, M.F.S.F. de Moura, and J.J.M.S. Domingues. Modelling single and double-lap repairs on composite materials. *Composites Science and Technology*, 65(13):1948 – 1958, 2005.

[23] José Machado, EAS Marques, Raul Campilho, and L.F.M. Silva. Mode i fracture toughness of cfrp as a function of temperature and strain rate. *Journal of Composite Materials*, 51, 12 2016.

[24] J.J.M. Machado, E.A.S. Marques, R.D.S.G. Campilho, and Lucas F.M. da Silva. Mode ii fracture toughness of cfrp as a function of temperature and strain rate. *Composites Part B: Engineering*, 114:311 – 318, 2017.

[25] Zainul Huda, Iskandar Taib, and Tuan Zaharinie. Characterization of 2024-t3: An aerospace aluminum alloy. *Materials Chemistry and Physics*, 113:515–517, 02 2009.

[26] W. Brockmann, O.D. Hennemann, H. Kollek, and C. Matz. Adhesion in bonded aluminium joints for aircraft construction. *International Journal of Adhesion and Adhesives*, 6(3):115 – IN1, 1986.

[27] T.J. De Vries and C.A.J.R. Vermeeren. R-curve testdata: 2024-t3, 7075-t6, glare 2 and glare 3. Delft University of Technology, 1995.

[28] 3M. 3m scotch-weld structural adhesive film af 163-2k technical datasheet. Technical report, 3M, 2009.

[29] D.G. dos Santos, R.J.C. Carbas, E.A.S. Marques, and L.F.M. da Silva. Reinforcement of cfrp joints with fibre metal laminates and additional adhesive layers. *Composites Part B: Engineering*, 165:386 – 396, 2019.

[30] Miguel Palmares. Strength of hybrid laminates aluminium carbon-fibre joints with different lay-up configurations. Master Thesis, Faculdade de Engenharia da Universidade do Porto, 2016.

[31] M. A. Morgado, R.J.C. Carbas, D.G. dos Santos, and L.F.M. da Silva. Reinforcement of cfrp single lap joints using adhesive layers. 2019.

[32] José Machado, A Hayashi, PDP Nunes, EAS Marques, RJC Carbas, and C Sato. Strain rate dependence of a crash resistant adhesive as a function of temperature for the automotive industry. *Proceedings of the Institution of Mechanical Engineers, Part L: Journal of Materials: Design and Applications*, page 146442071983691, 03 2019.

[33] H.A.M. Araújo, J.J.M. Machado, E.A.S. Marques, and L.F.M. da Silva. Dynamic behaviour of composite adhesive joints for the automotive industry. *Composite Structures*, 171:549 – 561, 2017.

[34] ASTM D5868 01(2014). Standard test method for lap shear adhesion for fiber reinforced plastic (frp) bonding. Technical report, ASTM, 2014.

[35] Diogo P.C. Antunes, António M. Lopes, Carlos M.S. Moreira da Silva, Lucas F.M. da Silva, Paulo D.P. Nunes, Eduardo A.S. Marques, and Ricardo J.C. Carbas. Development of a drop weight machine for adhesive joint testing. Accepted for publication, 2019.

[36] Khaled Giasin, Sabino Ayvar-Soberanis, Toby French, and Vaibhav Phadnis. 3d finite element modelling of cutting forces in drilling fibre metal laminates and experimental hole quality analysis. *Applied Composite Materials*, 24(1):113–137, Feb 2017.

[37] G.H. Majzoobi and F. Rahimi Dehgolan. Determination of the constants of damage models. *Procedia Engineering*, 10:764 – 773, 2011. 11th International Conference on the Mechanical Behavior of Materials (ICM11).

[38] M Burley, JE Campbell, J Dean, and TW Clyne. Johnson-cook parameter evaluation from ballistic impact data via iterative fem modelling. *International Journal of Impact Engineering*, 112:180 – 192, 2018.

Paper B

Reinforcement of CFRP Single Lap Joints with Adhesive Layers

M. A. Morgado[1], R.J.C Carbas[1,2], D.G. dos Santos[1], L.F.M da Silva[1]

[1]Department of Mechanical Engineering, Faculty of Engineering, University of Porto, Portugal

[2]Institute of Science and Innovation in Mechanical and Industrial Engineering (INEGI), Faculty of Engineering, University of Porto, Portugal

Abstract: Usage of composite materials like Fibre Reinforced Plastics for structural applications has been increasing in recent years. Delamination of adhesively bonded composite joints is a concern as it causes premature failure of the bond. A technique to reduce delamination in CFRP single lap joints (SLJs) by inserting additional adhesive layers in the adherends is analysed for quasi-static and impact conditions, with satisfactory results. For quasi-static conditions failure by delamination is avoided, while for a low velocity impact scenario its onset is delayed. In both cases the failure load is increased. A numerical model using finite element analysis is developed in ABAQUS to study the performance of the best configuration. Experimental and numerical results are compared.

Keywords: CFRP; Adhesive Bonding; Reinforcements; Composite Materials; Delamination; Mechanical; Impact; Numerical.

1 Introduction

Composites like fibre reinforced plastics (FRP) have been used more frequently in structural applications during the last decades, as was expected with the increase of knowledge of their properties and behaviour under different conditions like loading conditions, and under different temperatures or strain rates. They found their first use in military aircraft construction during World War II, having then spread to the aerospace industry and commercial aircraft industry. These industries must create structures with strong yet light structures, which plays plays right into one of composites major advantages: their extremely high specific strength and stiffness. The increase in material and manufacturing costs are then offsetted by reduced fuel consumption and emissions detrimental to the environment [1, 2]. Composite materials are therefore replacing more traditional

construction materials, such as steel or aluminium. Moreover, they have excellent fatigue properties and corrosion resistance [3].

The two aerospace giants Airbus and Boeing, already have models with composite materials representing half of the aircraft structural weight, the A350 and the 787 Dreamliner respectively, enhancing fuel economy whilst reducing maintenance times and operating costs [4–6]. However, aircraft manufacturers must find a balance between weight reduction and structural integrity, price/durability and, despite the increase in composite materials usage, metallic materials like high-strength low-alloy steel and titanium are expected to continue to be fundamental.

Due to their low bearing and shear strengths and the higher notch sensitivity when compared to metals [7], composite materials experience a major decrease in their mechanical properties when holes are drilled for joining methods like riveting or bolting. Adhesive bonding technology is therefore seen as the best option for joining composite materials, and it's a crucial technology for enabling large scale use of composites. Although adhesive bonding prevents the components from being detached for inspection or replacement unlike a mechanical coupling would, it allows for a higher joint stiffness, more uniform stress distribution while minimising added weight.

Delamination is another phenomenon that could occur when bonding composite substrates due to peak peel stresses at the extremities of the overlap in a SLJ, combined with low transverse tensile strength in the through-thickness direction, can cause premature interlaminar failure [8,9]. This can be mitigated using several techniques such as adherend and adhesive shaping and the utilisation of z-pins while the maximum stress values can be reduced by changing the geometry of the joint at the ends of the overlaps, by tapering the adherend and/or filleting the adhesive. This can often be the solution to prevent/retard the onset of delamination and force the failure to occur on the adhesive increasing the joint strength [10–12].

This study aims to study the influence of additional adhesive layers in reinforcing the peel strength of composite materials, based on the concept of introducing additional adhesive layers between laminae of the basic CFRP material. An adhesive with ductile properties and lower stiffness than the epoxy used in the CFRP prepreg was selected given previous studies showing that low strength, yet flexible adhesives outperform stronger but stiffer adhesives in delamination prevention [13–15].

Ideally, these layers can help better distribute the stress than the rigid epoxy and act as a damper in impact scenarios increasing overall toughness. Several material configurations were suggested for a CFRP adherend, and the failure loads modes were studied in order to identify the best performing joint.

A numerical study was carried out using a Finite Element Analysis (FEA). Cohesive zone models (CZMs) based on adhesive triangular/trapezoidal laws were used to simulate the fracture behaviour of CFRP only and hybrid adhesive carbon-fibre joints [16].

Due to the strain rate dependency of adhesives, fracture tests like TAST (Thick Ad-

herend Shear Test), DCB (Double Cantilever Beam) and ENF (End Notched Flexure) were carried out in order to experimentally obtain the necessary properties for the numerical simulation.

2 Experimental Details

2.1 Adherend

The CFRP used in this work was supplied by CIT Composite Materials from Italy, a 0° oriented carbon-epoxy composite prepreg roll sold under the product name HS 160 T700.

The CFRP elastic orthotropic properties were previously determined by Campilho et al. 2005 [17] and can be found on Table B.1.

Table B.1: CFRP elastic orthotropic properties [17]

Ex **(MPa)**	***Ey*** **(MPa)**	***Ez*** **(MPa)**	ν**xy**	ν**yz**	ν**xz**	***Gxy*** **(MPa)**	***Gyz*** **(MPa)**	***Gxz*** **(MPa)**
109000	8819	8819	0.342	0.342	0.38	4315	4315	3200

2.2 Adhesive

The adhesive used was the 3M Scotch Weld AF 163-2k, a "thermosetting modified epoxy structural adhesives in film form". [18] The film form with knit-supporting made it ideal for application in adhesively reinforced joints, with a clean manufacturing process and easy control of the bondline thickness. The adhesive was cured following manufacturer's recommendations, at 130°C for 1 hour.

2.3 Singe Lap Joints

The manufactured SLJs were based on the geometry shown in Figure B.1.

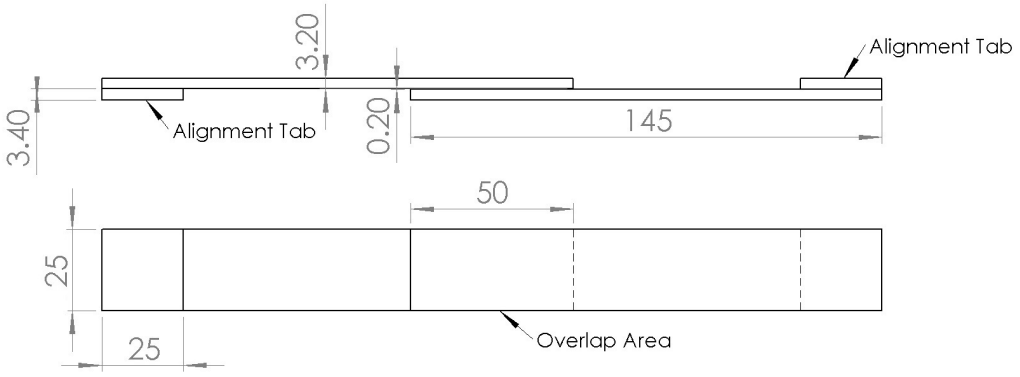

Figure B.1: Single Lap Joint Geometry (dimensions in mm)

For the stacking process of the final adherends a hand lay-up method was used, by stacking the metal laminates, the CFRP and the adhesive, in such a way, that the proposed configurations were obtained. To obtain a unidirectional final plate, every single layer must have the fibres oriented in the same direction as the previous one. The number of layers stacked in each configuration varied according with the lay-up, in such a way that the final adherends could be approximately 3.2 mm thick for all the specimens manufactured.

All adherends were manufactured by a hand lay-up method. For the Adhesive Layer Reinforced substrates, composite plies were replaced by a layer of adhesive creating three different configurations, Figure B.2. The number of CFRP layers stacked in each configuration varied depending on the lay-up configuration, in such a way that the final adherend had approximately 3.2 mm thickness for all the specimens manufactured.

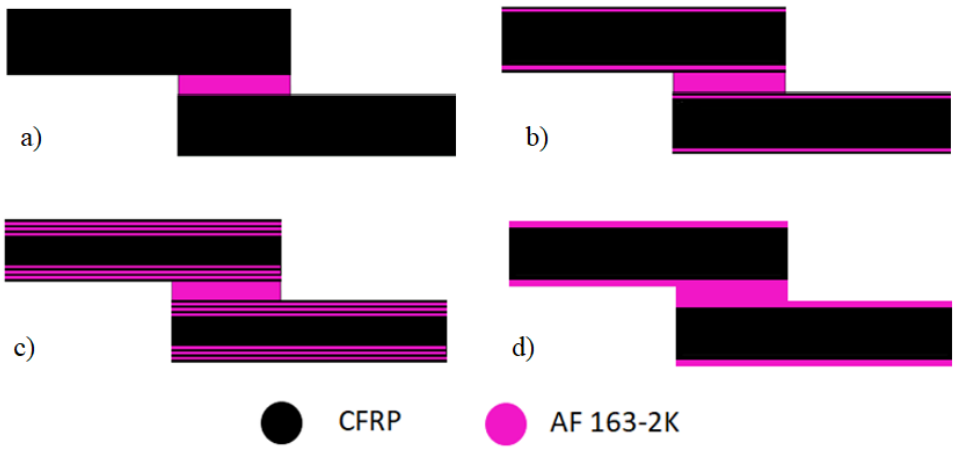

Figure B.2: Tested Configurations:a) CFRP-only b) 1 interlaminar adhesive layer; c) 3 interlaminar adhesive layers; d) 1 superficial adhesive layer

For the first configuration studied an adhesive layer is placed between the first and second layers of CFRP on each side of the adherend. For the second, 3 adhesive layers instead of 1 are used following the same alternate CFRP-ply adhesive layer. In the last configuration the top layer of CFRP is replaced by a superficial layer of adhesive on both sides of the adherend.

2.4 Testing Conditions

For quasi-static conditions the SLJs were tested using an Instron 8801 servo-hydraulic testing machine with a load cell of 100 kN at a constant crosshead speed of 1mm/min, according to the standard ASTM D5868 - 01(2014) [19].

For impact conditions, a drop-weight impact testing machine developed in-house was used [20]. This machine is capable of dropping a 56 kg mass off a maximum height of 1.27 m, achieving an impact speed of 5 m/s.

The displacements were indirectly obtained by trapezoidal integration of the load with

time, and validated using high speed camera footage.

The impact speed used was 3m/s for a weight of 31.3 kg, resulting in an impact energy of 140.85 J.

All tests were performed at laboratory ambient conditions (room temperature of 24°C, relative humidity of 55%), and repeated a minimum 5 times for each configuration tested.

3 Characterisation of the adhesive

The mechanical properties of the adhesive AF163-2K for quasi-static conditions (1mm/min) were determined by Palmares (2016) [21] and Gomes et al. (2019) [22].

Table B.2: Adhesive 3M Scotch-Weld AF 163-2k quasi-static properties [21, 22]

Young's Modulus [MPa]	1521.87 ± 118.29
Tensile strength [MPa]	46.93 ± 0.63
Shear strength [MPa]	46.86 ± 2.57
Shear Modulus* [MPa]	563.67
$\boldsymbol{G_{IC}}$ **(1mm/min) [N/mm]**	4.05 ± 0.07
$\boldsymbol{G_{IIC}}$ **(1mm/min) [N/mm]**	9.77 ± 0.21

* deducted from the Young's modulus

In order to determine the necessary properties of the adhesive for low velocity impact (3m/s) conditions, additional DCB (Double Cantilever Beam), ENF (End Notch Flexure) and TAST (Thick Adherend Shear Test) tests were performed.

3.1 Specimen Manufacturing

DCB and ENF tests use the same specimen geometry, shown in Figure B.3. Steel adherends were used to minimise the effect of plastic deformation during the test loading.

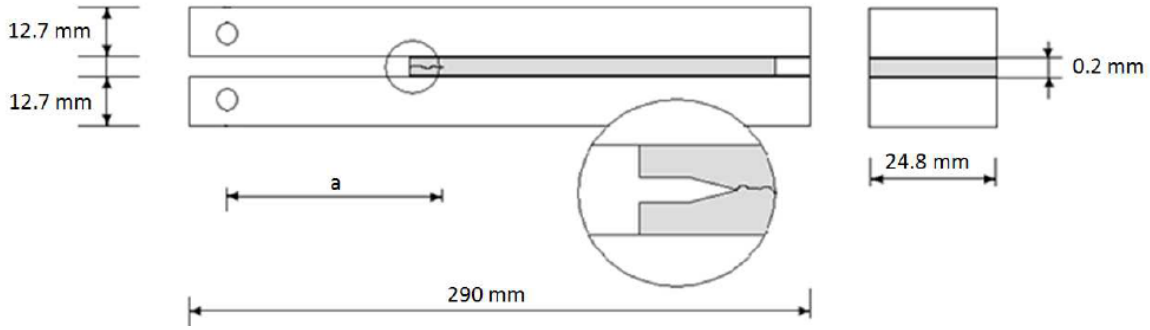

Figure B.3: DCB and ENF specimen geometry [22]

To promote a good adhesion the surface of the adherends was grit blasted and degreased with acetone.

To control the thickness of the adhesive layer, even though the adhesive being tested had knit supporting capabilities, additional precautionary measures were taken by adding calibrated steel spacers at the ends of the bonded area.

At the crack initiation zone, and in between the steel spacers a sharp blade was placed, introducing a pre-crack in the adhesive layer at mid adhesive thickness. The placement of this blade establishes the value for the initial crack length, a_0, of 44.6 mm.

TAST specimens were manufactured in accordance to the ISO 11003-2 standard [68], concerning test methods of an adhesive shear shear behaviour. The specimen geometry, which can be seen in Figure B.4, creates an adhesive bond area of 162.5 mm^2.

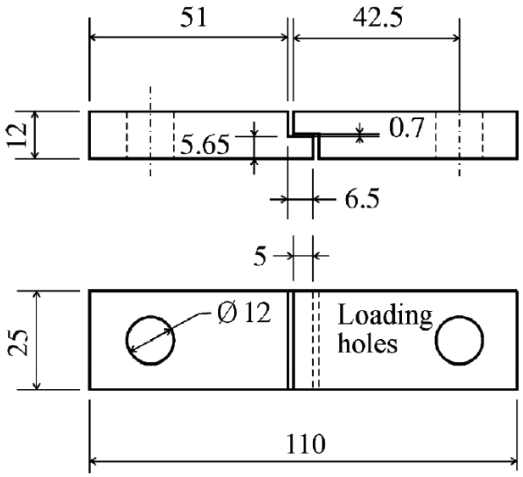

Figure B.4: TAST specimen geometry (dimensions in mm) [23]

3.2 DCB

The DCB and ENF tests use the same specimen geometry but differ in the load application method. To replicate pure peel mode I loading the specimen is loaded in the direction perpendicular to the adhesive layer for DCB testing [24], as shown in Figure B.5.

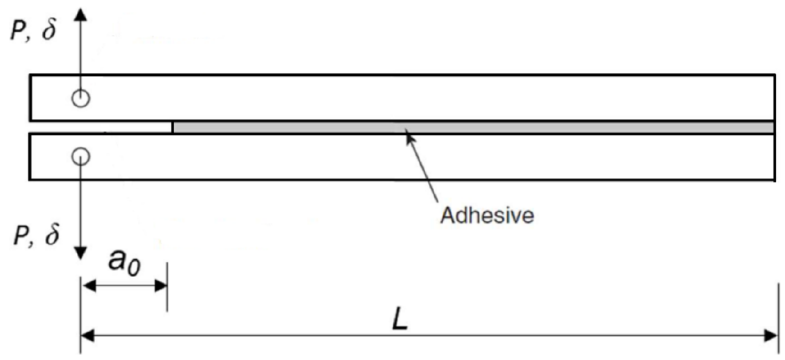

Figure B.5: Schematic representation of a DCB test

The fracture energy in mode I for AF 163-2k was previously determined to be 4.05 ± 0.07 N/mm for a testing speed of 0.2 mm/min [22].

For the low velocity impact testing speed of 3m/s, 3 specimens were tested using a drop-weight machine. A cohesive failure was obtained.

During crack propagation, the values of the load (P) and displacement (δ) were recorded, the first by the machine's load cell and the second indirectly by integration of the loads obtained. The displacement data was further validated with the help of high speed camera footage, B.6.

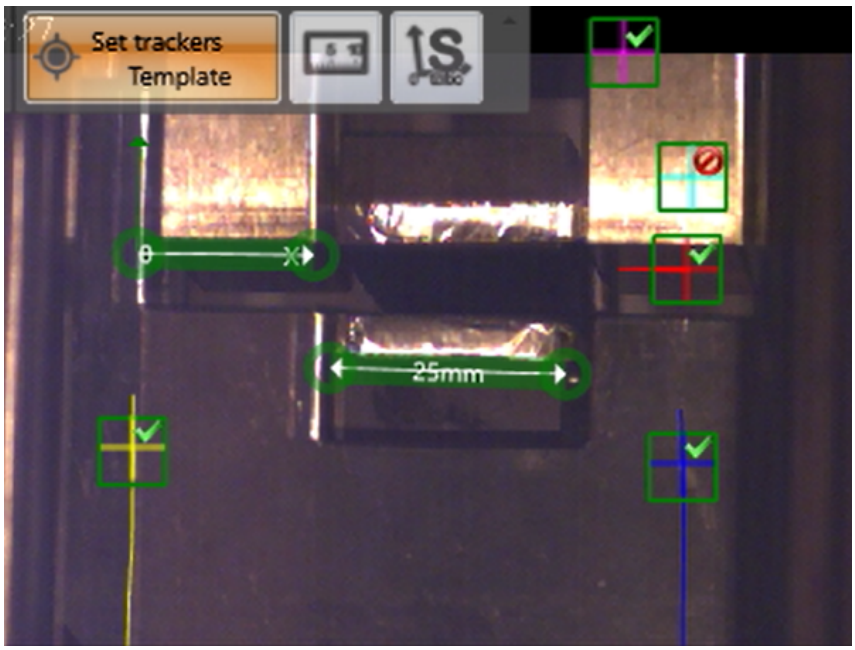

Figure B.6: High-speed Camera footage of DCB testing

Using the Compliance Based Beam Method (CBBM) data reduction scheme developed by de Moura et al. (2008) [25], that introduced a crack equivalent concept to DCB testing, the fracture energy in mode I could be calculated without measuring the crack length throughout the test duration, something impossible to do for impact testing. G_{IC} was obtained using the following expression

$$G_{\mathrm{Ic}} = \frac{6P^2}{B^2 h}\left(\frac{2a_{\mathrm{e}}^2}{h^2 E_{\mathrm{f}}} + \frac{1}{5G_{13}}\right) \tag{5}$$

where, E_f and G_{13} are, respectively, the corrected bending modulus and shear modulus of the specimens and a_{eq} is the equivalent crack length, estimated from the specimen compliance. B and h are specimen geometry parameters, the width of the specimen and the height of the adhesive layer respectively. P is the load obtained from the load-displacement curve.

The mode I fracture energy for AF163-2k at 3 m/s was experimentally determined to be 6.06 ± 0.30 N/mm.

3.3 ENF

For ENF tests, to induce shear stresses in the adhesive layer, three point bending loading is applied. A schematic representation of the test can be seen in Figure B.7. However, this test could not be performed for the impact velocity of 3m/s, due to excess plastic deformation of the steel specimens.

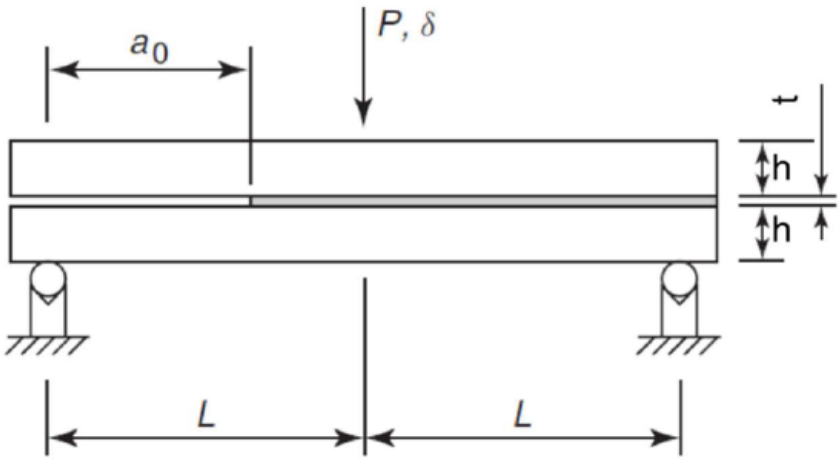

Figure B.7: Schematic representation of an ENF test

The fracture energy in mode II of 3 specimens was determined for a crosshead test speed of 100mm/min for, which in conjunction with the previously determined fracture toughness for quasi-static conditions, enables the logarithmic extrapolation of the G_{IIC} for 3m/s. The extrapolation of fracture energies using a logarithmic relation was first proposed by Zgoul and Crocombe and later [66] validated by Avendaño et al. [67].

The CBBM method for ENF specimens [26] was used. Just like for mode I, CBBM for ENF testing also does not require the measurement of the crack length. The fracture energy in mode II was calculated using the following expression

$$G_{IIc} = \frac{9P^2a_{eq}^2}{16B^2E_fh^3} \tag{6}$$

The fracture energy in mode II for 100mm/min was determined to be 13.83 ± 0.85 N/mm, which after logarithmically extrapolating to 3m/s corresponds to 18.73 N/mm.

3.4 TAST

Three TAST specimens were tested on the same drop-weight testing machine speed used for DCB testing for the same impact velocity of 3m/s. An average shear strength of 41.40 MPa with a standard deviation of 4.21 MPa was determined. Because of the small bond area typical TAST specimens, and the sudden violent nature of impact testing the precision of the measurement of the displacement of this test was not enough to accurately calculate the value of the shear modulus.

3.5 Results of adhesive characterisation under impact

The mechanical properties determined are shown in the summary Table B.3

Table B.3: AF 163-2k impact properties (3 m/s)

G_{IC} [N/mm]	6.06 ± 0.30
G_{IIC}* [N/mm]	18.73
Shear strength [MPa]	41.40 ± 4.21

* logarithmically extrapolated

4 Experimental Results

All adhesively reinforced SLJ configurations tested showed improvements in the failure load achieved when compared to the reference CFRP-only joint.

The best performing configuration, superficial/interface reinforcement, increased the reference joint average failure load of 29.82 ± 0.54 kN by 23.27 % to 36.76 ± 0.58 kN.

Typical load-displacement curves for the studied configurations can be seen in Figure B.8.

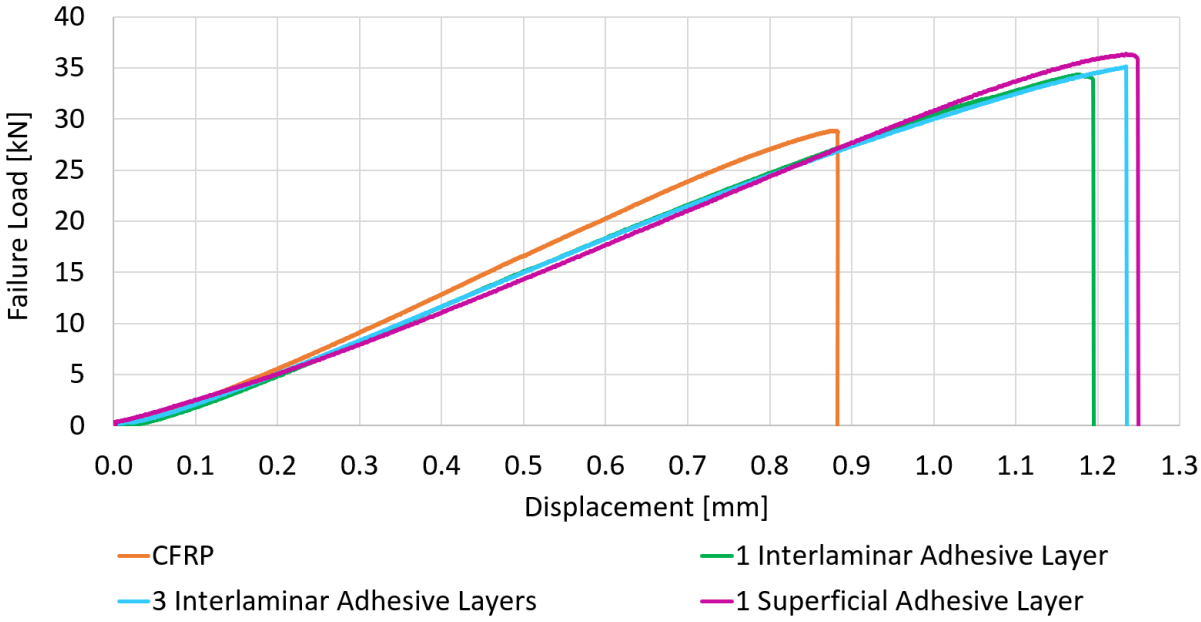

Figure B.8: Typical Quasi-Static P-δ curves for the configurations tested

Using a flexible adhesive with better mechanical properties than the epoxy resin bounding the fibres, the surface is toughened, and instead of the stresses being concentrated on the CFRP matrix at the ends of the overlaps, it is redistributed and absorbed along the superficial adhesive layer. Because of this, delamination was prevented for the final configuration and a cohesive failure mode was obtained.

For the interlaminar configurations although delamination could not be avoided, it was delayed, consequence of the absorbed stresses in the through thickness direction by the more flexible layers. The delamination path was also multi-layered, taking place through all the composite laminae in contact with the adhesive layers, increasing the energy needed to complete the delamination process - increasing the average failure load.

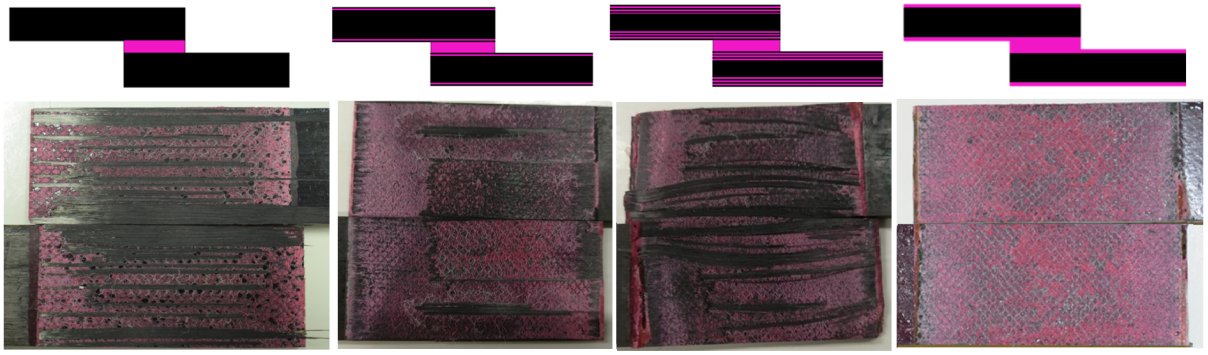

Figure B.9: Failure modes for the configurations tested under quasi-static conditions

The joint with the best quasi-static performance, the configuration reinforced at the CFRP-Adhesive interface, henceforth referred to as ALR was then tested under impact at 3m/s.

Typical load-displacement curves of these joints compared to a reference CFRP-only joint is shown in Figure B.10.

The adhesively reinforced specimen not only has a higher average failure load than the CFRP-only joint, but also a higher average displacement.

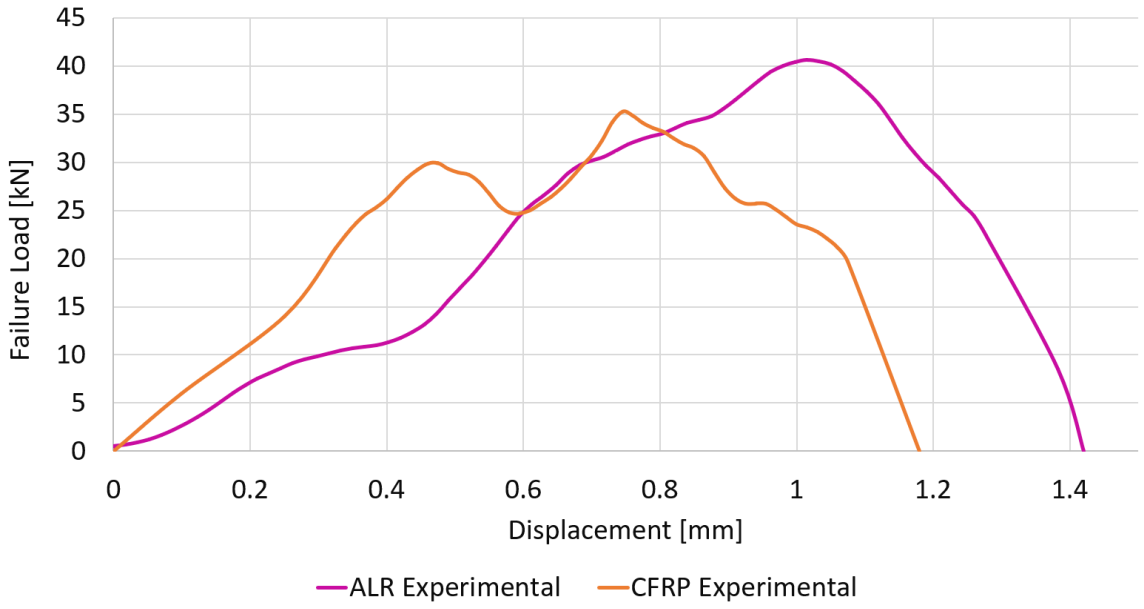

Figure B.10: Typical Impact P-δ curves for ALR and CFRP specimens

The superficial adhesive reinforcement increased the failure load of the CFRP-only joint of 35.41 $\pm$ 1.21 kN to 41.49 $\pm$ 1.42 kN, a percentage increase of 17.2%.

The areas beneath a load-displacement curve representing the work done by the specimen, or rather, the energy dissipated during the impact. The combination of a higher failure load and larger displacement for the ALR joint directly translates into a greater area, and thus energy absorption capabilities almost 22% greater than the CFRP-only SLJ.

The failure mode for the reference CFRP-only joint was delamination. For ALR joints, even though a few specimens showed a cohesive failure for impact conditions, the main failure mode was also delamination.

The change of failure mode from cohesive to delamination for the ALR joints can be attributed to the strain-rate dependency of the adhesive. For a higher strain rate, the adhesive becomes stronger and loads the CFRP matrix with more peel stresses than for quasi-static conditions, surpassing the peel strength of the CFRP.

5 Numerical Models

The numerical models were developed using ABAQUS. The FE analysis was carried out with the aim of predicting the failure load and failure mode of the modelled joints.

Two models were used, one for quasi-static conditions and one for the impact scenario. Both were based on a 2D planar deformable shell part and differed only in boundary conditions and the step-type analysis used.

Figure B.11 shows the boundary conditions used. An encastre is used in one of the extremities to replicate the gripping system. For the other end of the SLJ for quasi-static conditions (tensile testing) a displacement of 5 mm was imposed, and for impact conditions (drop-weight) a mass with the same weight as the one dropped on the specimen was modelled and given the same speed as the impactor, 3m/s.

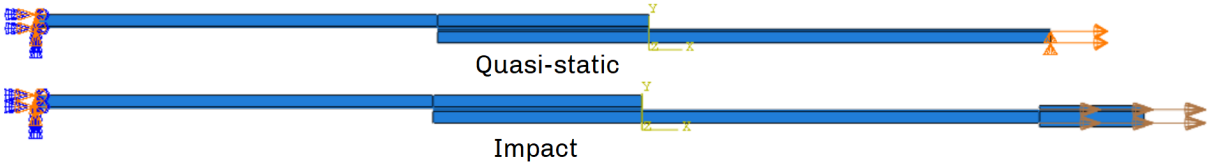

Figure B.11: Modelled boundary conditions

Static general and a dynamic explicit steps were used for quasi-static and impact conditions respectively.

The material properties previously shown in the experimental details section were used for the numerical modelling.

5.1 CFRP

A 0.2 mm adhesive layer, the same thickness of the adhesive layer in the real joint, was modelled with cohesive elements. Two triangular traction-separation laws, one for quasi-

static conditions and another for impact conditions, based on the properties previously presented, were used to model the adhesive behaviour.

Elastic orthotropic properties (engineering constants) were used for modelling the sections of CFRP substrates where no delamination is thought to occur.

Delamination failure of the CFRP was modelled by adding a 0.15 mm of thick layer of cohesive elements at a distance of 0.15 mm from the interface between adhesive and CFRP. The thickness of 0.15 mm corresponds to one ply of the prepreg used to manufacture the CFRP substrate. Cohesive properties of CFRP were used in these section's material properties.

The sections of the CFRP-only model can be seen in Figure B.12.

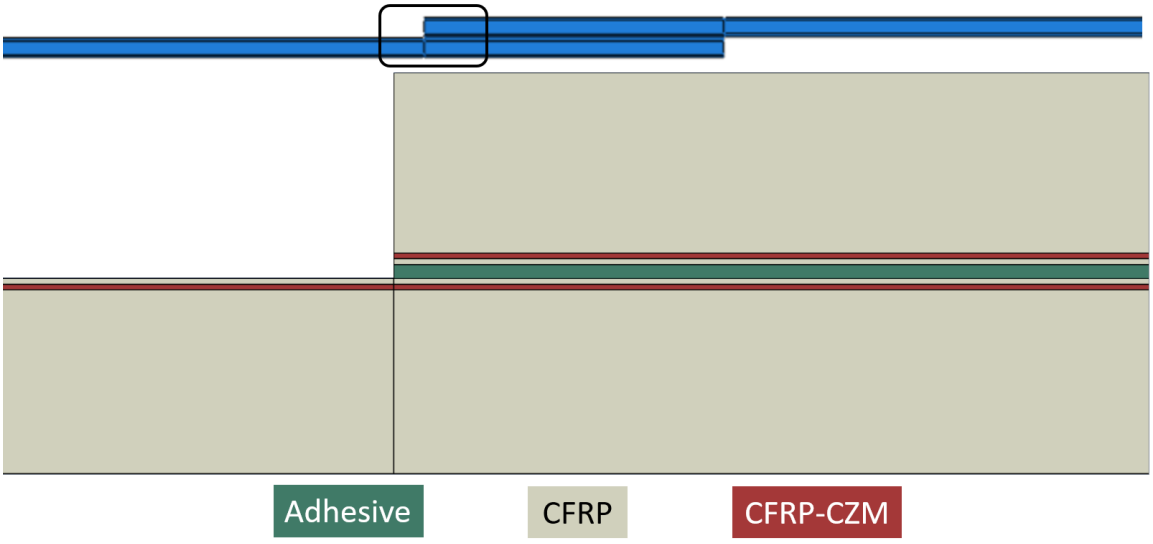

Figure B.12: CFRP-only model

5.2 ALR

The model used for ALR joint is shown in Figure B.13. Elastic and cohesive layers of the adhesive were placed on the tops of the adherend. With the sections used, possible numerical failure scenarios would include cohesive failure in the adhesive bond area, cohesive failure in the adhesive placed on the adherends and delamination of the CFRP. For quasi-static conditions since the observed failure was cohesive in nature no CFRP delamination was modelled.

The elastic sections of CFRP and adhesive used four-node plane strain elements (CPE4R). Finally, for the cohesive sections, adhesive and CFRP, a 4-node two-dimensional cohesive element, COH2D4, was employed.

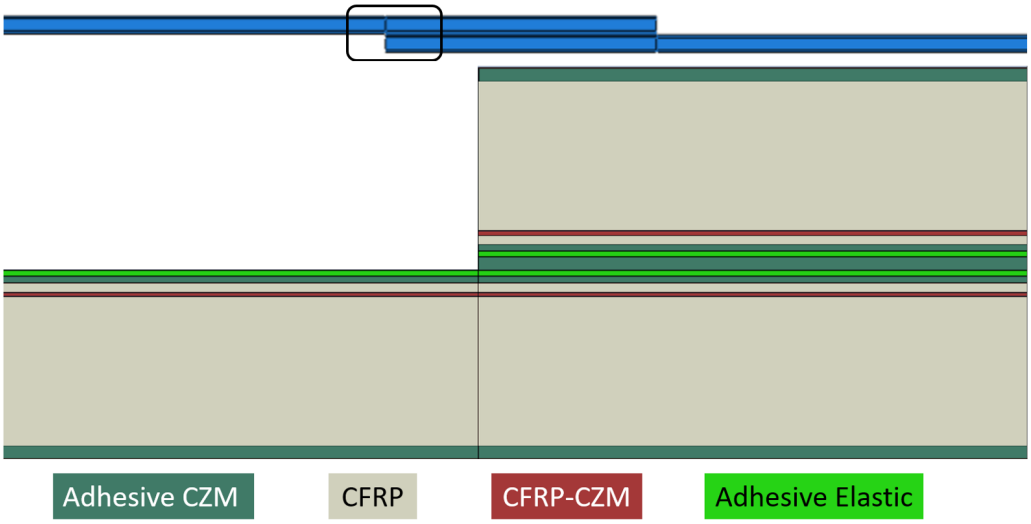

Figure B.13: ALR model

5.3 Numerical results

The numerical model correlated very well with the experimental results. The failure loads were predicted with minimal error for both CFRP-only and ALR joints. Figure B.14 shows a comparison between the numerically generated and typical experimentally obtained quasi-static load displacement curves.

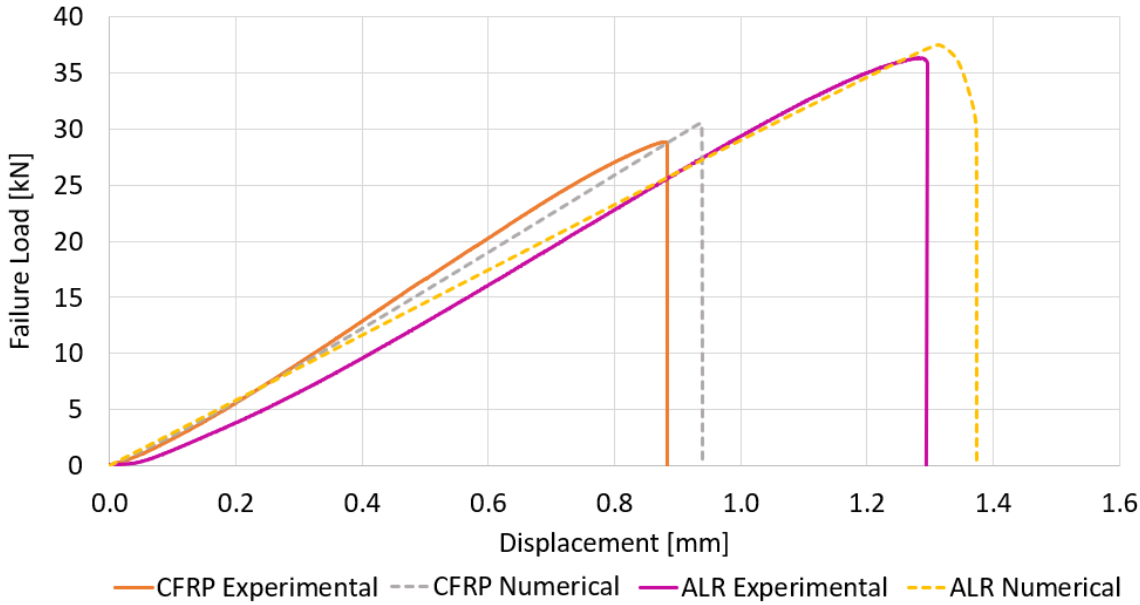

Figure B.14: Numerical vs Experimental quasi-static P-δ curves for CFRP

The failure modes obtained experimentally were also correctly replicated on the numerical models: delamination for CFRP-only and cohesive for ALR. It appears however that the cohesive failure in the ALR travels irregularly throughout the adhesive layer bonding the joint and the reinforcement layers of adhesive reinforcing the adherend. Figure B.15 shows a comparison between the numeric and experimental failures.

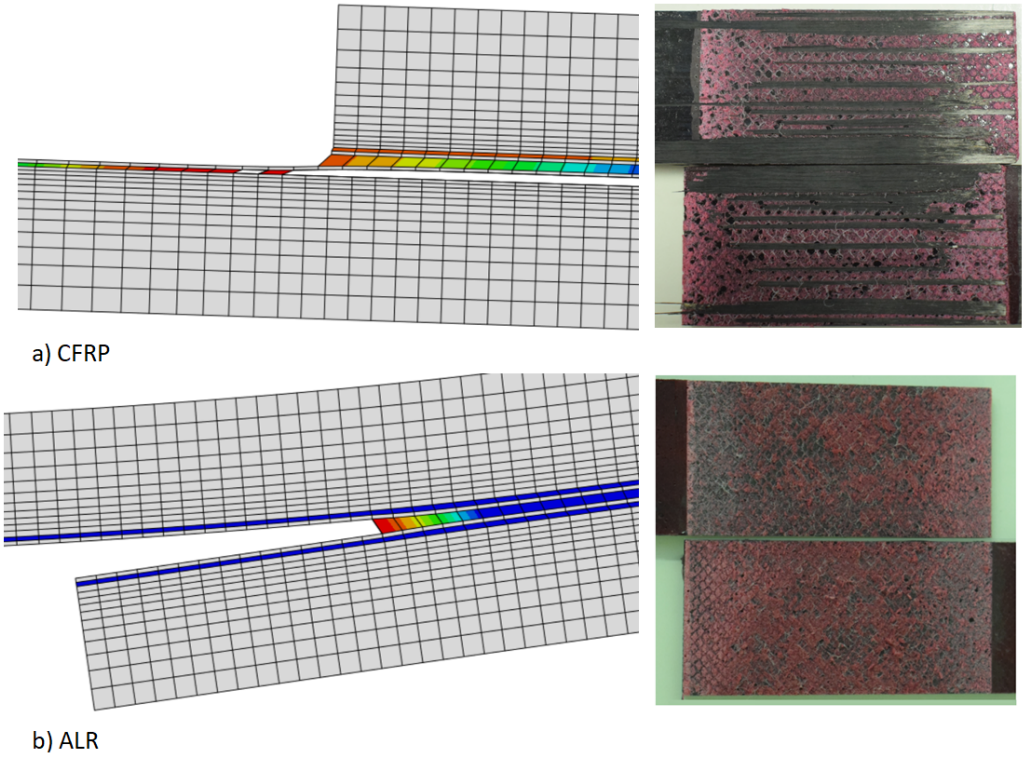

Figure B.15: Comparison between quasi-static numerical and experimental failure modes obtained: a) CFRP; b) ALR

The behaviour of the joints for impact conditions was also accurately predicted by the numerical models. The failure loads obtained numerically were within a 3% error of the experimental results. The load-displacement curve comparison between the numerical and experimental results can be seen in Figures B.16 and B.17, for the CFRP-only joint and ALR joint respectively.

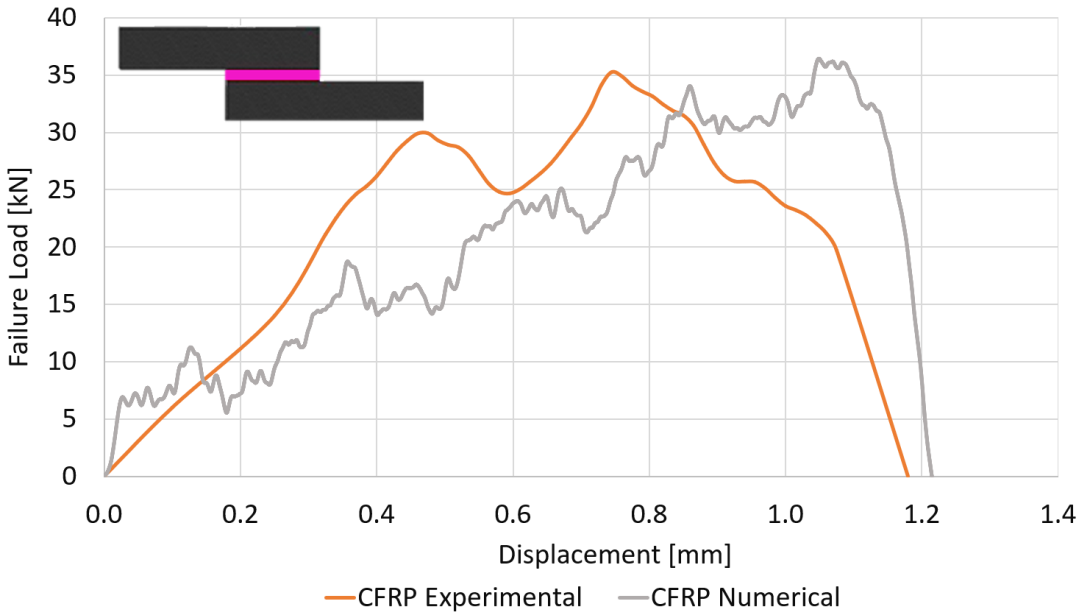

Figure B.16: Numerical vs Experimental P-δ curves for CFRP under impact conditions

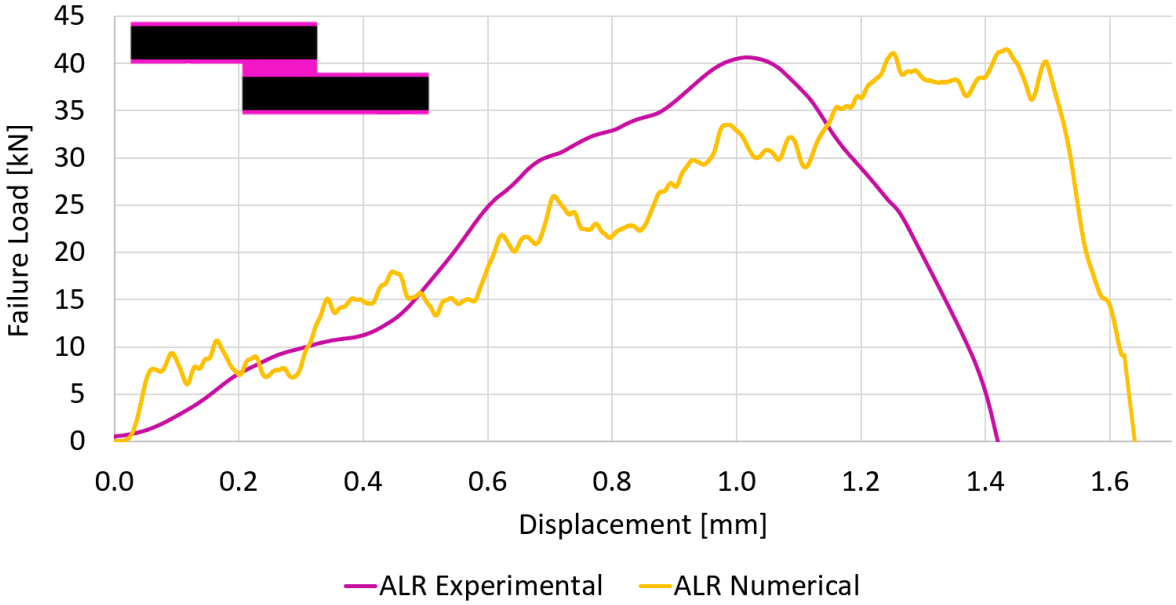

Figure B.17: Numerical vs Experimental P-δ curves for ALR under impact conditions

The experimental/numerical failure mode comparison is shown in Figure B.18. The model predicted the occurrence of delamination for both joints, with the start of cohesive failure for the ALR joint, a failure that, as previously discussed, was obtained for some of the specimens.

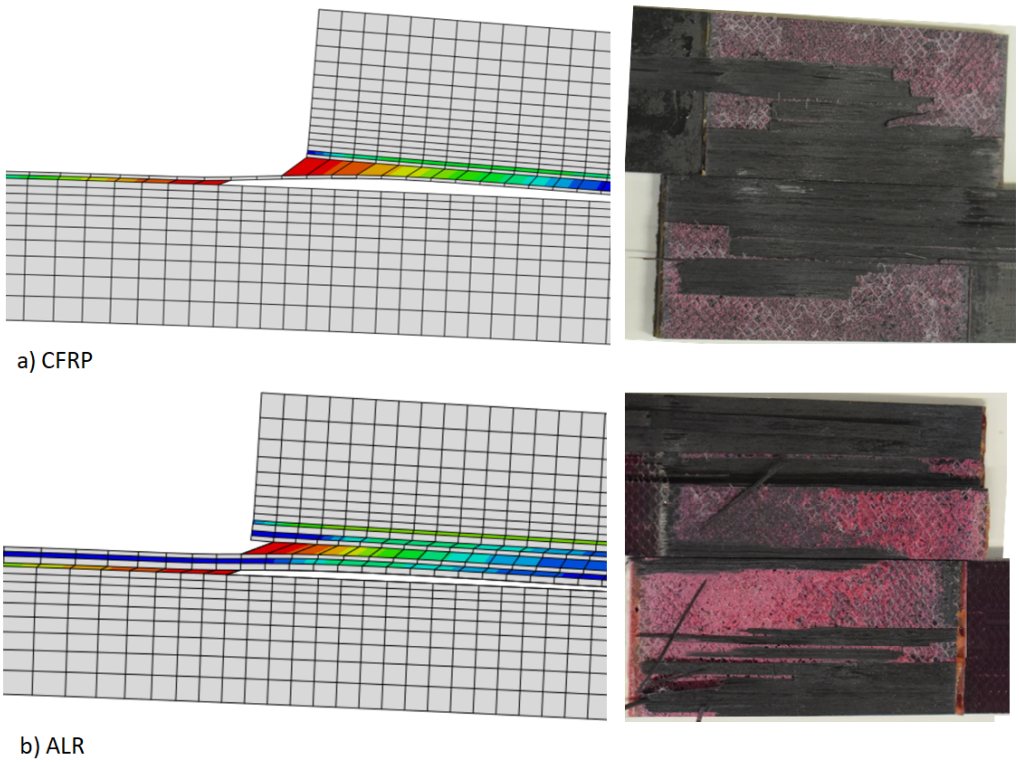

Figure B.18: Comparison between impact numerical and experimental failure modes obtained: a) CFRP; b) ALR

A summary of the performance of the reinforced ALR joints compared to the CFRP-only reference can be seen in Figure B.19. The same figure also illustrates the performance of the numerical models in the prediction of the failure loads for both loading conditions.

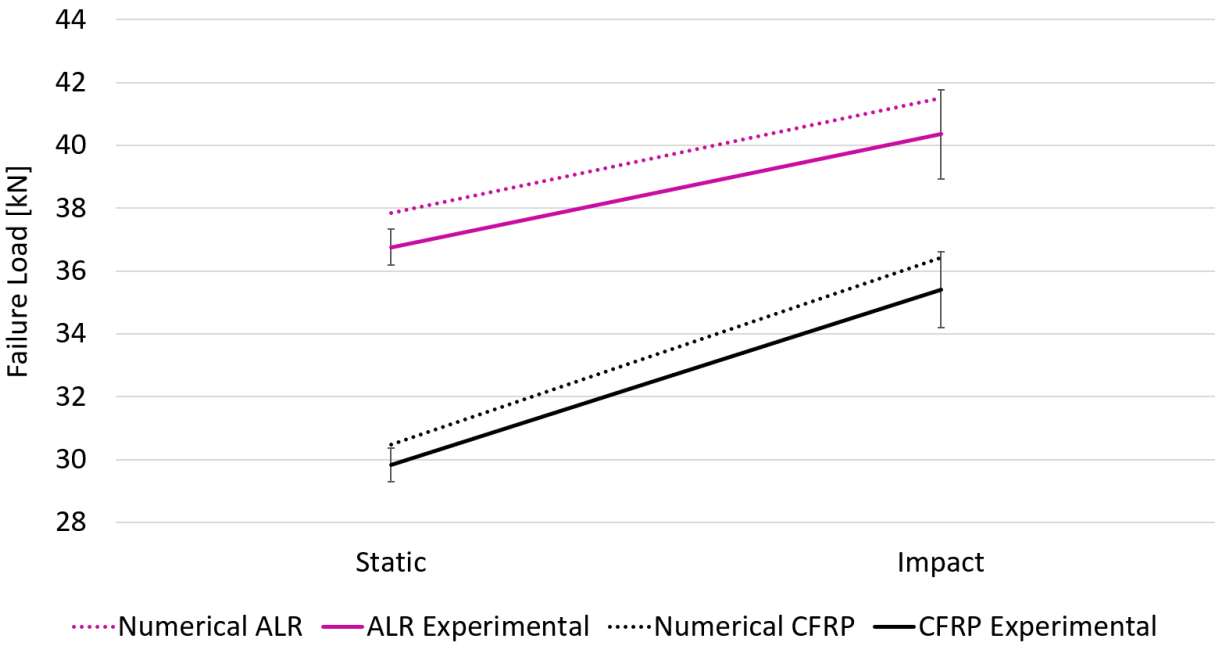

Figure B.19: Summary of the performance of ALR vs CFRP (Numerical and Experimental)

Shang et al. (2018) [9], in a "Strategy to reduce delamination of adhesive joints with composite substrates", analysed a similar novel reinforcement technique, using glass fibres embedded in a high toughness resin to reinforce the surface of the adherends. A change of the failure mode was observed with delamination failure being replaced by a cohesive failure.

The approach in this study suggest the complete replacement of the top surface with adhesive, instead of the reference CFRP ply, or the mix resin and glass fiber by Shang et al. For quasi-static conditions, the improvement percentage obtained using this technique, 23.31%, was very similar to the one obtained by Shang et al, 22.4%. Additionally, the improvement of the impact joint strength of ALR joints was also demonstrated.

Although a direct comparison is not possible due to different adhesives being used as reinforcements, this new approach is considerably easier to manufacture and logistically easier, as the reinforced joint uses the same materials as a traditional CFRP-only SLJ.

6 Conclusions

The role of adhesive layers in the reinforcement of adherends as a delamination prevention technique was numerically and experimentally studied. Several configurations were analysed, varying both the number of adhesive layers used and their location in the through thickness direction of the substrates.

A CFRP SLJ with 50mm overlap length and 3.2 mm thick adherends served as the reference to which the suggested configurations were benchmarked.

Several different adhesively reinforced joint configurations were developed, including joints reinforced with interlaminar adhesive layers and a joint with superficial adhesive layers. The performance of the suggested reinforced joints in a delamination prevention role was analysed for quasi-static conditions. Despite all suggested configurations displaying improvements regarding the maximum failure load, only one configuration, ALR, consisting of superficially reinforced adherends was shown to avoid delamination and fail cohesively in the adhesive layers. Instead of the stresses concentrated near the overlap ends being transmitted directly to the CFRP matrix, the plasticity of the adhesive layer redistributed them to the adhesive reinforcement layer and the substrate over a larger area, avoiding delamination.

This configuration was subsequently tested for impact conditions at 3m/s. However, and in spite of the encouraging results for quasi-static conditions it was not possible to eliminate the occurrence of delamination for impact conditions.

Nevertheless, the use of ALR as a delamination limiting technique is shown to be viable, increasing failure load levels and showing an increase in the energy absorbed in an impact setting. It is especially interesting because the reinforcement material is already used by the manufacturer of non-reinforced joints and is a reinforcement with very little weight added. The strain-rate dependency behaviour of the adhesive is thought to be the reason for this change in failure mode, with the increased strength of the adhesive for higher strain rates surpassing the strength of the CFRP matrix, causing delamination.

Finally, the numerical models correctly simulated the behaviour of the studied configurations of SLJs for both quasi-static and impact conditions. The numerically obtained failure loads were shown to be within a marginal error of the experimentally observed and the numerical failure modes accurately predicted the experimental failures.

References

[1] Jeevan Hanumanthu, Perumalla Ramulu, Vishnu Mukkoti, and CH Chandramouli. Failure prediction in fiber metal laminates for next generation aero materials. *IOP Conference Series: Materials Science and Engineering*, 149:012102, 09 2016.

[2] D. Gay. *Composite Materials: Design and Applications, Third Edition*. Taylor & Francis, 2014.

[3] Tamer Sinmazçelik, Egemen Avcu, Mustafa Özgür Bora, and Onur Çoban. A review: Fibre metal laminates, background, bonding types and applied test methods. *Materials & Design*, 32(7):3671 – 3685, 2011.

[4] Airbus. Experience and lessons learned of a composite aircraft. ICAS 2016, 30th Congress of the International Council of the Aeronatuical Sciences, 2016.

[5] The new-technology boeing 787 dreamliner, which makes extensive use of composite materials, promises to revolutionize commercial air travel. Technical report, Aviation Week & Space Technology Market Supplement, 2005.

[6] B. Kolesnikov, L. Herbeck, and A. Fink. Cfrp/titanium hybrid material for improving composite bolted joints. *Composite Structures*, 83(4):368 – 380, 2008.

[7] Pedro Camanho, Axel Fink, A Obst, and Soraia Pimenta. Hybrid titanium–cfrp laminates for high-performance bolted joints. *Composites Part A: Applied Science and Manufacturing*, 40:1826–1837, 12 2009.

[8] L.F.M. da Silva and M.F.S. de Moura. *Juntas Adesivas Estruturais*. Publindústria, 2007.

[9] L Tong. An assessment of failure criteria to predict the strength of adhesively bonded composite double lap joints. *Journal of Reinforced Plastics and Composites*, 16:698–713, 05 1997.

[10] Lucas F M Da Silva and RD Adams. Techniques to reduce the peel stresses in adhesive joints with composites. *International Journal of Adhesion and Adhesives*, 27:227 – 235, 4 2007. Publisher: Elsevier.

[11] R. D. Adams, R. W. Atkins, J. A. Harris, and A. J. Kinloch. Stress analysis and failure properties of carbon-fibre-reinforced-plastic/steel double-lap joints. *The Journal of Adhesion*, 20(1):29–53, 1986.

[12] Lucas F M da Silva and R D Adams. Techniques to reduce the peel stresses in adhesive joints with composites. *International Journal of Adhesion and Adhesives*, 27(3):227 – 235, 2007.

[13] J.A.B.P. Neto, R.D.S.G. Campilho, and L.F.M. da Silva. Parametric study of adhesive joints with composites. *International Journal of Adhesion and Adhesives*, 37:96 – 101, 2012. Special Issue on Joint Design 3.

[14] Lucas F. M. da Silva, T. N. S. S. Rodrigues, M. A. V. Figueiredo, M. F. S. F. de Moura, and J. A. G. Chousal. Effect of adhesive type and thickness on the lap shear strength. *The Journal of Adhesion*, 82(11):1091–1115, 2006.

[15] José Machado. A strategy to reduce delamination of adhesive joints with composite substrates. *Proceedings of the Institution of Mechanical Engineers, Part L: Journal of Materials: Design and Applications*, 233, 10 2018.

[16] Filipe J. P. Chaves, L. F. M. da Silva, M. F. S. F. de Moura, D. A. Dillard, and V. H. C. Esteves. Fracture mechanics tests in adhesively bonded joints: A literature review. *The Journal of Adhesion*, 90(12):955–992, 2014.

[17] R.D.S.G. Campilho, M.F.S.F. de Moura, and J.J.M.S. Domingues. Modelling single and double-lap repairs on composite materials. *Composites Science and Technology*, 65(13):1948 – 1958, 2005.

[18] 3M. 3m scotch-weld structural adhesive film af 163-2k technical datasheet. Technical report, 3M, 2009.

[19] ASTM D5868 01(2014). Standard test method for lap shear adhesion for fiber reinforced plastic (frp) bonding. Technical report, ASTM, 2014.

[20] Diogo P.C. Antunes, António M. Lopes, Carlos M.S. Moreira da Silva, Lucas F.M. da Silva, Paulo D.P. Nunes, Eduardo A.S. Marques, and Ricardo J.C. Carbas. Development of a drop weight machine for adhesive joint testing. Accepted for publication, 2019.

[21] Miguel Palmares. Strength of hybrid laminates aluminium carbon-fibre joints with different lay-up configurations. Master Thesis, Faculdade de Engenharia da Universidade do Porto, 2016.

[22] D.G. dos Santos, R.J.C. Carbas, E.A.S. Marques, and L.F.M. da Silva. Reinforcement of cfrp joints with fibre metal laminates and additional adhesive layers. *Composites Part B: Engineering*, 165:386 – 396, 2019.

[23] M Banea, L.F.M. Silva, and Raul Campilho. Mode ii fracture toughness of adhesively bonded joints as a function of temperature: Experimental and numerical study. *The Journal of Adhesion*, 88:534–551, 04 2012.

[24] ASTM D5528-13. Standard test method for mode i interlaminar fracture toughness of unidirectional fiber-reinforced polymer matrix composites. Technical report, ASTM, 2013.

[25] Marcelo De Moura, Raul Campilho, and J P. M. Goncalves. Crack equivalent concept applied to the fracture characterization of bonded joints under pure mode i loading. *Composites Science and Technology*, 68:2224–2230, 08 2008.

[26] M.F.S.F. de Moura, R.D.S.G. Campilho, and J.P.M. Gonçalves. Pure mode ii fracture characterization of composite bonded joints. *International Journal of Solids and Structures*, 46:1589–1595, 2008.